UNCLASSIFIED

UKNDC(84)P111
NEANDC(E)252 Vol.8
INDC(UK)-38/LN

UKNDC(84)P111
NEANDC(E)252 Vol.8
INDC(UK)-38/LN

United Kingdom Atomic Energy Authority

HARWELL

U.K. Nuclear Data Progress Report January - December 1983

Editor: D.J.S. Findlay
Nuclear Physics Division
AERE Harwell, Oxfordshire

July 1984

UNCLASSIFIED

UNCLASSIFIED

UKNDC(84)P111
NEANDC(E)252 Vol.8
INDC(UK)-38/LN

U.K. NUCLEAR DATA PROGRESS REPORT
JANUARY - DECEMBER 1983

Editor: D.J.S. Findlay

Nuclear Physics Division
AERE Harwell

July 1984

HL84/2719

CONTENTS

*For key see p. 44

CONTENTS

*For key see p. 44

PREFACE

This report is prepared at the request of the United Kingdom Nuclear Data Committee (UKNDC) and covers the period from January to December 1983.

Nuclear data are presented by laboratory. There are contributions this year from the Harwell and Winfrith Laboratories of the UKAEA, the National Physical Laboratory, the Birmingham Radiation Centre, the University of Birmingham, the University of Aston in Birmingham, the University of Edinburgh, the University of Oxford, and the University of Liverpool.

This report includes work from various collaborations between Harwell, Winfrith, the Universities of Oxford, Birmingham, Manchester and Guelph (Canada) and the Bureau International des Poids et Mesures, and between the National Physical Laboratory, the Institut für Radiumforschung and Kernphysik (Vienna) and the Institute of Atomic Energy (Beijing). Contributions on Chemical Nuclear Data are gathered by the Chemical Nuclear Data Committee and grouped under that heading.

Contributions to the report on nuclear data topics are welcome from all sources and we extend an invitation to researchers in other laboratories of industry, government, the universities and polytechnics to use this channel of communication.

Where the work is clearly relevant to requests in WRENDA 83/84 (INDC(SEC)-88/URSF) request numbers are given after the title of the contribution.

1983 NUCLEAR DATA FORUM

The seventeenth Nuclear Data Forum took place at the Imperial College Reactor Centre, Ascot on 12 Dec 82 with more than sixty participants. Two invited lectures were presented, one by N.M. Spyrou (University of Surrey) on the nuclear data requirements of medical physics, the other by A. Whittaker (BNFL) on nuclear data requirements of BNFL. Both these lectures are reproduced below. These were eleven contributed talks:

Neutron physics measurements relating to cancer therapy
M.C. Scott and J.G. Fletcher (Univ. of Birmingham)

Development of a charged particle detector for studies of neutron-induced reactions
R.A. Jarjis (AERE Harwell/Univ. of Birmingham)

A review of the Specialists' Meeting on yields and decay data of fission product nuclides, Brookhaven, Oct. 83.
D.R. Weaver (Birmingham Radiation Centre)

The UK CNDC data libraries: evaluated data for reactor applications
A. Tobias (CEGB Berkeley)

Delayed neutron spectrum measurements and covariance analysis
J.G. Owen, D.R. Weaver, J. Walker (Birmingham Radiation Centre)

Measurements of the $^{93}Nb(n,n')^{93m}Nb$ reaction by activation
D.B. Gayther and C.A. Uttley (AERE Harwell), M.F. Murphy and W.H. Taylor (AEE Winfrith), K. Randle (Univ. of Birmingham).

The angular distributions of 14 MeV neutrons scattered from large samples of iron and concrete
A.J. Cox, S.T. Anvarian (Univ. of Aston)

Resonance neutron radiography
E.M. Bowey, M.G. Sowerby (AERE Harwell), S. Woodward (AERE Harwell/ Imperial College).

The NEANDC task force on ^{238}U
M.G. Sowerby (AERE Harwell)

Measurements of the parameters of the pulsed neutron beams from the fast neutron target of HELIOS
D.B. Syme, G.D. James, A.D. Gadd (AERE Harwell)

Report on the IAEA Consultants' Meeting on nuclear data for structural materials, Vienna, 83
M.C. Moxon (AERE Harwell)

A Review of Nuclear Data Requirements in Medical Physics

Nicholas M. Spyrou
Department of Physics, University of Surrey

Lecture given at the Nuclear Data Forum, Ascot, Dec. 1983

1. Introduction

In this survey of nuclear data requirements in medical physics, it is intended to indicate in general, rather than in detail, some areas where the demand for nuclear data exists, and to highlight developments and applications in the field which may be of interest to the Nuclear Data Forum. By necessity therefore this review is selective.

Medical physics in this context is concerned with the interaction of ionising radiation with matter, and considers the role of radiation probes in diagnosis and in therapy. Physical methods of diagnosis are developed in order to study, non-invasively, the structure, composition and function of the body or regions within it, whilst minimising any hazard that may arise from the examination, i.e. the techniques employed in medical imaging and analysis are radiation dose limited.

In recent years clinicians, encouraged by physicists, have become increasingly aware that quantitative information can be extracted from medical images, which may be useful in the diagnosis of disease and treatment of the patient. To a certain extent, this awareness has been due to the impact that computerised tomography (CT) has had in medicine since the introduction of the first commercial CT-scanner, designed by Hounsfield, over a decade ago[1,2]. In tomography the aim is to provide a cross-section or slice through the body, which contains the information of interest, without contributions from underlying and overlying planes. In X-ray transmission tomography (Fig. 1a) the reconstructed image represents the distribution of the linear attenuation coefficient, a function of the density and the atomic number, whereas in gamma-ray emission tomography (Fig. 1b) it is the concentration and distribution of activity in the plane which is of interest. Making these techniques quantitative, implying 'how much and where', has led to the re-examination of theoretical and measured data. In the case of photon attenuation coefficients in the range 10 to 200 keV, of interest to X-radiography and tomography, discrepancies of the order

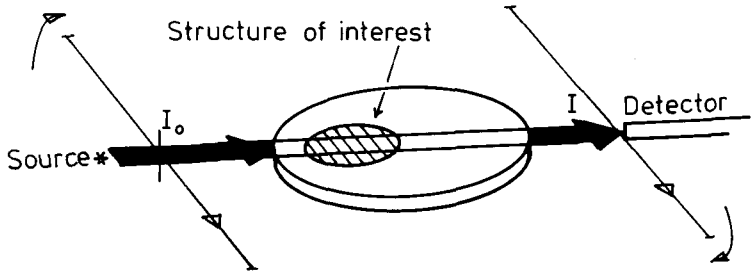

(a) Transmission tomography

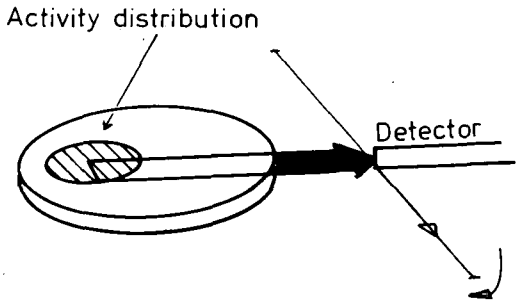

(b) Emission tomography

Fig. 1 (a) Transmission: source-detector rotated through small angle after each translation completed and repeated over at least 180°; the ray sum is here the average value of the linear attenuation coefficient along the beam paths and equal to

$$-\log I/I_0 = \int \mu(x,y)ds$$

where $\mu(x,y)$ is the attenuation coefficient at point (x,y) in the plane.

(b) Emission: detector rotated through small angle after each complete translation and sequence repeated round object plane; the ray sum is equal to

$$\int f(x,y)ds.\exp(-\int\mu(x',y')ds') \ ,$$

where f(x,y) denotes the activity concentration at (x,y) which is then attenuated before reaching the detector.

of 5% have been noted in measured values of the mass attenuation coefficient of materials, and because of the conditions for the 'mixture rule' to hold, errors are thought to be even larger below 10 keV although estimated at less than 2% if taken at 1 keV or more away from an absorption edge[3,4]. An

International Union of Crystallography project was set up in 1978 to resolve these problems in the region 0.5 to 50 keV. Measurements of photon attenuation coefficients may be used to determine elemental composition of materials[5].

Physical methods of diagnosis are not restricted to 'in vivo' investigations but encompass 'in vitro' examinations, not only of post mortem changes but also of biopsy specimens and other tissues (e.g. blood urine, hair) less traumatically obtained from the patient, since these measurements may provide the means for detecting abnormality and disease through biochemical changes.

The conventional radiation probes for therapy are X- and gamma-radiation. The aims of radiation treatment of disease, by destruction of cells in malignant tissue, are to enhance the effect of the radiation dose on these cells, in order to prevent recurrence of the disease and allow repair of the healthy tissue with which the radiation also interacted. In the interaction of photons with the body, the transfer of energy to molecules, mainly to water molecules, to form reactive free radicals makes normal biological tissue, with a well oxygenated blood supply, more sensitive to photons than oxygen deficient (hypoxic) and anoxic tissue, which may occur in diseased states. This has led to the search for other radiations as probes for therapy. Three quantities determine the effectiveness of absorbed radiation dose in tissue: the oxygen enhancement ratio (OER) which is the ratio of the dose required to produce an effect under anoxic conditions to that required to produce the same effect under well oxygenated (normal) conditions; the radiobiological effectiveness (RBE), which since different types of radiation produce different degrees of biological damage, is the ratio of the dose required for a standard or conventional radiation to have a certain effect, to the dose required of the radiation under consideration; and the linear energy transfer (LET), the energy transferred per unit track length in the material. (The RBE is not constant but is related to the LET.) For most biological materials the relatively high value of the OER for X- and gamma-rays, found to be between 2.5 and 3.0, has provided the impetus for radiobiological investigations with neutral and charged particles, in order to achieve a value closer to unity[6]. These investigations have shown that the effects produced by densely ionising particles are not as sensitive to hypoxic conditions, as is the case with photons and electrons.

2. Radiotherapy and Tomography

The reader is referred to the proceedings of a recent conference[7] and a review article[8] for greater detail on developments in the field and information about the adequacy of nuclear data, respectively. For the latter the position has improved only slightly since the article was written[9], so some of the salient features and conclusions will be quoted here, in particular with reference to H, C and O. In Table 1, the percentage composition by weight of the human body and the tissues, fat, muscle and bone, is listed in terms of bulk and minor elements but not trace elements.

Table 1

Bulk and minor elements in the human body[11] and in human tissues[10], expressed as percentages by weight

Element	Total Body	Fat	Muscle	Bone
H	10%	12.2%	10.2%	3.4%
C	23	76.1	12.3	15.5
N	2.6	NQ*	3.5	4.0
O	61	11.7	72.89	44.1
Na	0.14	NQ	0.02	<0.1
Mg	0.027	NQ	0.02	0.2
P	1.1	NQ	0.2	10.2
S	0.20	NQ	0.5	0.3
K	0.20	NQ	0.3	NQ
Ca	1.4	NQ	0.01	22.2

*Not quoted

Neutrons are densely ionising particles, with a low OER in the range 1.7 to 2.0, and are being used for therapy at about 20 centres, the first application having taken place in 1938. On neutron irradiation* of tissue, a large part of the energy is transferred to recoil protons and alpha particles emitted in the (n,α) reaction, as well as to recoiling carbon, nitrogen and oxygen nuclei in scattering collisions. As the neutron beam traverses the body, gamma-rays are also emitted as a result of neutron

*Neutron beams are never free from gamma-ray contamination

inelastic scattering and capture reactions. However, neutron data on C, N and O above 15 MeV are sparse, and therefore the energetics of the reactions and energies of resulting charged particles are incomplete, making it difficult for accurate energy transfer coefficients to be calculated. All other projectiles (π^-, p, α, C, Ne and A) being used or being considered for radiotherapy are charged particles, for which the main channel of energy loss in a material is ionisation, although nuclear interactions must be taken into account in certain cases. The well-known Bethe-Bloch formula adequately describes the stopping-power (the energy loss unit path length) of protons and heavier charged particles as well as pions:

$$-\frac{dE}{dx} = \frac{z_p^2 e^4}{m_0 c^2 \beta^2} NZ \left(\log(2m_0 c^2 \beta^2 / I(1-\beta^2)) - \beta^2 - s\right) \qquad (1)$$

where z_p is the charge of the projectile of velocity v in a medium of atomic number Z, $\beta = v/c$, m_0 is the electron mass, N is the number of atoms per unit volume, s is the shell correction and I is the mean ionisation energy. For energies in the range $I << E << m_p c^2$, where m_p is the mass of the projectile, the term in the parenthesis varies slowly with energy and hence

$$-\frac{dE}{dx} \alpha \frac{m_p z_p^2}{E} \qquad (2)$$

The projectiles would therefore deposit most of their energy at the end of a well-defined range, resulting in the characteristic Bragg peak. This has obvious advantages in radiation treatment for concentrating on the tumour and sparing healthy tissue, compared to photons (and neutrons) where attenuation of the radiation beam in the medium is exponential. The Bragg peak, however, does widen for heavy ions at the energies considered useful in radiotherapy and in radiography, because the mean free path for nuclear interactions in the material is comparable with the range at these energies, and therefore the primary beam will give rise to secondary particles of lower charge but approximately the same velocity. Most of the dose will then be deposited at the far side of the Bragg peak, because of the longer range of these secondary fragments. However, an advantage of using heavier charged particles is that they suffer less multiple scattering and so the

incident beam diverges less as shown in Fig. 2[12]. The Bragg peak of ionisation for protons offers the possibility that relatively high doses could be delivered to tumours at depth, with little energy being lost in the more superficial tissues; unfortunately this is only the case when very thin sections are irradiated. Most tumours are rather large compared to the dimensions of the Bragg peak and the proton beam must be 'modulated', either in range or energy to produce a beam covering the volume of interest. Protons have therefore become associated with the treatment of rather small volumes as found in the pituitary gland and in ocular melanomas.

There are only a few existing accelerators with energies and intensities appropriate for proton therapy and few available for clinical investigation. However, as early as 1957 at Uppsala, Sweden, proton therapy was applied using a 185 MeV synchrocyclotron beam. Machines from 75 MeV synchrocyclotrons to 12 GeV proton synchrotrons are now being used for clinical applications at major centres in Sweden, the USA, the USSR and Japan and are being considered for research in South Africa, France (Orsay), Switzerland (SIN) and Belgium (Louvain). Most of these centres are also investigating the usefulness of a range of heavy charged particles.

Interest in the negative pion as a probe for radiotherapy began some 22 years ago with the publication of a paper by Fowler and Perkins[14]. Capture of a negatively charged pion into an atomic orbit eventually leads to the absorption of the pion by the nucleus after the captured pion has cascaded through atomic states with the emission of X-rays and Auger electrons. The rest mass energy of the pion (140 MeV) is released on its absorption by the nucleus which breaks up into charged particles, neutrons and gamma-rays. It is the localised deposition of the energy of the densely ionising fragments in addition to the Bragg peak of the pion, forming the 'star peak', which makes the pion's use attractive in radiation treatment (see Fig. 3). Only the so-called 'meson factories' at LAMPF (USA), TRIUMF (Canada) and SIN (Switzerland) can currently produce pion beams with sufficient intensity for radiation therapy.

Computerised tomography is proving useful as a diagnostic tool and as an aid to radiotherapy, for in planning effective treatment the localisation of the tumour must be as accurate as possible, and also heterogeneities in the beam path selected within the patient must be accurately known in terms of variations in the chemical composition. In X-ray transmission

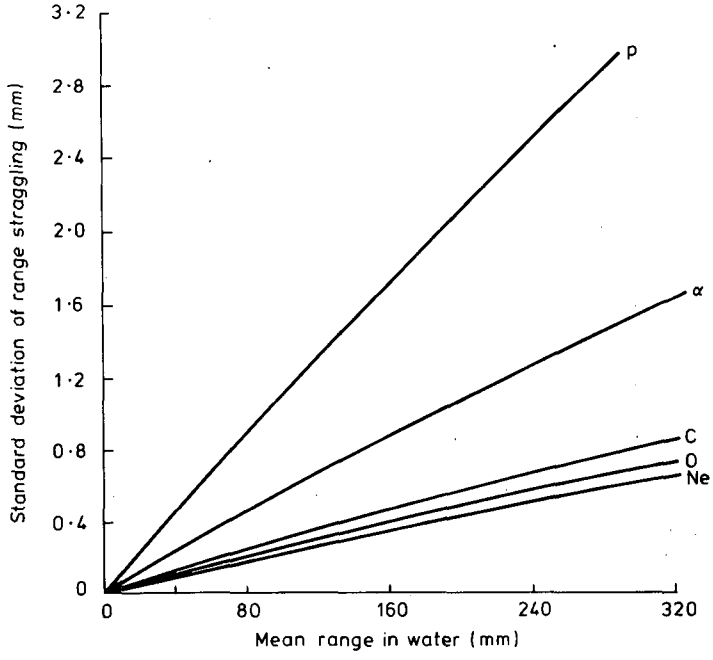

Fig. 2(a) The rms range straggling in water (soft tissue) for various projectiles as a function of range (not energy).

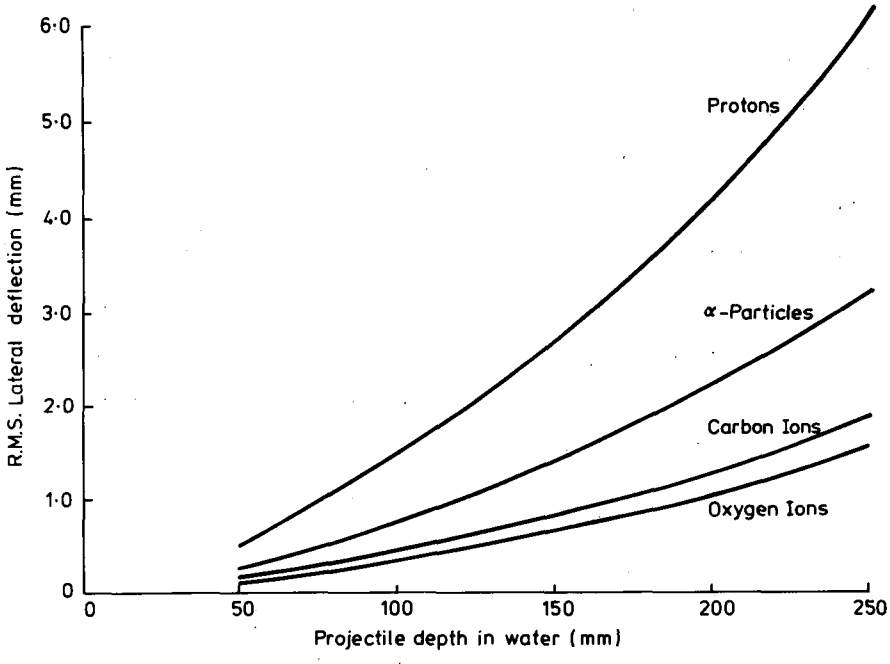

Fig. 2(b) The rms beam deflection due to multiple scattering of various projectiles (from ref. 12, redrawn from ref. 13) (the vertical axis is twice the rms lateral displacement (the full width of an originally infinitesimally narrow beam))

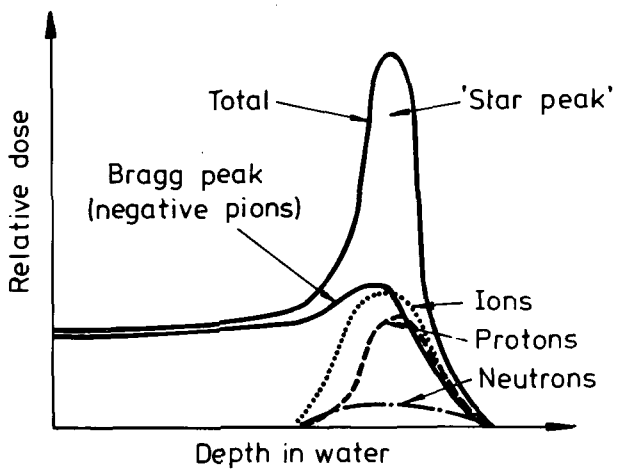

Fig. 3 The 'star peak' for negative pions (calculated values following pion capture in ^{12}C, in terms of numbers of particles produced and average kinetic energy (MeV) per negative pion captured, are[15]: n(2.79, 64.2 MeV) p(1.03, 20.1), d(0.26, 2.8), t(0.08, 1.0), ^{3}He(0.03, 0.4), α(1.10, 16.8) and Li + Be + B(0.33, 1.5))

tomography the distribution of the linear attenuation coefficient, a function of density and atomic number, is presented with a spatial resolution between 1 and 2 mm. However, by scanning the patient at two different energies, it is possible to obtain distributions of the effective electron density and an effective atomic number, separately. These data thus represent the input to a treatment plan at present, and it is clear therefore that if full advantage is to be taken of the precise dose localisation provided by heavy charged particle therapy these data must be accurate. Estimates of the required spatial resolution of these data have been made[16] and suggest that for tumour localisation a resolution no worse than 2-3 mm is required, whereas for heterogeneity measurements a minimum of 3, 1 and 0.3 mm for pions, protons and Ne ions respectively (ignoring secondary particles) is indicated. Although the present resolution limit

for X-ray tomography is 1-2 mm, it is possible that better resolution will be achieved by other radiation probes, and the centres involved with new means of therapy have intensive programmes in the study of imaging and CT not only with photons but also with heavy charged particles.

In summary, the radiation probes applied to or being considered for radiation treatment and in tomography present the following fundamental problems[8] if quantitative information, necessary for therapy, is to be reliable:

(i) Heavy charged particles, e.g. alpha-particles, ^{12}C and ^{20}Ne, interact with nuclei, and hence information is required about their production of secondary particles, their energy spectra and interactions. Atomic processes by which positively charged particles slow down and transfer energy to matter are quite well understood in the main.

(ii) Negative pion nuclear interactions must be understood so that reliable, quantitative predictions can be made of the number, types and energy spectra of secondary particles produced, since it is these secondary particles which provide the additional dose at the end of the range. As with heavy charged particles, information about the interactions of secondary particles and de-excitation of residual nuclei is required. Relative atomic capture probabilities of the pions must also be known or be calculable.

(iii) Neutrons are used as probes in therapy and are also produced as secondary particles in heavy ion and in pion-nuclear interactions. A significant proportion of the neutron interactions in tissue involve nuclei other than hydrogen and so detailed information must be available.

3. Elemental Analysis and Tomography

The role that elements play in health and disease is an area which has been receiving considerable attention in the past twenty years and is continuously expanding, not only in fundamental research where trace elements associated with enzymes and proteins are studied in the regulation of biochemical changes, but also in nutrition, in the determination of body burdens for environmental applications, and also in their detection as 'biological indicators' of diseased states. The significant contribution that nuclear- based methods of analysis have made to the determination of

the elemental composition of biological materials is well documented, and in the case of 'in vivo' analysis, where a variety of radiation probes have been applied but in which mainly neutrons have been extensively used, the contribution is unique. This section will largely be concerned with neutron activation analysis data requirements, and will be illustrated by three areas of application.

(a) In neutron activation analysis there is a growing trend towards the so-called absolute method of analysis, where elemental concentrations are calculated from the basic equations for activation and decay, without the use of comparators. Thus preparation and analysis of standards or reference materials, which must be carried out in conjunction with the samples of interest, are avoided. It is not unusual for analytical laboratories to report several thousand results annually and progress in this area would present a considerable saving in time and money. Table 2 lists the detector response for various activation modes and defines the parameters involved.

The disadvantage of the absolute method is its poor accuracy due to the uncertainty of listed nuclear data. A recent investigation[17], in which the irradiating and detecting systems were well characterised, showed that determination of elemental concentrations by the detection of prompt and delayed gamma-rays using the absolute method varied between elements from a few percent to a factor of two when compared with known values. This is not uncommon; for absolute activation analysis σ, I and f should be known to an accuracy of 1-2%, while for delayed measurements $\tau_{1/2}$ should be known to an accuracy of 0.1 - 0.5%. Attempts are being made to minimise these errors by measurement of a single factor, the k_0-factor (see Table 2), by a number of groups, notably the Institute of Nuclear Sciences at the University of Ghent and the Central Research Institute for Physics in Budapest in a collaboration which started in 1975[18].

(b) The demand for rapid and sensitive methods of analysis led us to develop a technique termed cyclic activation[19] over a decade ago. It is capable of detecting short-lived isotopes, e.g. ^{207m}Pb(0.8s) and ^{20}F(11s), in a multielemental matrix by enhancing the short-lived activity and suppressing the activation of longer liver nuclides. The technique involves

Table 2

Detector responses for prompt, delayed and cyclic modes of neutron activation

1. Prompt: $D_p = \varepsilon I_p \phi \sigma \frac{N_o f}{A_w} m\, t_c$

2. Delayed: $D_d = \varepsilon I_d \phi \sigma \frac{N_o f}{A_w} m \frac{(1-e^{-\lambda t_i})e^{-\lambda t_w}(1-e^{-\lambda t_c})}{\lambda}$

where
- σ = neutron cross-section
- ϕ = neutron flux
- I_p = number of photons of interest emitted per neutron captured
- I_d = the fractional intensity of the emitted gamma-ray
- ε = the detector efficiency for the gamma-ray energy of interest
- t_i = time of irradiation
- t_w = transfer time i.e. time elapsed from end of irradiation to the start of counting period
- t_c = time of counting (in prompt mode $t_i = t_c$)
- N_o = Avogadro's number
- f = fractional isotopic abundance
- A_w = atomic weight of element of interest
- m = mass of element

The k_o-factor = $\frac{I\sigma f}{A_w}$

3. Cyclic:

The detector response after n cycles

$$D_n = D_d \frac{(1-e^{-n\lambda T})}{(1-e^{-\lambda T})}$$

The cumulative response after n cycles i.e. $\sum_{i=1}^{n} D_i$

$$D_c = D_d \left[\frac{n}{(1-e^{-\lambda T})} - \frac{e^{-\lambda T}(1-e^{-n\lambda T})}{(1-e^{-\lambda T})^2} \right]$$

where T = cycle period = $t_i + t_w + t_c + t_r$

t_r = return time i.e. time elapsed from end of counting to start of irradiation.

the rapid transfer of the sample from the irradiation position in the reactor core, where it is irradiated for a short period of time, to the detecting system, where it is counted for an equally short period of time. The process is then repeated for a preselected number of cycles, depending on experiment time and the half-life of the nuclide of interest and those of the matrix nuclides, to give a cumulative detector response spectrum according to the equations in Table 2. By recording individual spectra for each cycle, an estimate of the half-life of the nuclide can also be made, which may be useful in identifying the source of a particular gamma-ray line in a complex spectrum.

Cyclic activation analysis has therefore increased the number of elements that could be determined accurately, but it also made demands on the availability of accurate nuclear data for short-lived isotopes. A compilation we made five years ago, now being updated, noted the areas of uncertainty - a significant number of these were associated with isomeric states. A number of reactor-based facilities have been designed and constructed for the detection of short-lived nuclides in activation analysis, and the first international meeting was held in 1980 at the Austrian Universities Reactor Centre in Vienna with fifty participants from sixteen countries[20].

(c) 'In vivo' neutron activation analysis comprises whole body methods where the elemental composition overall is determined, and partial body methods where elemental levels in a region of interest in the body are found and in which neutron irradiation is confined to that volume of interest, if possible. There are about fifteen groups working in the field, of which seven are in the UK. The measurement of Ca, P, Na, Cl, K, N and O in body composition studies can now be considered as routine; these are major and minor constituents of the body. H, I and Cl can also be measured and there are about eight trace elements (Mg, Al, Fe, Cu, Se, Pb and Hg) for which techniques exist or are being developed. Elements are determined by fast neutron reactions and thermal neutron capture, and detection is via prompt or delayed gamma-rays. Irradiation facilities include accelerators, 14 MeV generators and radioisotope neutron sources, with doses to the person kept below 10 mSv per examination and in some cases considerably lower. Because 'samples' cannot be homogenised or standardised into easily calculable shapes and person-to-person variations must be accounted for, considerable effort goes into the design of 'phantoms', made of tissue equivalent

materials, as comparators for measurement of elemental composition. However, 'in vivo' activation analysis, ideally, also ought to be carried out in an absolute sense. With the advent of X-ray transmission tomography and provision of information in terms of effective density and atomic number in cross-sections, it should be possible to develop computer codes to calculate the volume of interaction of the neutron probe with the tissues and the emission and attenuation of the gamma rays produced within it, taking into account variations in size and location of organs from person to person. However the lack of accurate nuclear data, as in radiation treatment, is a problem. For example, in the determination of body nitrogen for protein measurements through the fast neutron reaction $^{14}N(n,2n)^{13}N$ (a pure positron emitter), accurate information is required about the energy and interaction cross-section of the recoil protons and secondary emissions, since it has been estimated that 20% of the ^{13}N measured in the body is due to the $^{16}O(p,\alpha)^{13}N$ reaction. In applications where the amount of calcium in bone is to be determined, absolute calculations would have an error of at least 20%, because of the uncertainty in the (n,γ) cross-section of ^{48}Ca.

Cyclic activation has also been considered for 'in vivo' activation analysis in order to exploit its advantages and determine the concentration of elements in the body not previously possible to detect, as well as optimising the amount of elemental information obtained for the radiation dose imparted. Here, oscillation of the patient between neutron source and detector is not contemplated, but instead the neutron source is cycled between an irradiating position and a shielded position. In our system a 5Ci Am-Be source is used[21], although other designs may incorporate a pulsed or chopped neutron beam. Since neutron irradiation of the patient takes place, however small the dose, it is useful to extract maximum information about elemental composition and therefore, on a cyclic basis, prompt gamma-ray spectra are recorded whilst the source is at the irradiating position and delayed gamma-ray spectra of short-lived nuclides when it is shielded. In addition, at the end of cyclic activation, the gamma-ray spectrum from the longer-lived induced activities is also recorded. It has been shown, for example, that selenium (^{77m}Se, 17s) and cadmium (prompt gamma-rays) can be detected in the liver in the same investigation using cyclic activation, with detection limits of the order of 0.5 and 5 ppm respectively for a dose of about 5 mSv[22], thus providing an 'in vivo' method for the study of synergistic effects between the two elements.

What is ideally required, in a number of 'in vivo' studies, is to determine composition and elemental distribution, rather than a gross indication of elemental concentration. Neutron activation analysis can be considered to be a form of tomography since the primary neutrons create a distributed source of photon activity, characteristic of the nuclei present in the material, which can then be treated as a problem in emission tomography. In 'in vivo' neutron activation analysis, dose considerations make neutron induced tomography photon limited, but these restrictions are less severe in therapy. Any differences in composition between healthy tissue and malignant tumour may then be determined, imaged and studied. The radiation probe need not be confined to neutrons as long as characteristic induced radiation is emitted from the body. Very little work has been done in this area, although induced activities resulting from (γ,n) reactions following high energy electron therapy using a 33 MeV betatron were studied[23]. This does not preclude application of the technique to industrial problems and in the investigation of specimens where radiation dose is not a limitation.

In conclusion, quantitative information is becoming increasingly important in the clinical context, and there are a number of exciting developments in prospect which place a heavier demand for more and better nuclear and atomic data.

---

(1) G.N. Hounsfield, British Patent no. 1283915 (1972).

(2) G.N. Hounsfield, Br. J. Radiol. 46 (1973) 1016-1022.

(3) R. Deslattes, Acta Cryst. A25 (1969) 89.

(4) J.H. Hubbell et al. International Tables for X-ray Crystallography, (eds. J.A. Ibers and W.C. Hamilton) 4 (1974) 47.

(5) K. Kouris, N.M. Spyrou, D.F. Jackson, Materials analysis using photon attenuation coefficients, Research Techniques in Nondestructive Testing VI, (ed. R.S. Sharpe) (Academic, 1982) pp. 211-254.

(6) M.R. Raju et al., Br. J. Radiol. 51 (1978) 712.

(7) Proc. Conf. on Applications of Physics to Medicine and Biology, Trieste, 1982, (eds. G. Alberi et al.) (World Scientific, Singapore, 1983)
ISBN 9971-950-42-1.

(8) D.F. Jackson and D.J. Brenner, Nuclear interactions for medical purposes, Prog. Nucl. Phys. 5 (1981) 144-205.

(9) D.F. Jackson (private communication).

(10) D.R. White, Phys. Med. Biol. 22 (1977) 219.

(11) Report of the Task Group on Reference Man, ICRP 23, (Pergamon, 1975).

(12) K. Kouris, N.M. Spyrou, D.F. Jackson, Imaging with Ionising Radiations, vol. 1, Progress in Medical and Environmental Physics, (Surrey University Press/Blackie, Glasgow, 1982).

(13) A.A.M. Mustafa, Ph.D. thesis, University of Surrey (1981).

(14) P.H. Fowler and D.H. Perkins, Nature 189 (1961) 524.

(15) M.P. Guthrie, R.G. Alsmiller and H.W. Bertini, Nucl. Instr. Meth., 66 (1968) 29.

(16) M. Goitein, Int. J. Radiat. Oncology Biol. Phys. 3 (1977) 271.

(17) C.A. Adesanmi, Ph.D. thesis, University of Surrey (1983).

(18) A. Simonits, F. De Corte, L. Moens, J. Hoste, J. Radioanal. Chem. 72 (1982) 209-230.

(19) N.M. Spyrou, J. Radioanal. Chem. 61 (1981) 211-242.

(20) Proc. Workshop on Short-lived Nuclides in Activation Analysis, Vienna, Feb. 1980, J. Radioanal. Chem. 61 (1981).

(21) I.P. Matthews and N.M. Spyrou, Int. J. Appl. Radiat. 33 (1982) 61-68; N.M. Spyrou and I.P. Matthews, J. Radioanal. Chem. 61 (1981) 195-209.

(22) G.E. Nicolaou, I.P. Matthews, L.G. Stephens-Newsham, N.M. Spyrou, J. Radioanal. Chem. 71 (1982) 519-532.

(23) D. Pearson, Ph.D. thesis, University of Surrey (1979).

Some Aspects of BNFL's Nuclear Data Requirements

A. Whittaker
British Nuclear Fuels plc

Lecture given at the Nuclear Data Forum, Ascot, Dec. 1983

1. Introduction

British Nuclear Fuels plc (BNFL) is a Government owned company which was formed in 1971 to take over the nuclear fuels business of the Production Group of the UK Atomic Energy Authority. This business is concerned with enriching, manufacturing and reprocessing nuclear fuel for customers at home and abroad. BNFL employs about 15,700 employees, 43% of whom are staff and 57% industrials. The Company's establishments are all located in the north-west of England with headquarters at Risley in Cheshire and three main industrial sites situated at Capenhurst near Chester, Springfields near Preston and Sellafield near Seascale in Cumbria. In addition BNFL owns and operates two small nuclear power stations, situated at Calder Hall in Cumbria and Chapelcross in Dumfrieshire.

Because of the dangers inherent in the handling of radioactive materials, detailed safety assessments have to be made to permit safe plant design and operation and to satisfy the Regulatory Authorities. Accurate nuclear data is needed otherwise the designers will need to err on the side of safety by overdesign, and this is turn will lead to unnecessary expense and perhaps less edge over our competitors.

With a general framework of safety, efficiency and economy, nuclear data is used within the Company in ten main contexts:

(i) flowsheeting,
(ii) process control,
(iii) shielding calculations,
(iv) health physics calculations,
(v) instrumental measurements,
(vi) research and development,
(vii) radiochemical analysis,
(viii) criticality assessment,
(ix) safeguards and accountancy,
(x) accident investigation.

During the course of this presentation I shall endeavour first to indicate BNFL's accuracy requirements for this nuclear data; secondly I shall pick out a few interesting examples of the use of nuclear data in these different areas, and thirdly I shall attempt to forecast some of the Company's likely requirements for nuclear data in the future. My aim will be to show that BNFL, operating as it does in the high technology industry of nuclear fuel services, has need of a wide range of nuclear data to achieve its objective of continuous improvements in the safety and efficiency of its operations. My section is responsible for providing a nuclear data service to the Company and this entails having at our finger-tips up-to-date information on all aspects of nuclear data as well as maintaining and updating computerised libraries allied to particular computer codes.

2. Generation of Fission Product and Heavy Isotope Inventories

The main effort in my section goes into generating fission product and heavy isotope inventories for particular reactors for any enrichment, irradiation, power history and cooling time. These inventories are used in a very wide range of contexts, but especially for flowsheeting and shielding calculations. In view of the importance of these inventories to the Company, I shall highlight a number of improvements that we would like to see in the future.

At present the calculation is broken down into two steps. In the first step, the cross-sections of eleven heavy isotopes are generated as a function of burn-up using the reactor physics code WIMS. Because the code is expensive to run, this is only done for a limited number of reactors at a limited number of enrichments. In the second step, these burn-up dependent cross-sections are then used in the code FISPIN to generate point fission product and heavy isotope inventories at any irradiation and cooling time. At the moment, this two-step process is not very efficient because the full output from WIMS has to be edited using a subsidiary code called FRATES in order to extract three-group cross-sections for the eleven key isotopes and to put them into the correct format for use with FISPIN. However, I am glad to say that joint discussions with AEE Winfrith have taken place in the last few weeks, and plans are now being laid to link WIMS to FISPIN so that automatic linked runs can be performed[1]. This should lead to much greater accuracy and efficiency.

In future, we want to be able to calculate channel or assembly-averaged fission product and heavy isotope inventories. Channel or assembly-

averaging is important in the reprocessing context because some of the fission products and many of the heavy isotopes are produced non-linearly due to multiple neutron capture. Thus, use of point inventories for flowsheeting can, for example, greatly underestimate the arisings of the americium and curium isotopes. Fig. 1 illustrates how the calculation might be performed. A modified version of FISPIN needs to be written which will perform the axial-averaging using a set of axial form-factors. Because the running time of this modified version of FISPIN will be long, it is economically expedient to have a third step which will perform a three-way interpolation to obtain assembly-averaged fission product and heavy isotopes for any enrichment, burn-up and cooling time.

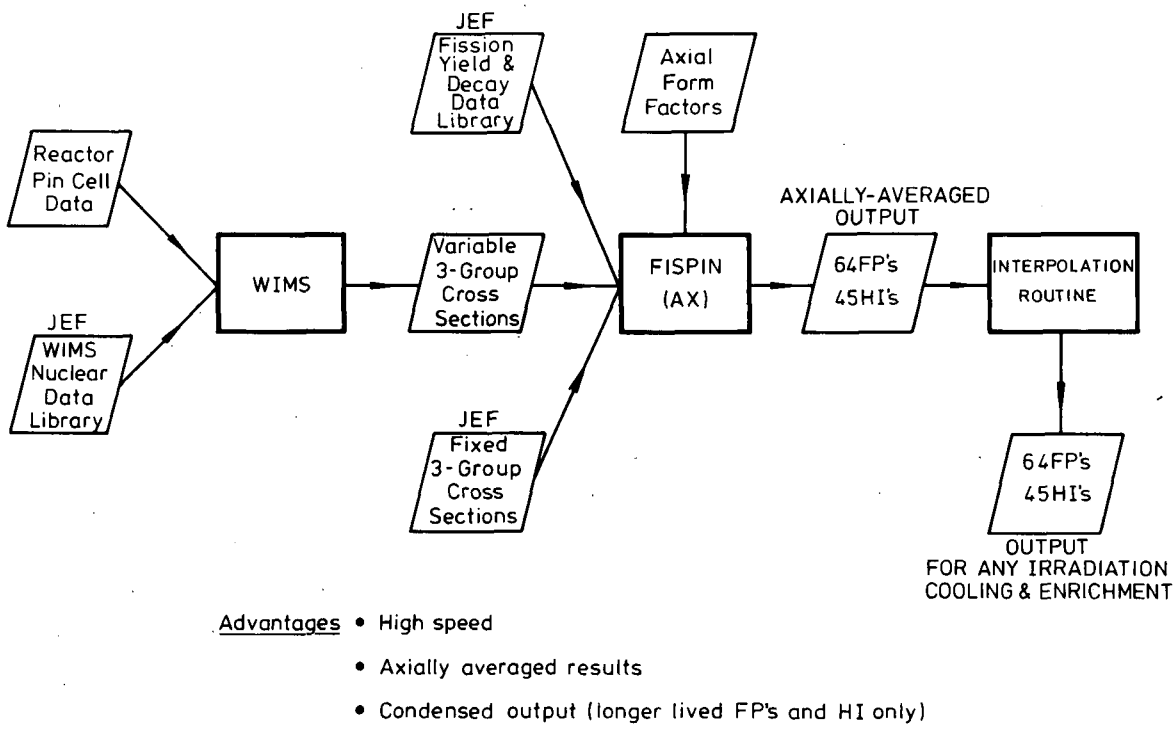

Fig. 1 Proposed three-step calculation with axial averaging and condensed output

Turning now to the nuclear data used in FISPIN, an important part of our work is the acquisition of suitable nuclear data libraries and these also require updating regularly. This is done in collaboration with the UKAEA through three committees:

The Differential and Integral Data Working Group (DIDWG),

The Chemical Nuclear Data Committee (CNDC), and

The Irradiated Materials Activity Committee (IMAC).

Very broadly the DIDWG is responsible for the accuracy of all nuclear data used in reactor physics calculations but tends to concentrate on evaluating the accuracy of cross-section data (particularly in the fast reactor context). The CNDC is broadly responsible for generating and evaluating fission yields, half-lives and decay data. It reports to the DIDWG. Development of the FISPIN code and its libraries is steered by the IMAC. BNFL requests, where necessary, measurements or evaluations of particular items of nuclear data if these are of insufficient accuracy for our purposes[2]. Complete libraries of cross-sections are created for us by Winfrith for particular reactor systems on a repayment basis[3-5].

Table 1 summarises those reactors for which WIMS calculations have been done. The adequacy of this list in the light of that fuel which is currently scheduled for reprocessing in the Thermal Oxide Reprocessing Plant (THORP) (the so-called THORP 'baseload') is presently being reviewed and further calculations will probably be required.

Table 1

Burn-up dependent cross-section libraries

Reactor type	Station	^{235}U enrichment (percent)
Magnox		Natural
CAGR	Dungeness Hinkley Point Hartlepool, Heysham A	2.2, 2.9, 3.5 2.016, 2.658, 2.9 2.016, 2.6, 3.2
SGHWR	Winfrith	2.1
PWR	Beaver Valley Bugey	2.0, 3.2 2.8, 3.2, 3.6
BWR	Garigliano Oskarshamn 'BWR 5' Fukushima 1	2.3, 2.42 1.7, 2.6 1.0, 2.0 2.19, 2.5 and 2.74

3. Accuracy Requirements

Turning now to BNFL's accuracy requirements for the fission products, these have been well summarised by Merz and Laser at the 1973 Bologna meeting on Fission Product Nuclear Data[6]. Merz and Laser stated that the total decay heat should be known to ±5%, and this is the most crucial parameter. At relatively short cooling times, a large number of fission products contribute to the total decay heat and it is statistically probable that this latter accuracy is achieved even if the individual fission products are only known to poor accuracy. At longer cooling times, only a limited number of fission products contribute towards the total decay heat, and it is quite possible that, because of the relatively large uncertainties in the mean beta energy of these particular fission products, the accuracy requirements are not met. Table 2 shows the percentage contributions of individual fission products to the total beta heating at cooling times of 5, 30 and 50 years, for PWR fuel irradiated to 40 GWd/t, and illustrates this point.

Table 2

The main fission products contributing to the beta heating after 5, 30 and 50 years (PWR fuel, 40 GWd/t)

5 y cooling		30 y cooling		50 y cooling	
^{90}Y	39.5%	^{90}Y	62.4%	^{90}Y	62.3%
^{106}Rh	16.8	^{137}Cs	17.0	^{137}Cs	17.6
^{144}Pr	10.8	^{90}Sr	13.3	^{90}Sr	13.3
^{137}Cs	10.4	^{137m}Ba	6.2	^{137m}Ba	6.4
^{90}Sr	8.4	^{85}Kr	0.6	^{85}Kr	0.3
^{134}Cs	5.2	^{154}Eu	0.5	^{154}Eu	0.2
^{137m}Ba	3.8				
^{154}Eu	1.3				
^{147}Pm	1.3				
^{85}Kr	1.1				
^{144}Ce	0.8				
^{155}Eu	0.2				
^{125}Sb	0.2				
^{106}Ru	0.1				
^{125m}Te	0.1				
All FP	100.0%	All FP	100.0%	All FP	100.0%

The following is a list of fission products of importance in reprocessing long cooled fuel and is reproduced from Merz and Laser's paper:

^{3}H, ^{85}Kr, ^{89}Sr, ^{90}Sr, ^{90}Y, ^{91}Y, ^{95}Zr, ^{95m}Nb, ^{95}Nb, ^{103}Ru, ^{103m}Rh, ^{106}Ru, ^{106}Rh, ^{125}Sb, ^{125m}Te, ^{129}I, ^{131}I, ^{134}Cs*, ^{137}Cs, ^{137m}Ba, ^{140}Ba, ^{140}La, ^{141}Ce, ^{143}Pr, ^{144}Ce, ^{144}Pr, ^{147}Nd, ^{147}Pm, ^{151}Sm, ^{154}Eu* and ^{155}Eu.

(* denotes an isotope produced by neutron capture in a stable fission product)

The accuracy required for these isotopes is ±10% and, with the exception of ^{3}H, ^{129}I, ^{134}Cs and ^{154}Eu, this is probably achieved. Because of the growing interest in reprocessing at increasingly longer cooling times[7] (currently 5 years for THORP, but possibly increasing progressively to 30 or even 50 years in later years), some of these fission products will be too short-lived to be of any interest, and the list becomes much shorter.

A further very useful review of the needs and accuracy for fission product nuclear data in the out-of-pile fuel cycle was given by McKay[8] at the Petten meeting on FPND in 1977. Table 3 is taken from McKay's paper and lists those radioactive fission products which are of importance in reprocessing plant streams.

Table 3

Radioactive fission products in reprocessing plant streams

Stream	Radioactive fission products which may be present
Off gases	^{3}H, ^{85}Kr, ^{125}Sb, ^{129}I, ^{131}I
Zircaloy hulls	^{3}H, traces of all FPs
Stainless steel hulls	Traces of all FPs
Fission product insolubles	$^{95}Zr/Nb$ (traces), ^{99}Tc, ^{103}Ru, $^{106}Ru/Rh$ ^{107}Pd
High-level waste	All non-volatile FPs
Medium- and low-level wastes	^{3}H, $^{95}Zr/Nb$, ^{103}Ru, $^{106}Ru/Rh$
U and Pu products	$^{95}Zr/Nb$, ^{99}Tc, ^{103}Ru, $^{106}Ru/Rh$
Fuel pond storage water	^{89}Sr, $^{90}Sr/Y$, ^{103}Ru, $^{106}Ru/Rh$, ^{134}Cs, $^{137}Cs/Ba$

Turning now to the heavy isotopes, the accuracy requirements for these is not as stringent as it is for the fission products. They have been summarised by Burstall in his review paper[9] to the Karlsruhe meeting on TND in 1975 as:

total decay heat ±20% and

total neutron emission ±20%

but as emphasised in his paper, much depends on the relative magnitude of the fission product effects to the heavy isotope effects. A further review[10] of the accuracy requirements for the heavy isotopes was given by Bouchard at the 2nd meeting on TND at Cadarache in 1979. This highlighted the need for accurate calculations for ^{232}U, ^{236}U, ^{237}Np, ^{236}Pu and ^{238}Pu in the context of uranium recycling. The paper concludes with a very large table summarising the accuracy requirements for the cross-sections and half-lives of nineteen heavy isotopes. I shall have more to say about some of these isotopes shortly.

Turning to the subject of the disposal of high level waste - as glass - into geological formations or into deep ocean sediments, here we are concerned wth a very different list of fission products and heavy isotopes whose half-lives are very long and which are important radiologically. The following list of radionuclides which are radiologically important in a variety of different disposal routes and scenarios was drawn up by the National Radiological Protection Board[11]:

^{79}Se, ^{90}Sr, ^{93}Zr, ^{99}Tc, ^{126}Sn, ^{129}I, ^{135}Cs, ^{137}Cs, ^{210}Po, ^{210}Pb, ^{225}Ra, ^{226}Ra, ^{229}Th, ^{237}Np, ^{238}Pu, ^{239}Pu, ^{240}Pu, ^{241}Pu, ^{242}Pu, ^{241}Am, ^{243}Am and ^{245}Cm.

No accuracy requirements have been stated explicitly, but owing to the other uncertainties associated with these assessments I think it is unlikely that an accuracy of better than ±20% (1σ) is justified.

So much for the accuracy requirements. I will now go on to give some examples of the use of nuclear data by the Company in some of the ten main contexts set out above.

4. Flowsheeting

In the course of designing a plant, a specimen flowsheet is first drawn up to achieve a particular purity in the main products (uranium and plutonium) coupled with minimum losses of uranium or plutonium in the process and minimum discharges of radioactivity to the environment. The design also has to conform with the very highest safety standards and must

also be easy to operate and to maintain. Because of the current interest in the recycling of uranium and plutonium, there is a strong interest in being able to predict the isotopic compositions of these products with good accuracy, particularly in respect to minor isotopes. I now propose to give an example of a minor isotope, ^{232}U, which I am currently working on and which has proved unexpectedly difficult to predict.

Fig. 2 shows the main production routes by which ^{232}U is formed in irradiated enriched oxide fuel. The two most important routes start at ^{230}Th and ^{231}Pa. Both these isotopes are believed to be absent from the

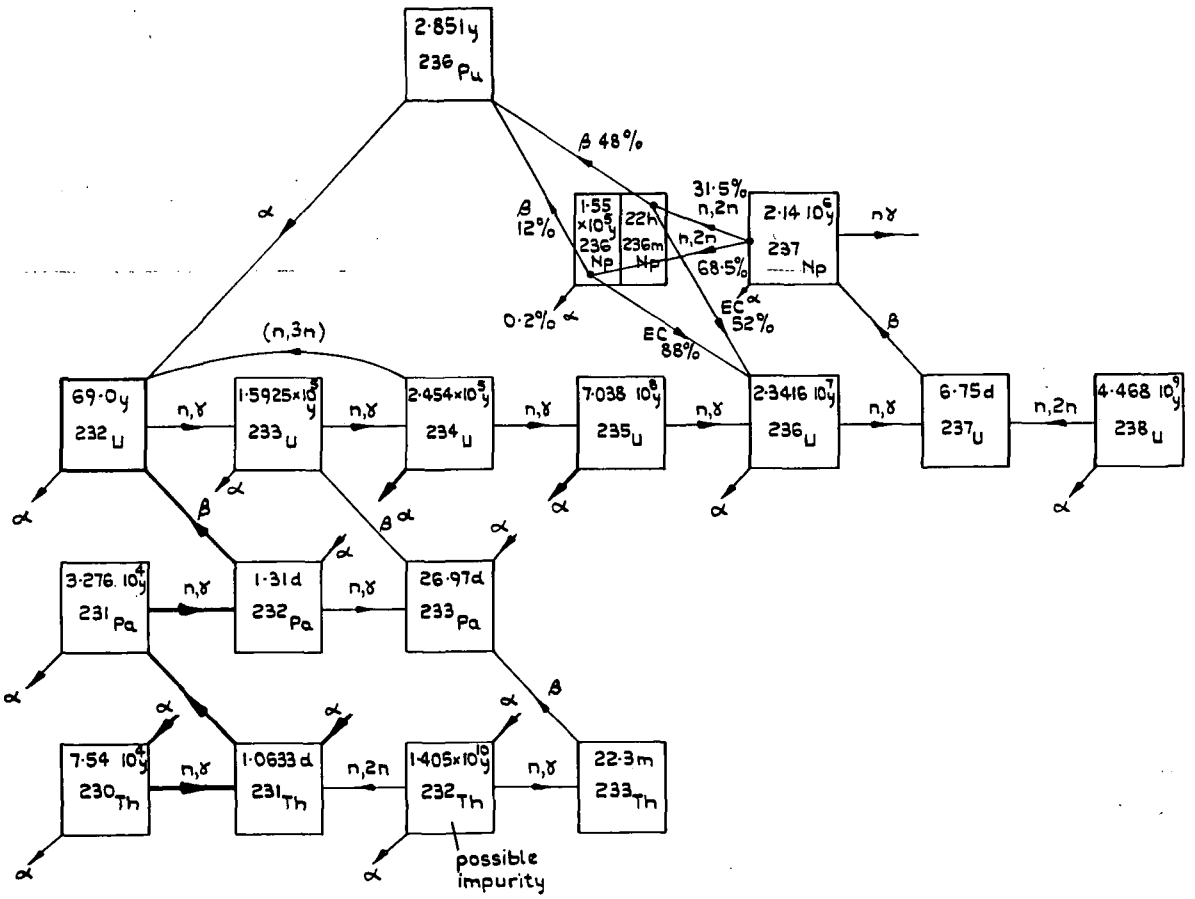

Fig. 2 The main routes for formation of ^{232}U. The two most important routes are shown with heavy lines

uranium immediately after volatilisation of the UF_6 prior to conversion to UO_2. After volatilisation these isotopes grow in linearly with time due to the decay of ^{234}U and ^{235}U respectively. Calculations of ^{232}U arisings using FISPIN for high burn-up PWR fuel (40 GWd/t) are given in Fig. 3. As can be seen, the ^{232}U is linearly dependent on the initial ^{234}U concentration in the fuel and on the storage time of the fuel prior to being irradiated.

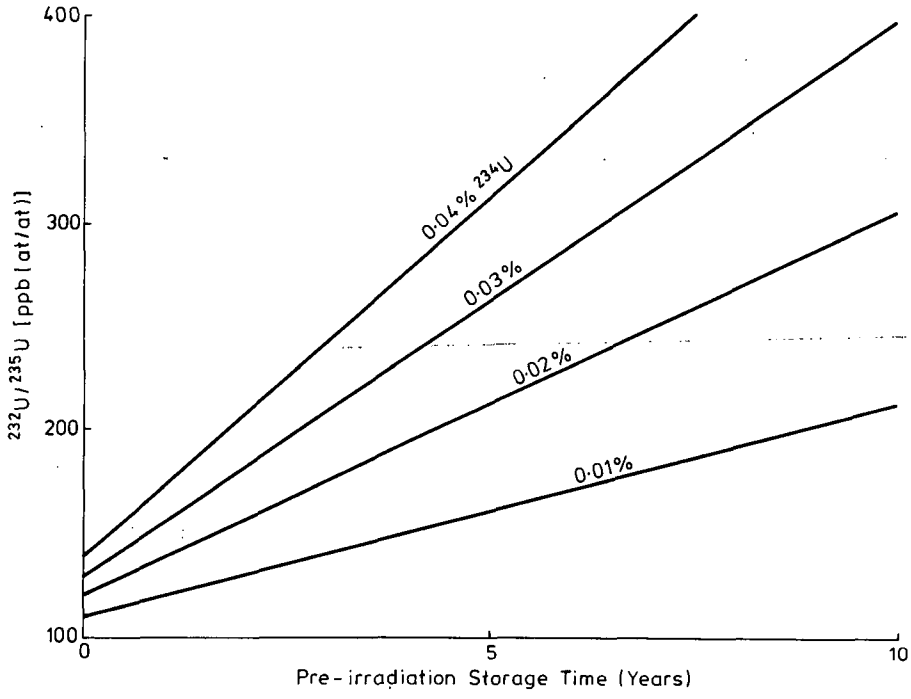

Fig. 3 Calculated $^{232}U/^{235}U$ ratios in PWR fuel (40 GWd/t at 40 MW/t) as a function of time for different initial ^{234}U concentrations in the fuel.

Because of the complexities of the routes for formation of ^{232}U, a programme of experimental measurement has been started to validate the calculations. Two validations have so far been performed and are summarised in the following table:

^{235}U (%)	Reactor	Irradiation (GWd/t)	Calc/Exp
3.4	Yankee Rowe (PWR)	28.1	0.33
2.79	Dodewaard (BWR)	31.7	0.52

Thus, in the case of Yankee Rowe fuel we appear to be undercalculating by a factor of 3, and in the case of Dodewaard fuel by a factor of 2. At the moment we do not know the reason for these discrepancies. It is possible that it is a nuclear data problem, though we are in fact using reasonably up-to-date cross-sections from BNL 325 (3rd edition) and I have no reason to suspect these. However there are grounds for believing that small amounts of ^{230}Th and ^{231}Pa could be introduced adventitiously during fuel manufacture and this is being looked into.

Other isotopes of importance in reprocessing are ^{14}C, ^{99}Tc and ^{129}I. ^{14}C is formed predominantly by neutron capture in nitrogen impurity in the fuel and by (n,α) reactions on the oxygen in the fuel. It is important biologically because of its long half-life (5730 y) and because carbon is a major constituent of all living organisms. Consequently, discharges to atmosphere (e.g. in the form of $^{14}CO_2$ or $^{14}CH_4$) must be closely controlled[12]. At the present time there are considerable uncertainties about the amounts of ^{14}C that will be formed in oxide fuel, due mainly to uncertainties in the nitrogen levels in customers' fuels from all parts of the world. For flowsheeting purposes it is therefore necessary to take the maximum credible values for the nitrogen impurity levels and to design the scrubbing systems to deal with this maximum level.

^{99}Tc is a fission product whose chemistry is such that it can have an important effect on the operation of THORP.

Finally ^{129}I is a fission product which is important environmentally because of its long half-life (1.57×10^7 y) and because of pathways leading back to man[12]. Discharges of this isotope to the atmosphere must therefore be very closely controlled and monitored. However the accuracy with which the fission yield of this isotope is known leaves a good deal to be desired as is evidenced by the large discrepancies between the evaluation of Crouch[13] and that of Rider and Meek[14] shown in the following table[15]:

Fissile Species	^{129}I Fission Yield (%)		R and M / C
	Crouch	Rider and Meek	
^{235}U (thermal)	0.574	0.705	1.23
^{239}Pu (thermal)	1.54	1.50	0.97
^{241}Pu (thermal)	0.937	0.756	0.81
^{238}U (fast)	0.260	1.003	3.86
Mean for PWR	0.831	0.946	1.14

Apart from one very old measurement, the fission yield of ^{129}I has never been measured directly and its fission yield has therefore had to be inferred from that of its precursors using theoretical fractional independent yields and branching ratios. In the particular case of ^{241}Pu no measurements for the 129 mass chain exist at all and it is therefore necessary to infer its yield from the chain yields of adjacent chains. The yield of ^{129}I is therefore predicted with a relatively poor accuracy of the order of $\pm 25\%$ ($1\ \sigma$) which worsens rapidly with increasing burn-up.

These are just a few examples of where accurate predictions are of importance to the Company in its planning of operations.

5. Process Control

A special computer program for calculating the ^{242}Cm content of fuel discharged from the Magnox stations has been written recently and is currently undergoing testing. This datum is required by the reprocessing plant operator in order to give advanced warning of the occurrence of high alpha activity in the solvent of stage 13 of the first mixer settler. Without it, the detection of high alpha activity here must be taken as evidence of maloperation, and the plant must be shut down. It would be too expensive and too slow to run a code such as FISPIN for every batch of fuel discharged, and therefore a simplified analytical solution[16] has been employed. This simplified solution provides a rapid means of predicting the build-up of ^{242}Cm during a complex irradiation history which involves many shutdowns and power variations. The calculations are written into a number of FORTRAN subroutines which can easily be incorporated into other computer programs which contain, or which are able to extract, the necessary irradiation histories. The route for formation of ^{242}Cm from ^{241}Pu is illustrated in Fig. 4.

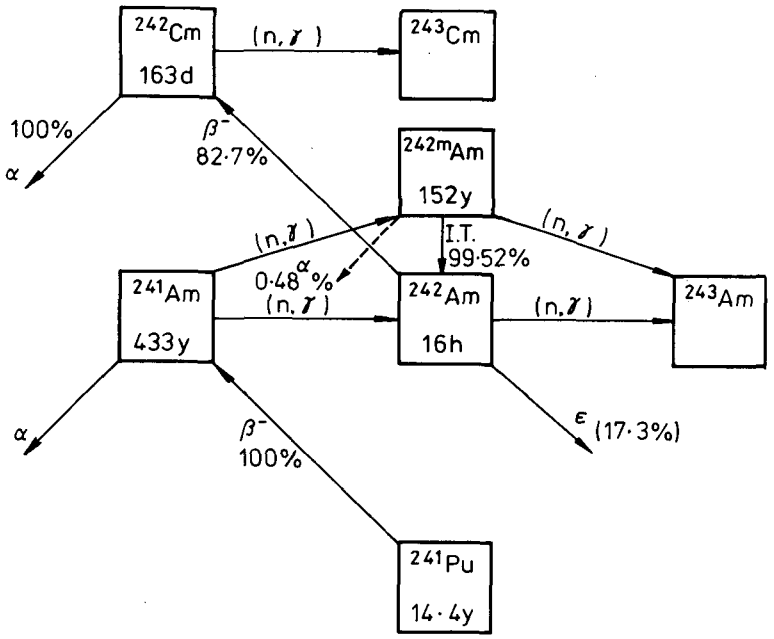

Fig. 4 Routes for the formation of ^{242}Cm

This code has now been validated against experimental data for seven fuel specimens from the Dungeness Magnox station and the following table lists the separate C/E values:

Irradiation (MWd/t)	Calc / Exp
2318	0.72
2520	0.60
5111	0.79
5120	0.69
6497	0.68
6551	0.76
7135	0.73
Mean	0.71

From this table it is apparent that the code undercalculates the ^{242}Cm

concentration by about 30%. Nair of the CEGB has also observed similar C/E values using the code RICE and has suggested that the capture cross-section of ^{241}Pu may have been set too high, or the capture cross-sections of ^{239}Pu, ^{240}Pu and ^{241}Am may have been set too low[17]. However, in our case it is most unlikely that the capture cross-sections of ^{239}Pu, ^{240}Pu and ^{241}Pu are seriously in error since these are derived from WIMS calculations, and therefore it is more likely that it is the capture cross-section of ^{241}Am which is in error.

6. Shielding Calculations

The Company has a large section at the Risley headquarters which specialises in shielding calculations. The code FISPIN is used extensively to provide fission product, activation product and heavy isotope inventories and gamma ray emission rates, but the ORIGEN code is also used occasionally, mainly to check the FISPIN code. Various US and UK shielding codes are used by the Shielding Section to model particular plant configurations for design purposes.

There is a distinct lack of information in the following areas:

(a) neutron flux and spectra for particular fuel components (e.g. grids, end-pieces),

(b) cobalt impurity levels for particular fuel components (e.g. various grades of stainless steel and inconel),

(c) gamma build-up factors for particular materials (e.g. barytes concrete, super shot concrete),

(d) production of secondary gamma rays in the shielding code MACBEND, and

(e) position of the 10 rem boundary in criticality incidents.

Referring to the latter problem, the 10 rem boundary in a hypothetical criticality incident is not crucial, but it is useful to know. If it lies within the building this is acceptable, if it lies outside the building this is less satisfactory, and if it lies outside the perimeter fence this is unacceptable. The recent update in the FISPIN decay data library to include a much larger number of short-lived fission products and their associated gamma rays has had a big effect on the gamma ray emission rates at times of the order of minutes after the incident, and this has caused a change in the 10 rem contour. Therefore the thickness of concrete used in future buildings may need to be increased to control the 10 rem contour. This is clearly an area where nuclear data is important and can affect the cost of construction of the Company's plants.

A study has been made recently at Sellafield to estimate the probable savings in the cost of building a new reprocessing plant in the early part of the 21st century which would be dedicated to the reprocessing of long cooled fuel[18]. For this study, cooling times of 30 and 50 years were taken and a rough estimate of the probable savings in concrete were made using the code FISPIN. These calculations, which are summarised in the following table,

Thickness of concrete for different cooling time to give the same transmitted gamma ray dose rate (3.6% PWR at 40 GWd/t)

Group	Energy range (MeV)	Percentage of total transmitted gamma ray dose rate		
		5 y	30 y	50 y
1	0.390 - 0.635	0.06	0.01	0.00
2	0.630 - 0.880	3.20	71.64	88.00
3	0.880 - 1.275	3.20	13.45	4.83
4	1.275 - 1.875	41.09	13.73	4.40
5	1.875 - 2.350	40.18	1.15	1.70
6	2.350 - 2.700	7.45	0.06	0.07
7	2.700 - 3.200	4.11	0.00	0.00
8	3.200 - 4.000	0.22	0.00	0.00
Shield thickness (cm)		150	122.6	118.2

indicate that savings of the order of 20% are possible. This, although not an over-riding consideration, is certainly useful. The longer cooling means that certain isotopes, such as ^{106}Ru, ^{144}Ce and ^{144}Pr, have decayed away completely and this means that extra shielding is no longer required to absorb their relatively high energy gamma rays (in groups 4-8).

7. Instrumental Measurements on Irradiated Fuel

There is a great deal of interest within the Company in designing instruments to measure non-destructively certain properties of irradiated fuel such as burn-up, cooling time and enrichment, since the information supplied by the reactor operator may need to be checked for criticality or operational purposes. Fox of the R&D Department at Sellafield has made a systematic search for fission product ratios which are sensitive to irradiation and independent of other parameters, and has discovered the following relationship:

$$\text{Irradiation} \propto \frac{(^{137}Cs) \times (^{106}Ru)}{(^{134}Cs)^2}$$

This is almost independent of cooling time and only slightly dependent on reactor rating. Barnes of the Nuclear Data Section at Sellafield has suggested that this ratio can be improved in certain respects by raising the activities of the individual isotopes to non-integer powers as follows:

$$\text{Irradiation} \propto \frac{(^{137}Cs)^{0.3162} \times (^{106}Ru)^{0.2793}}{(^{134}Cs)^{0.5955}}$$

This ratio is completely independent of cooling time and is plotted in Fig. 5 as a function of irradiation for Magnox fuel. Barnes has also shown how the technique can be applied generally to any number of isotopes (greater than two) in such a way as to minimise perturbations from unwanted properties. Several other isotope ratios look promising and are being studied. These ratios are likely to be very useful to us for checking the burn-up of oxide fuel fed to THORP.

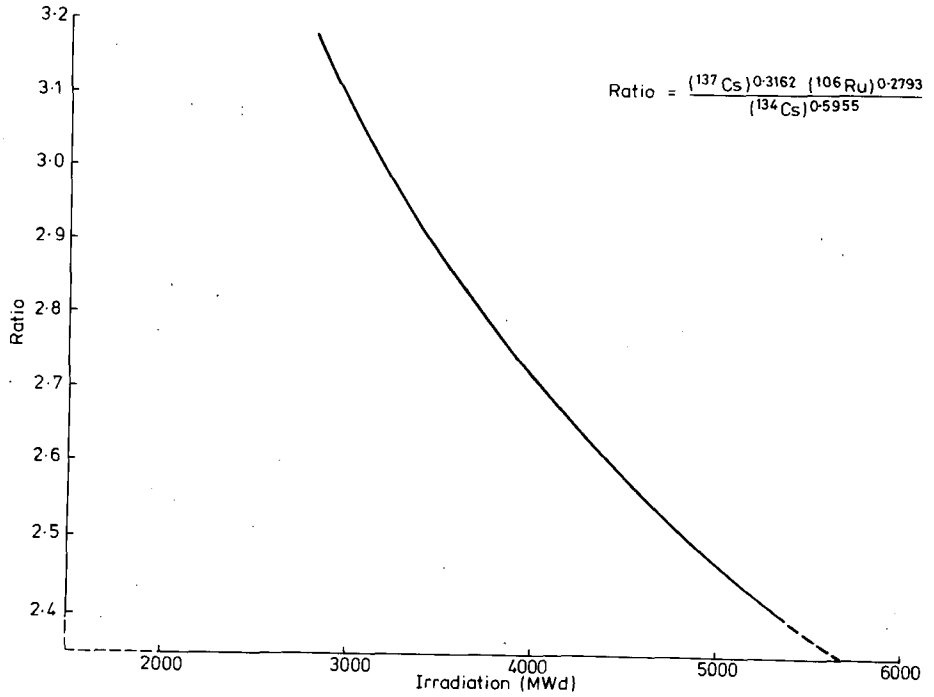

Fig. 5 The Barnes ratio for Magnox fuel

An entirely different approach for determining the properties of irradiated fuel by a least-squares technique has also been studied theoretically by Barnes. The basis of the idea is quite simple. Firstly the activities of a number of fission products in a sample are measured, and then each is expressed as a fraction of the total activity. In a similar manner, fractional activities for these same fission products are calculated at zero cooling time for a wide range of irradiation parameters (burn-up, rating, enrichment etc.). It is then a simple non-linear least-squares problem to obtain that cooling time, which when applied to a given set of calculated fractional activities, will give a best fit to the measured fractional activities. The cooling time and the χ^2 goodness-of-fit parameter are then recorded. The next set of calculated fractional activities is then taken and the cycle repeated. Thus 'best-fit' values of cooling time and χ^2 are evaluated for all combinations of irradiation parameters. The result is a multi-dimensional χ^2 space and the most appropriate set of properties are those giving the minimum value of χ^2 in this space. In the case of Magnox fuel, only irradiation and rating need to be taken into account and a two-dimensional plot of χ^2 is sufficient. Fig. 6 shows such a plot where a minimum is clearly shown at an irradiation of 5250 MWd/t and a rating of 2.75 MW/t.

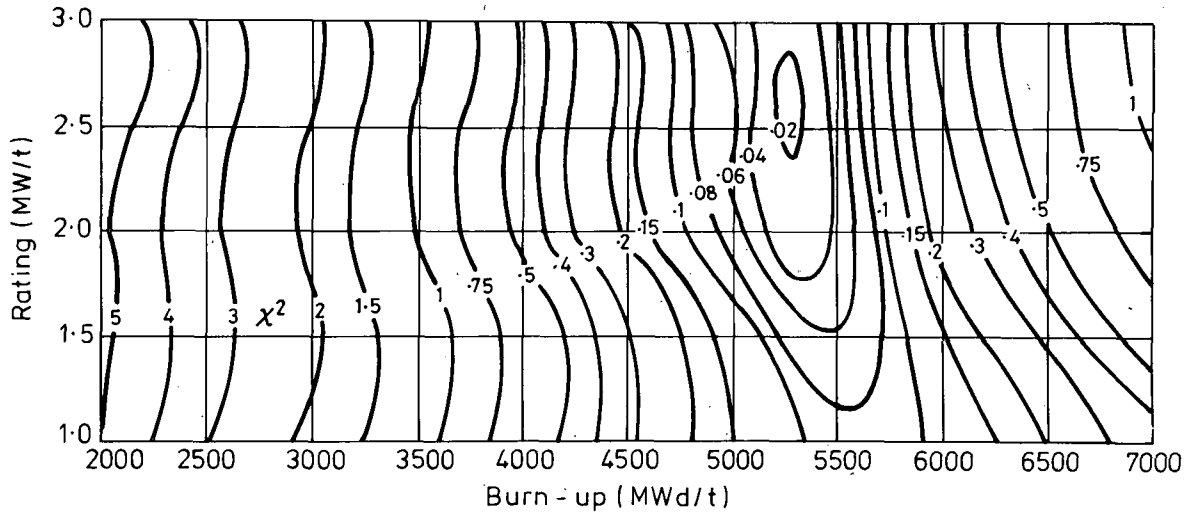

Fig. 6 Two-dimensional χ^2 plot for a Magnox fuel specimen

Comparing and contrasting the least-squares method to the ratio method, one can say that the least-squares method has the advantage that any number of isotopes can be used and it automatically estimates all the unknown irradiation parameters simultaneously, but it has the disadvantage that it is totally dependent on accurate nuclear data. The ratio method, on the other hand, need not be dependent on nuclear data since it can be calibrated by direct measurement with fuel of known irradiation history.

8. Research and Development

The Research and Development Department at Sellafield makes a great deal of use of nuclear data in the course of its work. Sometimes these uses are unusual and the nuclear data obscure. One such example was the calculation of the activity of short lived iodine isotopes in the aerial effluent from Highly Active Storage Tanks associated with THORP. This work followed from reports that traces of ^{131}I (8 day half-life) had been detected in the aerial emissions from long cooled highly active waste from the German WAK plant. The most probable source of this activity in high burn-up oxide fuel is from the spontaneous fission of the higher actinides, particularly the curium isotopes. Calculations using FISPIN revealed that the spontaneous fission rate from highly active waste derived from reprocessing 3.2% enriched PWR fuel (irradiated to 40 GWd/t) was dominated by the two isotopes ^{244}Cm and ^{246}Cm.

The following table gives the calculated equilibrium activity of four short lived iodine isotopes (^{131}I, ^{132}I, ^{133}I and ^{135}I) which would be present in the highly active waste resulting from reprocessing 8000 tonnes of such fuel:

Iodine activities produced by spontaneous fission in highly active storage tanks associated with THORP (8000 t of PWR fuel)

Cooling (years)	Isotope activities (curies)						
	5	10	25	50	100	500	1000
^{131}I	1.65	1.37	0.77	0.30	0.05	0.01	0.01
^{132}I	2.29	1.89	1.07	0.42	0.08	0.01	0.01
^{133}I	2.83	2.34	1.33	0.52	0.09	0.02	0.02
^{135}I	3.07	2.54	1.44	0.57	0.10	0.02	0.02

This calculation would not have been possible had not spontaneous fission yields for ^{244}Cm and ^{246}Cm been published recently[19]. These activities, although significant, are quite small in relation to the total amount of long-lived ^{129}I activity still remaining in the highly active waste which would be of the order of 280 Ci.

9. Safeguards and Accountancy

Because of the decay of 14 y ^{241}Pu to ^{241}Am there is a steady loss of elemental plutonium from stored plutonium. To attempt to make this correction by direct analysis would be extremely expensive and is out of the question on the grounds of radioactive contamination and exposure. Therefore this correction must be made theoretically using the best figure for the half-life of ^{241}Pu.

Using the recommended value of 14.4 years from the latest evaluation of Nichols and James[20] results in a total loss of about 8 kg per tonne being calculated since manufacture. Because of the comparatively large uncertainty in this half-life of ±3.4% (1 σ), or roughly ±0.5 years, there is a corresponding uncertainty in the loss of about ±200 g per tonne. The IAEA Safeguards Inspectors and our accountants regard this uncertainty as rather unsatisfactory and would like it reduced.

I hope that these few examples have conveyed, at least in general terms, the extensive use of nuclear data within the various phases of our activities within BNFL, and have indicated those areas where there is a need for improvements in the basic data.

---

(1) Minutes of a Meeting to Discuss Linking WIMS and FISPIN - IMAC/P(83)126, (Dec. 1983).

(2) J.L. Rowlands and R.W. Smith - AEEW-M 2015 (Feb. 1983).

(3) I.H. Gibson - AEEW-M 1299 (Dec. 1974).

(4) W. Aylen, C.J. Dean and J.L. Rowlands - AEEW-M 1379 (Mar. 1976).

(5) G. Reddell - AEEW-R 1193 (June 1978).

(6) E. Merz and M. Laser - IAEA-169 Vol. 1, p 213 (1974).

(7) R. Castaign - Report of the Working Group on 'Spent Fuel Management'. Supreme Council for Nuclear Safety, Paris, (1 Dec. 1982).

(8) H.A.C. McKay - IAEA-213 Vol. 1, p 91 (1978).

(9) R.F. Burstall - IAEA-186 Vol. 1, p 175 (1976).

(10) J. Bouchard - IAEA-TECDOC-232, p 1 (1980).

(11) I.F. White - IMAC/P(80)74 (1980).

(12) G.N. Kelly, J.A. Jones, P.M. Bryant and F. Morley - CEC Report V/2676/75 (1975).

(13) E.A.C. Crouch - Atomic Data Nucl. Data Tables 19 (1977) 419.

(14) B.F. Rider and M.E. Meek - NEDO-12154-2 (1977).

(15) H.A.C. McKay, P. Miquel and I.F. White - unpublished information.

(16) V. Barnes and P. Little - Internal BNFL Report (to be published).

(17) S. Nair - CEGB Report RD/B/N4349 (Aug. 1978).

(18) P.C. Davidge, A. Whittaker, W.P. Holland and J.Y. Martin - Internal BNFL Report (to be published).

(19) J.E. Gindler - J. Inorg. Nucl. Chem. 43 (1981) 895.

(20) A.L. Nichols and M.F. James - AEEW-R 1407 (Dec. 1981).

Element Z	A	Quantity	Type	Energy (eV) min	max	UKNDC (84)P111 (May 84) page no.	Lab	Comments
Li	6	(n,t)	expt,prog				BIR	Naylor+ t prod in fusion blanket
Li	7	(n,t)	" "				BIR	Naylor+ t prod in fusion blanket
Li	7	(n,n't)	" "	4.6 +6	14.1+6		HAR	Swinhoe mult scatt corr recalculated
Cu	65	(n,2n)	" "	13.7+6	14.8+6		NPL	Winkler+ Ann Nucl Energy 10 601
Nb	93	inelastic γ	" "	1.1 +6	2.1 +6		HAR	Gaythert+ meas + anal continuing
In	nat	n scat spec	" "	2.5 +6			EDG	Erduran+ en spec scat neuts
In	113	(n,2n)	" "	14 +6	18 +6		NPL	Ryves+ J Phys G 9 1549
In	113	inelastic γ	" "	14 +6	18 +6		NPL	Ryves+ " " "
In	115	inelastic γ	" "	14 +6	18 +6		NPL	Ryves+ " " "
In	115	(n,p)	" "	14 +6	18 +6		NPL	Ryves+ " " "
In	115	(n,α)		14 +6	18 +6		NPL	Ryves+ " " "
In	115	(n,2n)	" "	14 +6	18 +6		NPL	Ryves+ " " "
Sn	nat	n scat spec	" "	2.5 +6			EDG	Erduran+ en spec scat neuts
I	127	n scat spec	" "	2.5 +6			EDG	Erduran+ en spec scat neuts
Eu	152	half life	" "				NPL	Christmas+ prov res 4934±4 d
Eu	154	half life	" "				NPL	Christmas+ prov res 3138±6 d
Hg	nat	n scat spec	" "	2.5 +6			EDG	Erduran+ en spec scat neuts
Bi	209	n scat spec	" "	2.5 +6			EDG	Erduran+ en spec scat neuts
Th	232	diff inelas	theo				OXF	Hodgson+ calc inelas scat xsec
U	235	delayed n	expt,prog	1.5 +6	7.4 +6		BIR	Owen+ del neut spec from thick target using Be(d,n)
U	238	diff inelas	theo				OXF	Hodgson+ calc inelas scat xsec
Np	235	decay data	expt,prog				HAR	Whittaker+ intens K + L X-rays
Np	235	α decay	" "				HAR	Whittaker meas α branch decay
Np	235	half life	" "				HAR	Whittaker prov res 385±4 d
Pu	237	half life	" "				HAR	Whittaker meas continuing
Am	241	(n,γ)	" "	fast			HAR	Wiltshire+ activ in ZEBRA core
Am	241	(n,γ)	" "	fast			HAR	Wiltshire+ activ in PFR core
Am	243	(n,γ)	" "	fast			HAR	Wiltshire+ activ in ZEBRA core
Am	243	(n,γ)	" "	fast			HAR	Wiltshire+ activ in PFR core
Cm	242	half life	" "				HAR	Wiltshire 163.03±.16 d fiss half life meas planned

1. NUCLEAR PHYSICS DIVISION, AERE, HARWELL

(Division head: Dr. J.E. Lynn)

Introduction

Nuclear data measurements in Nuclear Physics Division are diverse and are performed on a variety of sources. Individual research items are labelled with a single letter indicating on which accelerator the experiments were performed. These labels are as follows:

Cockcroft-Walton Generator	A
3 MV pulsed Van de Graaff Generator IBIS	B
6 MV Van de Graaff Generator	C
14 MV Tandem Generator	D
136 MeV Electron Linear Accelerator	E
Variable Energy Cyclotron	G
500 kV Van de Graaff	I

In the contents pages there is a reference to the accelerator on which a measurement was made.

The material for this contribution is taken from the chapter on Nuclear Data and Technology for Nuclear Power in the 1983 Nuclear Physics Division Progress Report AERE PR/NP 31.

1.1E HELIOS - The new machine for the electron linac laboratory (J.E.Lynn, M.S. Coates, B.P. Clear, J. Down, R.A.J. Riddle and P.W. Swinden)

Experimental operation has continued successfully on the Fast Neutron, Low Energy, and Condensed Matter Cells of the Harwell electron linear accelerator HELIOS. The contracted beam time for the joint Harwell/SERC programme on the Condensed Matter Cell has been provided, with extended runs at the maximum beam power of 45 kW.

The operational programme was interrupted for ~3½ months to allow the Litton klystron (UKNDC(82)P105, p.25) to be installed and tested by Radiation Dynamics Ltd. They met unexpected technical difficulties during the work, connected firstly with matching the new klystron impedance with the existing modulator pulse forming networks, and secondly with the new SF_6 circulation system needed for the waveguide arrangement that links the klystron to the linac itself. Although the linac is fully operational again some further modification work is still necessary in these areas.

The Neutron Booster Cell has been commissioned following the rectification of the faults reported previously (UKNDC(82)P105, p.24). However, an unrelated fault in the coils of an important steering magnet prevented optimisation of the electron beam transport conditions. Nevertheless a neutron pulse brightness nearly three-quarters of that expected was observed, and we expect to achieve full performance when the faulty magnet element is replaced.

Significant progress has been made with the pulsed magnet system (UKNDC(79)P94, p.27) needed for simultaneous (multiplexed) cell operation. Following extensive modifications to improve reliability and cooling, a pulsed magnet recently has been excited off-line at 50 pps to produce the field needed to steer a 100 MeV electron beam. It is expected that the required operating conditions needed to steer a 150 pps 120 MeV electron beam will be demonstrated shortly. A new type of magnet box made from silicon carbide (REFEL) has been successfully developed in conjunction with Springfields Nuclear Laboratories. The material has sufficiently low conductivity to restrict eddy current losses to an acceptable level but has a high enough value to allow any stray electric charge accumulated during operation to leak away safely. The problem of producing vacuum seals for the box has been solved, and the box is expected to be installed into the electron beam line shortly. We hope to test the whole pulsed magnet system on-line during 1984.

The design of the new accelerator section (UKNDC(83)P109, p.37) has been completed and manufacture has started.

1.2E Background investigations on a neutron transmission spectrometer (M.C. Moxon, A.G. Clare (University of Reading), J.B. Brisland and A.P. Guntrip

A neutron transmission time-of-flight spectrometer has been set up on the Condensed Matter Cell of the Harwell electron linear accelerator HELIOS to obtain total cross-sections needed for the interpretation of solid state and nuclear physics experiments. There are two measurement positions 8.7 and 15 m from the target. The detectors are lithium glass scintillators, 1 mm thick, 75 mm dia. at 8.7 m, 3 mm thick, 130 mm dia. at 15 m. Both scintillators are viewed edge-on by single 5" EMI 9823QB photomultipliers with aluminium foil reflectors surrounding the scintillators. The 8.7 m detector acts as an overlap filter for the 15 m detector. The edge-on configuration means that the photomultipliers are placed out of the neutron beam thus reducing the effect of scattered neutrons on detector resolution and background.

A number of measurements have been carried out during the last year to study background effects, using Co, Hf and Gd samples to provide 'black' resonances. The first measurements were made in December 1982 using conventional 2000 series electronics. The signal-to-background ratios observed in the minimum of the 'black' resonances for the 8.7 m detector in the energy region below 10 eV were several hundred to one, but those for the 15 m detector were poorer with backgrounds of 20% at 8 eV and 17% at 1 eV relative to the neutron counts being observed. Measurements on graphite and silica samples gave cross-sections in good agreement wth recommended values for both detectors.

Several modifications to the shielding of both detectors were carried out prior to the next runs in April-May 1983. The 8.7 m detector shield was lined with boroflex, which reduced the machine-dependent background by a factor of 1.5 in the energy region below 10 eV, and improvements to the bulk shielding around the 15 m detector reduced the background to 15% at 8 eV and 8% at 1 eV.

During the course of these runs we noticed, while carrying out electronic dead-time measurements, that some of the detector pulses were very much shorter (~10-20 nsec duration) than the characteristic pulses

(~120 nsec duration) produced by the charged particles from the $^{6}Li(n,\alpha)t$ reaction. Measurements with radioactive sources indicated that the short pulses were gamma-ray induced, which suggested the use of the pulse shape discrimination (PSD) technique[1,2], normally used with organic scintillators, as a means to further improve the signal-to-background ratios. A PSD unit* was used with the 1 mm thick detector at 8.7 m, and this resulted in an improvement of a factor of two in the signal-to-background ratios, with a clean separation between neutron and gamma-ray events. Before a later run in August 1983 a second PSD unit was installed for use with the 3 mm thick detector at 15 m. Although the discrimination between neutrons and gamma-rays is not as clear-cut as with the 1 mm detector, a dramatic improvement in the neutron signal-to-background ratio was observed, as demonstrated in Fig. 1.1 and Table 1.1. The differences in the shapes of the time-of-flight spectra for the neutron and gamma-ray channels of the PSD unit suggest that much of the background at the 15 m position is due to gamma-rays produced when scattered neutrons from the detector are captured in the surrounding shield materials. These investigations will continue. At this stage we are not certain of the

Table 1.1

Normalised counts at different energies observed in background measurements using PSD equipment

		8 m detector				15 m detector			
		n chan.	γ chan.	n chan.	γ chan.	n chan.	γ chan.	n chan.	γ chan.
'Black' resonance		No sample (open beam)		Sample+ (filtered beam)		No sample (open beam)		Sample+ (filtered beam)	
Energy (eV)	Nucleus								
130	Co	1393	7.0	50.0	6.1	989	801	120	439
8	Hf	1219	0.52	3.2	0.37	686	550	3.9	166
2	Hf	1130	0.19	1.9	0.22	557	437	1.9	107
1	Hf	1082	0.14	0.62	0.067	386	403	0.81	60
0.05	Gd*	0.022	0.045	0.020	0.037	0.16	16.0	0.12	7.0

*Overlap filter permanently in neutron beam
+3 mm Co + 5 mm Hf; counts tabulated are in minimum of 'black' resonances

*Designed by G.S. White of Harwell's Instrumentation and Applied Physics Division.

mechanism which gives rise to the gamma-ray induced short pulses, but it seems likely that they are produced by Cerenkov radiation from electrons.

---

(1) F.D. Brooks, Prog. Nucl. Phys. 5 (1956) 252.

(2) R.B. Owen, IRE Trans. Nucl. Sci. NS-5 (1958) 198.

1.3 Work related to the NEANDC task force investigating the discrepant resonance parameters in ^{238}U above 1.15 keV (D.B. Syme and M.C. Moxon) (WRENDA 1067-1069)

Under the auspices of the NEANDC task force investigating the discrepancies in the resolved resonance parameters of ^{238}U above 1.15 keV, we have concentrated on an analysis of the published ORNL data[1] as the most completely documented and potentially accurate available data set. Our purpose has been to confirm the resonance parameter values derived by ORNL themselves[2], but using a different shape analysis code. The Harwell shape analysis code REFIT[3] has the advantage of an extremely detailed and flexible input for the background and resolution parameters important for proper analysis in this region.

This work has proceeded with emphasis on the 1.45 - 1.76 keV region where we have attempted to reproduce the fits obtained by the ORNL code SIOB using our initial evaluation of the ORNL resolution function. We found that the ORNL resonance parameters (not the same as the UK evaluated file, the ORNL ones are all s-wave) fitted the data for all four measured samples reasonably, but not exactly, the largest discrepancies being near the resonance bottoms of the three thick samples. This may have been partially because we used our own detailed evaluation of the ORNL resolution function, rather than the quite different mathematical approximation actually used in SIOB to obtain the original fits. We have since spent considerable time understanding and reproducing that approximation in REFIT subroutines.

Several generations of resolution function have been used by ORNL themselves[4] and we have pointed out how this has added inconsistency to the resonance parameters previously extracted. We have compared the common approximations made to the resolution functions with the proper convolution of their measured components and it is clear that in some cases severe systematic errors can be introduced into the resonance parameters by adoption of an insufficiently complete approximation. We are now in the process of separately analysing the 1.45 - 1.76 keV region with the ORNL resolution function approximation and with what we believe to be its more exact form, in order to establish whether there is any significant systematic error from this source.

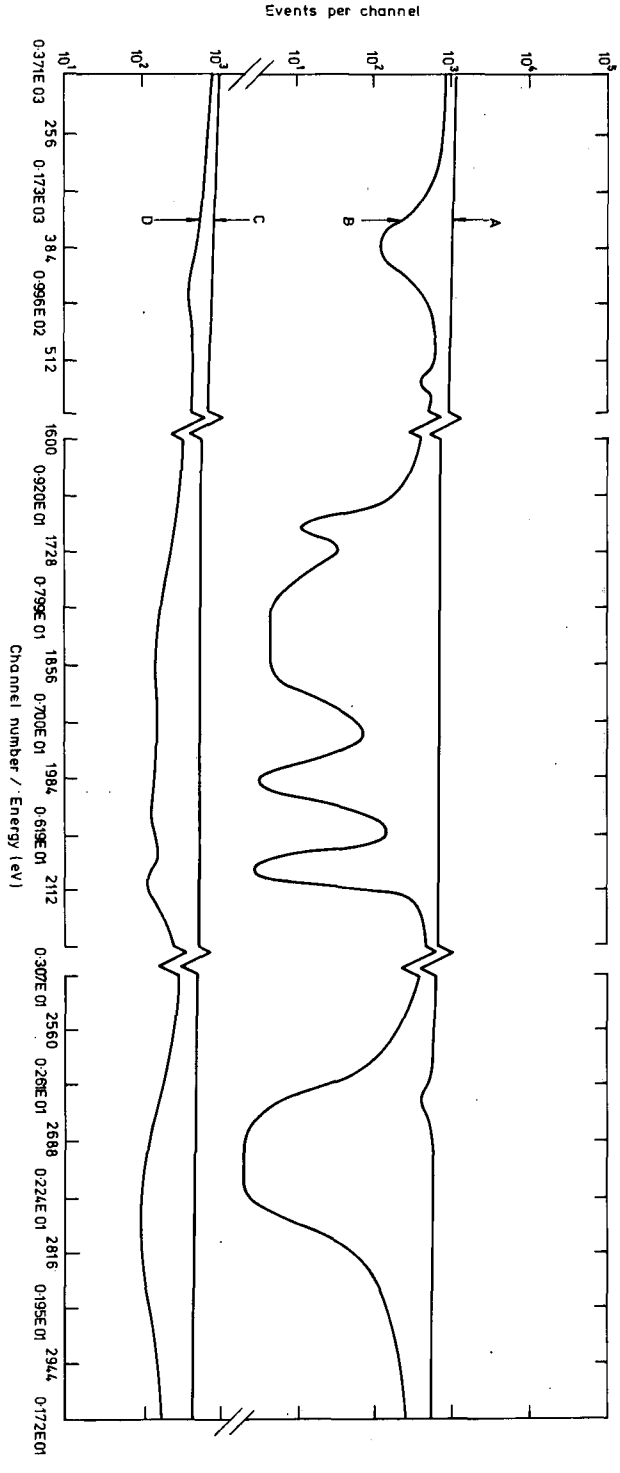

Fig. 1.1 The observed count rate from a lithium glass scintillator using the pulse shape discriminator (PSD) unit for:

A open beam data from the neutron channel of the PSD unit;

B filtered beam data from the neutron channel of the PSD unit (filters are Co (~130 eV) and Hf (~8, ~6, ~5 and 2.3 eV);

C open beam data from the gamma-ray channel of the PSD unit; and

D filtered beam data from the gamma-ray channel of the PSD unit.

It has become clear through this work that there has been insufficient documentation in the literature of the main components of the resolution function in most neutron time-of-flight measurements of nuclear data. This was the subject of a paper given at the 1983 Vienna Consultants' Meeting on Nuclear Data for Structural Materials[5]. Some of the work described elsewhere in this report is intended to improve the knowledge of the resolution function for experiments on HELIOS.

---

(1) D.K. Olsen, G. de Saussure, R.B. Perez, F.C. Difillipo, R.W. Ingle and H. Weaver, Nucl. Sci. Eng. 69 (1979) 202.

(2) Ref. 1, ibid, also private communications between task force members.

(3) M.C. Moxon, Proc. Spec. Meeting on Nucl. Data of Struct. Materials for Fast Reactors, Geel (1977) 644.

(4) Ref. 1, ibid, also D.K. Olsen and P.S. Meszaros, Nucl. Sci. Eng. 83 (1983) 174.

(5) M.C. Moxon and D.B. Syme, 'Neutron resolution functions', Proc. Consultants' Meeting on Nucl. Data for the Struct. Materials, IAEA, Vienna, Nov. 1983, in course of publication.

1.4 E Measurements of the performance of the Fast Neutron Target of HELIOS (D.B. Syme, G.D. James and A.D. Gadd)

Last year we described a series of measurements of various characteristics of the pulsed neutron beams from the Fast Neutron Target (FNT) of the Harwell electron linear accelerator HELIOS (UKNDC(83)P109, p.39). We have since extended these measurements to examine in more detail the spectrum shape, some of the backgrounds and the target resolution function.

(1) Neutron spectrum

Measurements of the neutron spectrum shape have been made for neutron beams from both the central region and the exterior regions of the FNT. Neutrons from the central region had a harder energy spectrum as expected for the source of fast neutrons, while neutrons from the exterior regions had a softer spectrum consistent with their role as a surrounding moderator. The analysis is not yet complete.

Resonance absorption from the tantalum plates in the centre of the target was expected to become obvious for the highest resolution experiments at low energies. This has been observed, and the resonant structure

confirmed as characteristic of tantalum (Fig. 1.2). With increasing energy the structure reduces and essentially disappears by about 8 keV because of increasing resonance overlap and deteriorating resolution. Future experiments below 20 keV will use a separate polythene moderator adjacent to the target thereby removing the resonant structure from the spectrum, and simultaneously improving the resolution (UKNDC(83)P109, p.40). Low energy neutrons are removed by the moderator which has a transmission of less than 0.001 below 20 keV, while the intense high energy neutron burst from the target is moderated to regenerate fresh low energy neutrons. The time resolution is improved since neutrons slow down most rapidly in hydrogen and there is obviously no tantalum to introduce structure. The moderator and its support structure have been designed and fabricated and will shortly be installed.

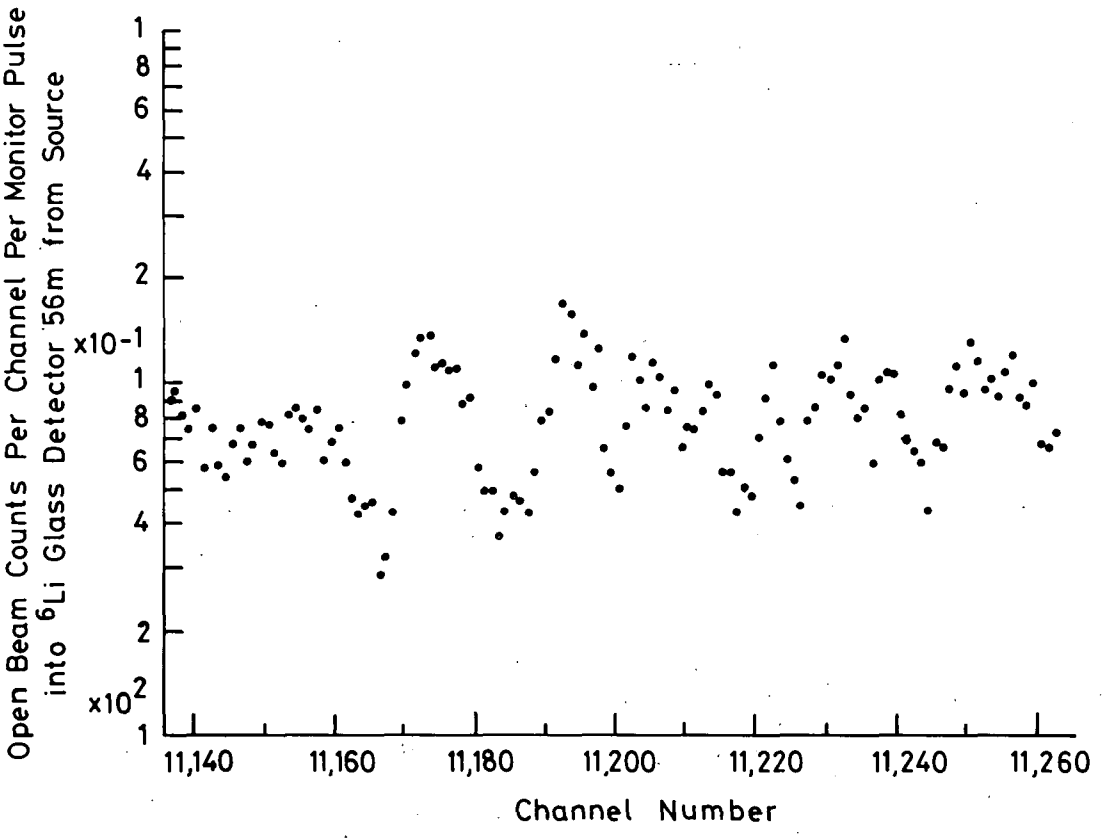

Fig. 1.2 Partial neutron time-of-flight spectrum in the low keV region from the HELIOS FNT. The structure is due to scattering from resonances in the Ta target plates and was measured by a ^{6}Li glass neutron detector 56 m from the source.

(2) Backgrounds

The results of measurements of neutron backgrounds in the fast neutron flux above 100 keV were described in UKNDC(83)P109, p.42. We have since measured the backgrounds due to accelerator dark current and those from neutron capture gamma rays generated in the FNT itself. Preliminary measurements with notch filters indicate that backgrounds due to out-of-time neutrons are less than 3.5% below 60 keV.

The background due to accelerator dark current was measured with the electron gun pulser turned off then on. The time-of-flight spectra obtained by a detector in the flight path in the two cases are shown in Fig. 1.3. The wide rectangular distribution is the shape of the r.f. pulse in the accelerator, made visible due to the stray electrons (dark current) present even when the gun is not pulsed. When the gun is on, a strong pulse of

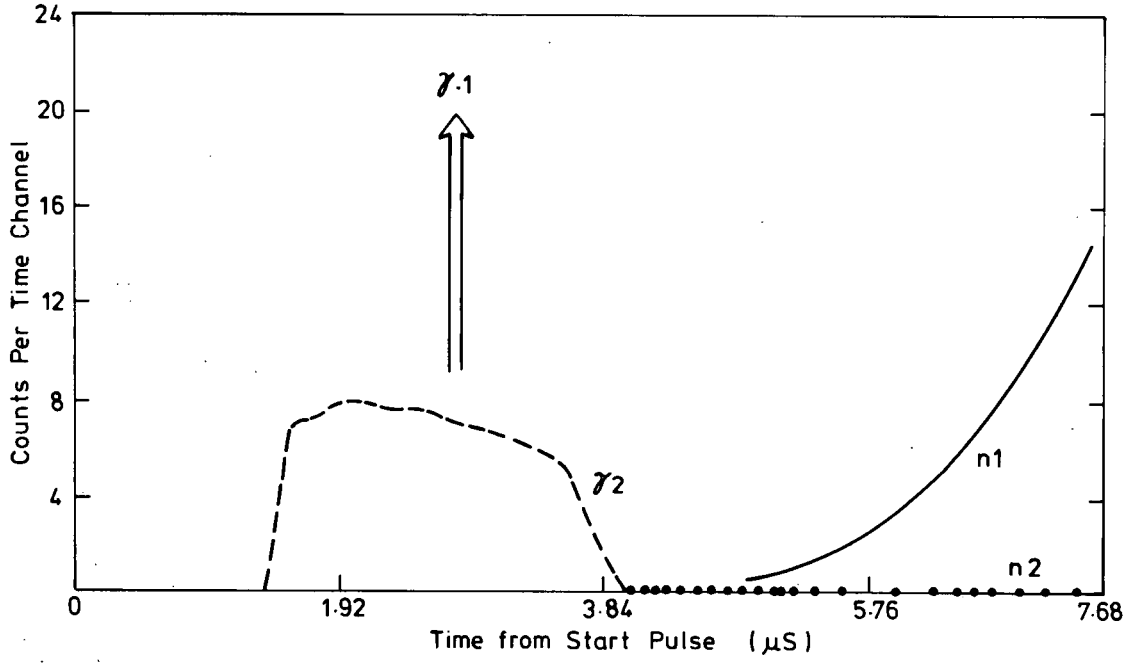

Fig. 1.3 Details of the early channels of a time-of-flight spectrum from the HELIOS FNT, taken with a ^{6}Li glass neutron detector 150 m from the source. Curve 1 (full): taken with the gun pulsed; a strong, narrow gamma flash γ1 precedes the high energy neutrons n1. Curve 2 (dashed): taken with the gun unpulsed but the accelerator on; dark current electrons accelerated during the presence of the r.f. are revealed by their gamma rays γ2 which show the shape of the r.f. pulse; a few neutrons n2 are also produced - under normal operation these neutrons constitute a small background under the proper events of curve n1.

gamma rays is produced at the time of the electron burst and, after a delay, this is followed by the fast neutron events. A much smaller number of neutrons are produced by the dark current (Fig. 1.3) and these constitute a background out of time with the proper neutrons. For the same width of electron beam and r.f. pulse the fast neutron background was measured to be 5×10^{-7} of the proper events. This is a measure of the linac dark current and is within specification.

Thermal neutron capture on the hydrogen in the water-cooled FNT gives rise to a background of 2.2 MeV gamma rays, emitted with an exponential time dependence with decay time determined by the target geometry and macroscopic absorption cross-section. The gamma rays were observed in a ^{6}Li glass neutron detector after removing the neutrons below 100 keV by a 70 mm thick polythene filter, which transmits about 70% of the gamma rays. The results are shown in Fig. 1.4. There are two time constants in the observed gamma ray flux from the target. For this particular detector and in these conditions these gamma rays constitute a background of about 7% at energies above 50 keV, but this reduces to less than 1% below a few keV.

(3) Direct measurement of source resolution functions

The source resolution function can be measured directly by observation of the shape of the capture gamma ray yield from narrow resonances, provided the experiment is mounted on a short flight path (UKNDC(83)P109, p.40). These measurements have been extended to cover a wide energy range using narrow resonances in Al, Fe and Cu samples. In Fig. 1.5 is shown the fit to the capture gamma ray yield from the 5.9 keV resonance in Al, made using the shape analysis code REFIT[1]. A best fit value was obtained for the parameter λ of the target resolution function expressed in the slowing-down form $f(x) = \frac{1}{2} x^2 e^{-x}$, $x = \lambda v$. We have been able to obtain a good fit and a precise value for λ despite the dominance of the electron pulse width component of the total resolution function because that component was directly measured (as described in UKNDC(83)P109, p.40). The doppler-broadened resonance lineshape was narrow by comparison, but was included in the shape calculations.

Preliminary values for the widths of the function f are given in Table 1.2 as $d = 3.4 \lambda$. The calculated values are derived from a Monte Carlo calculation for the same geometry of target, but with uranium plates instead of tantalum[2]. The different mean free paths in tantalum and uranium have

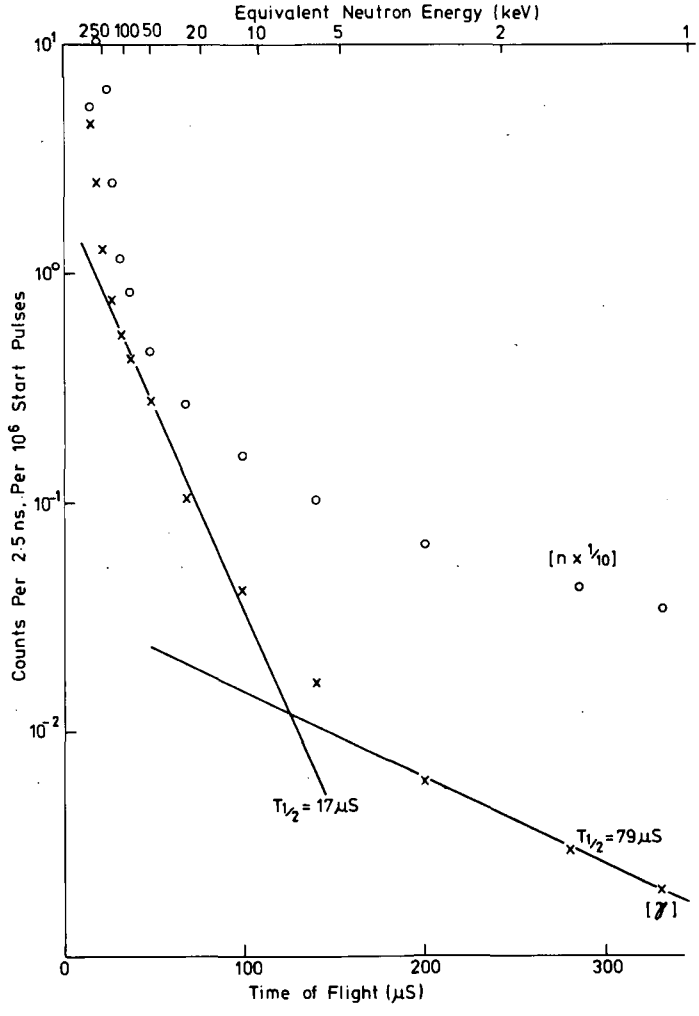

Fig. 1.4 Averaged neutron time-of-flight spectrum from the HELIOS FNT as measured by a ^{6}Li glass scintillator detector on a 150 m flight path (circles, drawn as one tenth of their true values). The spectrum shown by the crosses was measured by inserting a 69 mm filter of polythene to remove neutrons below 100 keV and reveals the time dependence of 2.2 MeV gamma rays emitted following neutron capture in the target cooling water.

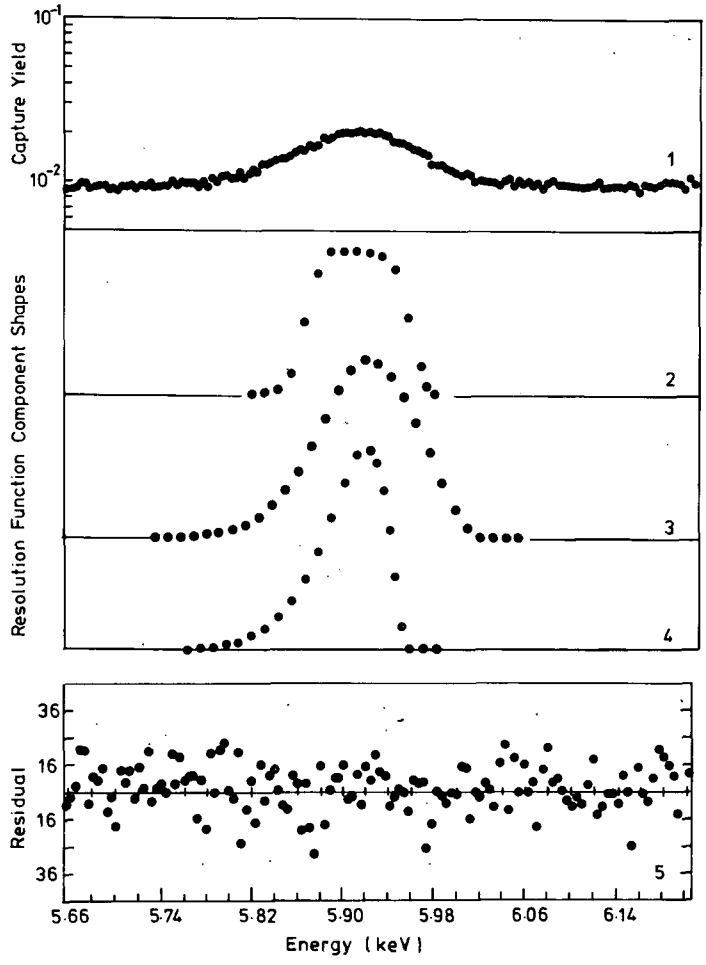

Fig. 1.5 Unfolding of source resolution function for the HELIOS FNT. 1: data and fit - this is shown on a log scale, while the other figures are shown on linear scales; 2: measured electron pulse shape used in unfolding; 3: total resolution function derived from fit 1 after deconvoluting the effects of the doppler-broadened resonance line shape (narrow and not shown) from the fit; 4: FNT slowing down spectrum derived from 3, after deconvoluting the electron pulse (2); 5: residual to fit 1.

been taken into account and the errors increased appropriately. Calculation and experiment are in good agreement and this constitutes some of the first direct evidence that these calculations can usefully predict the detailed response of such targets. More detailed calculations are being undertaken and the experimental data have yet to be finally corrected for the effects of resonant structure in the target spectrum.

Table 1.2

Measured f.w.h.m. values for the resolution function of the HELIOS Fast Neutron Target (water-cooled Ta plates)

Resonance		f.w.h.m. d (mm)	
Element	E_n (keV)	Experimental (mm)	Calculated (mm)
Cu	227	36.0 ± 0.5	36 ± 3
Fe	1150	39.8 ± 1.8	38 ± 3
Al	5906	41.8 ± 1.7	42 ± 3

For the above case there are no directly comparable data from elsewhere, but for the case of a separate moderator adjacent to the fast neutron source, our measurements agree well with the only previous direct data[3]. This is shown in Table 1.3.

Table 1.3

Measured f.w.h.m. values of resolution functions for targets with separate polythene moderators

Element	E_n (keV)	f.w.h.m. 'd' (mm)*	Reference
Fe	1150	22.1	Patrick et al[3] (U sphere + 25 mm $(CH_2)_n$)
Fe	1150	22.6 ± 2	Present work (HELIOS FNT + 25 mm $(CH_2)_n$)

*Preliminary values

(1) M.C. Moxon, Proc. Spec. Meeting on Nucl. Data of Struct. Materials for Fast Reactors, Geel (1977) 644.

(2) G. Constantine, private communication to M.S. Coates (1977).

(3) B.H. Patrick, E.M. Bowey, M.C. Moxon and E.R. Rae, Proc. Third Conf. on Accel. Targets

1.5 E Generation of backgrounds from shields in pulsed neutron experiments (D.B. Syme)

There is little direct experimental evidence of the effect of neutron scattering in adjacent shielding as a source of background in neutron time-of-flight spectrometers (UKNDC(83)P109, p.43), but we have observed such effects while setting up a temporary experiment to measure the resolution function of the Fast Neutron Target of the Harwell electron linear accelerator HELIOS. A collimated neutron beam impinged on a 6.4 mm thick iron sample 7.5 m from the source. The sample was viewed by a capture gamma ray detector placed out of the direct neutron beam and both were enclosed in a radiation shield comprising 10 cm lead inside 30 cm borated resin (Fig. 1.6).

At low neutron energies the time-of-flight spectrum of the gamma ray yield revealed resonances characteristic of neutron capture in the antimony which was present in the lead shield at the few percent level (Fig. 1.7).

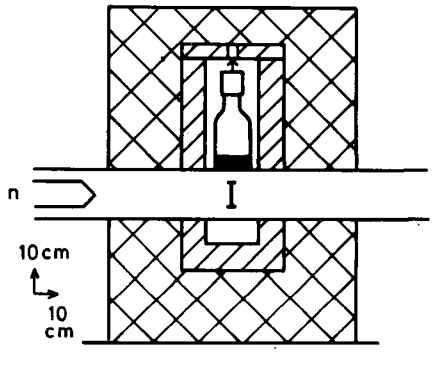

Fig. 1.6 Neutron capture detector and shielding arrangements. The 6.4 mm iron capture sample is in the neutron beam. The Moxon-Rae detector sits outside the beam viewing the sample. Both are enclosed by a 10 cm thick lead shield inside a 30 cm thick shield of borated resin.

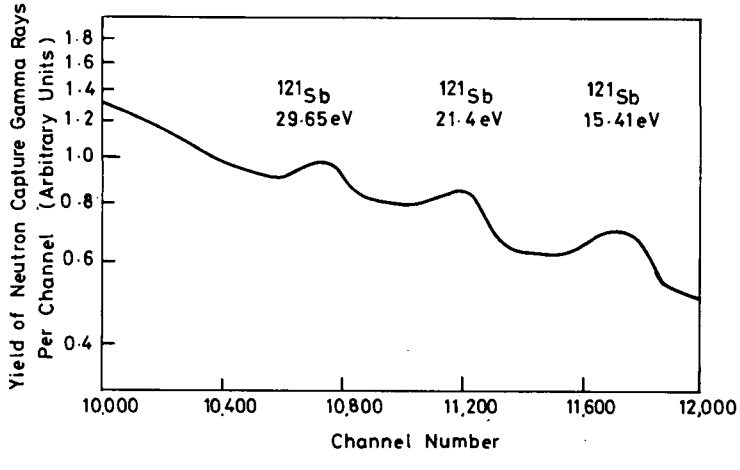

Fig. 1.7 Time-of-flight spectrum of neutron capture gamma rays from the apparatus of Fig. 1.6. The resonances are from antimony in the lead shielding surrounding the detector. Neutrons scattered from the iron capture sample have been captured in the lead shield, making a background for the intended measurements of iron neutron capture.

Neutrons entered the shield following scattering from the thick iron sample and the resulting capture gamma rays were detected as background. This demonstrates that the return effects from shields can be significant sources of background. The internal dimensions of shields should be as large as practicable and of carefully chosen materials to minimise generation of backgrounds in neutron time-of-flight spectrometers.

1.6 Fission chambers for the intercomparison of fast neutron flux density measurements (D.B. Gayther)

The chambers were at the National Bureau of Standards (USA) during the period February-June 1983, measurements being performed with the ^{235}U chamber on the linac from ~0.1 to 1.0 MeV and on the Van de Graaff from 0.5 to 0.6 MeV. After returning to the UK the chambers were not used for six months due to postponements in the previously arranged measurement programme caused by problems in operating accelerators. Because of these scheduling difficulties, the International Bureau des Poids et Mesures undertook, at short notice, a three month period of measurements commencing in February 1984.

1.7 Some comments on the ^{235}U fission cross-section data base above 1.5 MeV (D.B. Gayther and B.H. Patrick)
(WRENDA 949-956, 959)

A paper with the above title was presented at the IAEA Consultants' Meeting on the ^{235}U Fast Fission Cross-Section, Smolenice, Czechoslovakia, 28 March - 1 April 1983. Proceedings will be published, and the paper had the following abstract:

> The main experimental requirements for making accurate fission cross-section measurements are presented and some of the most important experiments which form part of the ^{235}U data base above 1.5 MeV are critically examined in the light of these criteria. The examples discussed are taken entirely from the published literature.

1.8 E Resonance neutron capture gamma-rays in structural materials (J.P. Mason and B.H. Patrick)
WRENDA 391, 486, 487)

Neutron capture in structural materials continues to be of considerable importance in relation to the neutronics characteristics of fission reactors and other effects, such as gamma-ray heating, temperature coefficients of reactivity and the activation of coolant circuits. Improved capture cross-section data are required and to this end a major programme of measurements

is currently under way. The emphasis is on improving the knowledge of resolved resonance parameters so that better calculations of the unresolved and higher energy region can be carried out. An important part of these calculations is the need to understand the capture reaction mechanism. For example, does the statistical model hold or are there non-statistical effects which need to be taken into account?

One of the ways in which non-statistical effects can be uncovered is to study the capture gamma-ray spectra from resolved resonances. An experiment is currently under development to investigate any such effects, particularly by comparison with the predictions of the valence capture model. Calculations using the valence model have shown that the isotopes ^{54}Fe, ^{52}Cr and ^{62}Ni appear to be of especial interest and samples of these isotopes have been loaned to us by the USA from the Department of Energy Research Pool. The measurements achieve high resolution gamma-ray detection with an n-type germanium detector and the time-of-flight technique is used to establish the energy of the neutrons produced by the Fast Neutron Target of the Harwell electron linear accelerator HELIOS.

Initial measurements with low accelerator output have been made on an existing 42 m flight path to confirm calculations of the expected count rates and to assess the recovery of the detector system from the gamma flash. An Fe sample of 10 mm thickness was placed in the neutron beam and the detector was placed outside the flight tube, at a distance of about 15 cm from the centre of the sample. A timing gate was set to allow accumulation of the gamma-ray spectrum from the 1.15 keV Fe resonance and the observed total gamma-ray count rate in that resonance, 180 per hour, was close to predictions. Since a resolution of at least 2000 channels is required for the gamma-ray energy, this count rate was clearly too small for practical purposes. With increased accelerator output and alterations to the detector geometry, it was predicted that the count rate would rise to more than 1000 per hour, but to reach an acceptable count rate further steps were necessary.

Firstly, the design and construction of a new flight path and experimental station was undertaken. The flight path is to be 12.5 m long, giving an increase in count rate of more than an order of magnitude. The blockhouse has been constructed and once the small amount of remaining pipework has been delivered, the flight path itself can be constructed. It should be completed early in 1984.

Secondly, the count rate can be doubled by using two germanium detectors simultaneously. To achieve this without duplicating the system throughout, a logic unit has been designed and constructed which routes the signals from the detectors to the computer and maintains the correct correlation between pulse height and timing information.

To compare the relative strengths of the gamma-ray transitions, it is necessary to know the efficiency of the germanium detector as a function of gamma-ray energy. For energies up to about 3 MeV, the measurements of the efficiency have been carried out using calibrated sources. Above these energies the relative efficiency has been determined by observing gamma-rays of known intensity emitted following thermal neutron capture in a variety of materials. The absolute efficiency at these higher energies may then be determined by normalising the data to those obtained from the sources. The data were collected using a neutron beam from the DIDO reactor and thermal capture was observed in Fe, Ti, Cr, Ni, Cl, Cu and N. A preliminary analysis has provided a satisfactory efficiency curve fitted by eye, and shortly an attempt will be made to fit an analytic function of an appropriate form for which a full covariance error analysis can be carried out.

1.9 The $^{93}Nb(n,n')^{93m}Nb$ reaction (D.B. Gayther and C.A. Uttley, K. Randle (University of Birmingham), W.H. Taylor and M.F. Murphy (AEE Winfrith))
(WRENDA 563-569, 571-573, 582)

Since the last report (UKNDC(83)P109, p.48) the measurements planned have been carried out at neutron energies of 1.1 and 2.1 MeV on the 3 MV Dynamitron accelerator at the Birmingham Radiation Centre. Adequate ^{93}Nb K X-ray counting rates were achieved during these runs, the results of which are still being analysed. Additional data have been obtained at neutron energies of approximately 3.2, 3.7, 4.5 and 5.6 MeV to investigate a slight anomaly in the earlier measurements. Two more irradiations are now planned at neutron energies of about 1.6 and 0.6 MeV, which are important energies for monitoring damage response in light water reactor pressure vessels.

1.10 Nuclear data computer codes

1.10.1 The computer code NJOY (E.M. Bowey and B.H. Patrick)

After some difficulties, the Los Alamos nuclear data file processing code NJOY has been fully implemented on the Harwell mainframe computer.

1.10.2 The status of FISPIN on the Harwell Computer (D.A.J. Endacott)

(1) FISPIN coding

There have been no changes to coding during the past year as the new coding for FISPIN (version 6) has not yet been received.

A command macro has been written which generates the required Job Control Language and also a data input file, for FISPIN runs. This list provides the correct burnup-independent and fission-product data libraries for a given thermal reactor case, and selects a burnup-dependent library with enrichment nearest to that specified by the user. It also provides certain necessary codewords and prompts the user for other data required for execution of the run. The user is prompted also for selection of load module and condensed fission-product library, and whether to stream selected output to a disk file.

(2) FISPIN data libraries

Two new files have been added to the FISPIN facility:

(a) AGRDAT2, a new 90 nuclide CAGR actinide decay data and cross-section library;

(b) ISYIELD, a file for flagging metastable states on the Risley generated condensed fission-product libraries.

1.11 Studies of neutron induced charged particle reactions: detector development (R.A. Jarjis (University of Birmingham) and B.H. Partick)

It is widely recognised that neutron induced charged particle reactions can play important roles in radiation damage of both reactor and biological materials. The reactions make substantial contributions to material damage through nuclear transmutation and through the build-up of helium and hydrogen. A knowledge of these effects is important for both fission and fusion reactor technology, and at a fundamental level this implies ideally a detailed knowledge of the reaction cross-sections. Experimentally this involves the measurement of charged particle yields, spectra, and angular distributions as the incident neutron energy is varied. Apart from their applied value, such measurements are important from the point of view of fundamental nuclear physics. For example, clustering of nucleons can be investigated by the formation of 'hot spots' on the nuclear surface via the interaction of an incoming neutron and few nucleons. This is manifested by the occurrence of pre-equilibrium emission which can be detected by the measurement of charged particle spectra.

To develop a suitable charged particle detector system to study these experimental areas a collaboration between the University of Birmingham and AERE Harwell is under way using the Harwell electron linear accelerator HELIOS as the neutron source. The advantage of using an accelerator pulsed neutron source is that measurements can be carried out over broad energy regions using the time-of-flight technique. However, problems associated with such measurements can be considerable. Due to the characteristics of the pulsed neutron source, the arrival of a neutron burst at the detector is preceded by an intense gamma flash, which makes measurements difficult at short flight times. Furthermore, due to the range limitations and the energy straggling characteristics of charged particles, thin samples have to be used, which usually result in low charged particle count rates. The situation is further worsened by the small magnitude of most reaction cross-section values. Therefore, an ideal detection system should have fast recovery time, high efficiency, low sensitivity to neutrons and gammas, and large solid angle for improved count rate. In addition it should be able to distinguish between charged particles of different kinds over a wide energy range.

In order to fulfil the above requirements it is obvious that a sophisticated charged particle detector will have to be devised. We have chosen to develop a detector with basic principles similar to the 'Phoswich' system of Wilkinson[1]. The detector provides ΔE and E signals which are produced by two scintillators processing distinctively different fluorescence decay characteristics. It is envisaged that an array of such detectors will be used to produce the required geometry. We have carried out tests on a detector which consists of 0.03 mm NE102A and 10 mm CsI(Tl) scintillators mounted on a fast photomultiplier tube. A typical pulse shape output from this detector is shown in Fig. 1.8. The fast decaying component is due to NE102A (ΔE) whilst the slow decaying component is due to CsI(Tl) (E).

We have conducted experiments with alpha-particles from the Tandem Van de Graaff accelerator at Harwell in order to study the characteristics of this detector. Our measurements include energy loss and straggling, scintillation efficiency, energy resolution and fluorescence response. The energy loss data from thin plastic scintillators agree with theoretical predictions based on the Bethe formula. Furthermore, in the alpha-particle

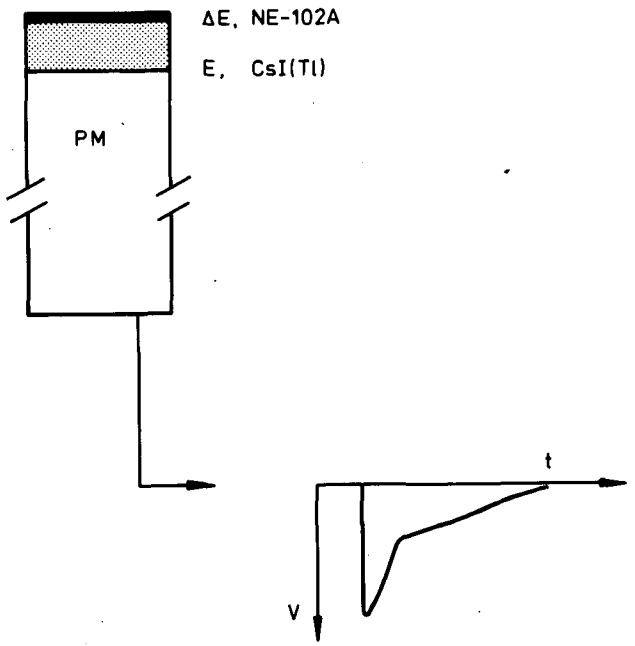

Fig. 1.8 Schematic diagram of detector and output pulse shape. E and ΔE components are separated with the aid of linear gates and integrating circuitry.

energy region below 12 MeV, the 0.03 mm NE102A plastic scintillator exhibits a non-linear fluorescence response, whereas a linear response is observed for the CsI(Tl) crystal. Future experiments are intended to cover broader alpha-particle energy regions, and to demonstrate charged particle identification. Further experiments with other plastic scintillators are also planned.

---

(1) D.H. Wilkinson, Rev. Sci. Instr. 23 (1952) 414.

1.12 Recalculation of multiple scattering effects in ^{7}LiOH irradiations (M.T. Swinhoe)
(WRENDA 63, 65, 67, 68)

There is considerable worldwide interest in the present status of the

^{7}Li(n,n'αt) reaction from threshold to 14 MeV. Recent measurements[1,2] since Swinhoe and Uttley[3] are also lower than the ENDF/B-IV values. Before our work was submitted for publication the multiple scattering correction was recalculated with a more precise Monte Carlo representation using MORSE (AERE PR/NP 30, p.145). The new multiple scattering correction increases our ^{7}Li(n,n'αt) cross-section values by about 6% below 10 MeV, and 3% above 10 MeV, roughly equivalent to one standard deviation of the measurement. The new values are given in Table 1.4. Fig. 1.9 shows the recent measurements together with the ENDF/B-IV values and a recent evaluation of Young[4]. A new evaluation of the cross-section is under way at Karlsruhe.

Table 1.4

New ^{7}Li(n,n'αt) cross-section values

Neutron energy (MeV)	^{7}Li(n,n'αt) cross-section (mb) (errors: ±1 st.dev.)
4.57	73 ± 14
5.47	303 ± 30
7.35	344 ± 29
9.72	335 ± 20
9.77	327 ± 21
11.76	300 ± 16
14.1	235 ± 11
14.1	242 ± 11

(1) D.L. Smith, M.M. Bretcher and J.W. Meadows. Nucl. Sci. Eng. 78 (1981) 359.

(2) H. Liskien, R. Wölfle and S.M. Qaim. Proc. Int. Conf. on Nucl. Data for Sci. and Tech. Antwerp, 1982 (ed. K.H. Böckhoff) p.349 (D. Reidel, Dordrecht, 1983).

(3) M.T. Swinhoe and C.A. Uttley. Report AERE-R 9929 (1980).

(4) P.G. Young. Report LA-8874-PR (1981) 2.

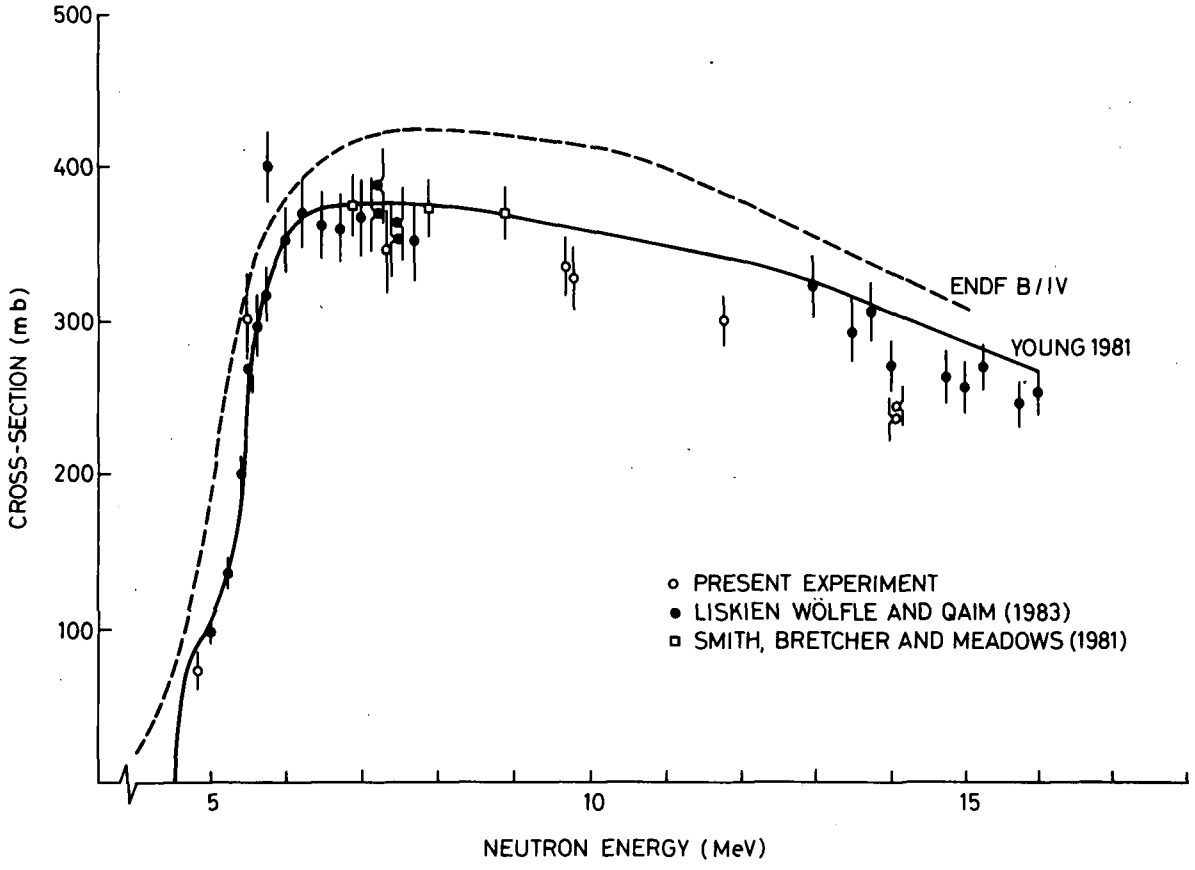

Fig. 1.9 The $^{7}Li(n,n'\alpha t)$ cross-section

1.13 Safeguards Research

1.13.1 Neutron die-away interrogation as a means of fissile material assay (B.H. Armitage, T.E. Sampson and T.I. Morgan)

Future requirements for the assay of fissile materials by neutron die-away interrogation have arisen in the decommissioning and decontamination of nuclear facilities, process control, material accountancy and in waste disposal. We aim here to develop a better understanding of neutron die-away interrogation and to contribute towards the solution of outstanding problems.

The measured performance of a die-away chamber of sufficient size to assay a 208 litre barrel has been compared with results obtained by Monte Carlo modelling. A systematic study is in progress on the effects encountered on assaying the fissile content of waste in barrels when the

waste is embedded in different matrices. An initial attempt to assay barrels of real waste has provided a practical demonstration of the method. An experimental examination of the feasibility of package monitors for nuclear safeguards purposes is being undertaken. A contract has been placed with the objective of producing a more reliable and longer lived pulsed neutron source suitable for neutron interrogation.

1.13.1.1 The performance of neutron die-away chambers (T.I. Morgan, T.E. Sampson and B.H. Armitage

A report has already been given (UKNDC(83)P109, p.52) of a study of the properties of die-away chambers capable of assaying 208 litre barrels. The work was concerned with the calculation of design parameters such as wall thickness and detector position, and was made with the Monte Carlo computer code MONK. Following the construction of a die-away chamber of internal dimensions 73 x 74 x 107 cm, a study is being made of the measured performance of the chamber compared to the results obtained by Monte Carlo modelling. The die-away chamber consists of a volume enclosed by graphite and polyethylene walls (CH_2) containing a compact pulsed source of 14 MeV neutrons. Neutrons from the pulsed source are moderated and thermalized in the walls of the chamber. The resulting thermal neutron flux is used to assay fissile material present inside the chamber. Fast neutron detector packages in the walls of the chamber are insensitive to thermal neutrons and detect only fast neutrons from thermal-neutron-induced fissions in the fissile material in the period between successive pulses of 14 MeV neutrons. The detector packages are each composed of a ^3He detector encased in 1.3 cm of polyethylene and wrapped in cadmium.

The objective of the work is to compare the value of the thermal neutron flux obtained as a result of modelling the die-away chamber with the measured value. Calculations made with the Monte Carlo computer code MONK give a value for the thermal neutron flux per source neutron at the centre of the die-away chamber. The measurements are therefore being undertaken in two parts, firstly measuring the neutron tube output, and secondly measuring the thermal neutron flux relative to the neutron source.

After isolating the pulsed neutron source from the die-away chamber the neutron yield was measured with a calibrated NE213 scintillator and photomultiplier with pulse shape discrimination. Room and air scattering corrections were made by interposing a steel block between the neutron source and scintillator. Monitoring of the neutron tube output was made by

Cu foil activation and subsequent γ-counting with a NaI detector. Finally, with the neutron source replaced, the thermal neutron flux in the chamber was measured with a calibrated BF_3 detector and again the neutron tube output was monitored by Cu foil activation. The results are currently being evaluated.

1.13.1.2 Assay of fissile material in 208 litre barrels (T.I. Morgan, T.E. Sampson and B.H. Armitage)

The primary function of the die-away chamber is to assay the fissile material content of low level waste in barrels. A description of the functioning of the system has already been given (UKNDC(83)P109, p.54). Measurements were also reported of the spatial variation of the thermal neutron flux in an empty barrel, a barrel filled with tissues and a barrel containing stainless steel tubes. It was also shown that the spatial variations of the number of fission neutrons counted when a ^{235}U sample was placed at a number of locations in the barrel did not exceed ±17% for the empty barrel or for the tissue or steel tube matrices.

The idealized objective of the work is to define a procedure for the assay of the fissile content of a barrel which does not require a prior knowledge of the matrix in which the fissile material is embedded. However, we are not yet in a position to know if a suitable method of matrix compensation can be devised for a range of matrices with variable elemental constitution, density, slowing down power and thermal absorption.

The progress we can report on this so far is limited but nevertheless real. The procedure has been to place a 6 g sample of ^{235}U at the centre of each matrix filled barrel and count the number of fission neutrons detected in the fast neutron detector packages. The extent of the problem can be appreciated from the first column in Table 1.5 where the number of fast fission neutrons per 14 MeV interrogating neutron is given for a range of matrices. The improvement obtained when the fast fission neutron count is expressed in terms of the BF_3 thermal monitor placed on the inside wall of the chamber is modest.

If we assume that the flux at the centre of the barrel is approximately proportional to the thermal flux measured by the BF_3 monitor, then normalization of the fission neutron response to the thermal monitor yield will take into account matrix to matrix variations in the thermal flux at the centre of the barrel. We also have a further factor to take into account and that is the effective detector efficiency for fission neutrons

Table 1.5

Variation of thermal neutron flux and fission neutron detection efficiency for different matrices

Matrix	Relative fission neutron count per 14 MeV neutron	Relative fission neutron count per thermal neutron count (F)	Relative detection efficiency for ^{252}Cf source (ξ)	$\frac{F}{\xi}$
Empty barrel	1.00	1.00	1.00	1.00
Vermiculite	1.03	0.99	1.00	0.99
Tissues	1.19	0.96	0.96	1.00
Rags	1.42	1.02	0.81	1.26
Zircaloy	0.85	1.06	1.05	1.01
Stainless steel	0.31	0.60	1.00	0.60
Water/poly bottles	0.87	0.61	0.55	1.11
Polyethylene chips	0.17	0.14	0.18	0.78

produced at the centre of the matrix. Relative values for this quantity were obtained by placing a Cf source at the centre of each matrix and are also given in Table 1.5. In the final column values are given for the relative fission neutron response per thermal monitor count divided by the detector efficiency.

The fact that the standard deviation of the values given in the final column is only 20% indicates that some form of matrix compensation has been achieved. However, for a barrel of real waste it will not be possible to place a Cf source at the centre. We plan to investigate whether placing a ^{252}Cf source immediately below the barrel will provide an equivalent indication of detector efficiency.

Although encouraging results have been obtained it has to be stated that preliminary data from additional matrices indicates that the present approach is not sufficiently comprehensive.

1.13.1.3 Waste assay (B.H. Armitage and T.E. Sampson)

An initial attempt has been made to assay the fissile material content of 100 litre and 50 litre barrels containing real Pu waste arising from operations at Harwell. The fission neutron yield obtained by neutron die-away interrogation has been compared with values obtained from Pu standards*. Assignment of precise values for the Pu content awaits the development of adequate matrix compensation methods (see Sect. 1.13.1.2 above).

*These standards were made available by Harwell's Instrumentation and Applied Physics Division.

A demonstration of the sensitivity of the method was provided by one particular barrel where a significant fissile material content was observed, although a null result had previously been obtained from γ-ray scanning and coincidence well counting.

1.13.1.4 Package Monitor Studies (B.H. Armitage and T.E. Sampson)

In order to safeguard nuclear facilities it may be appropriate to include a device to examine large packages at entry and exit to detect significant quantities of uranium present in the package. Calculations made with the computer code MONK, described in UKNDC(82)P105, p.39 and UKNDC(83)P109, p.57, showed that attempts to conceal fissile material in bulky shielding should result in the fissile material being observed during interrogation in a differential die-away system either by delayed neutron detection or by the change in the thermal neutron die-away time induced by the bulky shielding in the package. This report is concerned with attempts to observe shielded fissile material by delayed neutron detection.

A die-away chamber designed for the assay of 208 litre barrels has been used to verify experimentally the feasibility of a package monitor operating on these principles. A fissile sample of 4.4 kg UO_2 enriched to 1.46% ^{235}U was surrounded with neutron shielding. Neutrons from a pulsed 14 MeV neutron generator induced fissions in the sample and the delayed fission neutrons were detected by fast neutron counter packages embedded in the walls of the assay chamber. The data shown in Fig. 1.10 were acquired with about 3600 pulses of 14 MeV neutrons (15 μs duration at a rate of 10 s^{-1}). The 14 MeV neutron output was about 1 x 10^6 neutrons $pulse^{-1}$ for a total of about 3 x 10^9 source neutrons per measurement.

The data in Fig. 1.10a were obtained with the sample surrounded by 7.6 cm CH_2. During the initial 10 ms after the pulse prompt fission neutrons induced by the thermal neutron flux die-away in the chamber are detected. These fast neutrons arise from thermal neutron induced fission of ^{235}U in the sample. Delayed neutrons are observed at times longer than 10 ms. The delayed neutrons arise from thermal neutron induced fission in ^{235}U during the thermal flux die-away and also from fast neutron induced fission in both ^{235}U and ^{238}U. In Fig. 1.10b the fissile sample is surrounded by 1 mm Cd inside the 7.6 cm thick CH_2 shield. The Cd prevents the thermal neutron die-away flux from inducing fissions in the sample hence the absence of the fission neutron response in the 1-10 ms range. Also, fewer delayed neutrons are produced since no thermal fission is occurring in the sample.

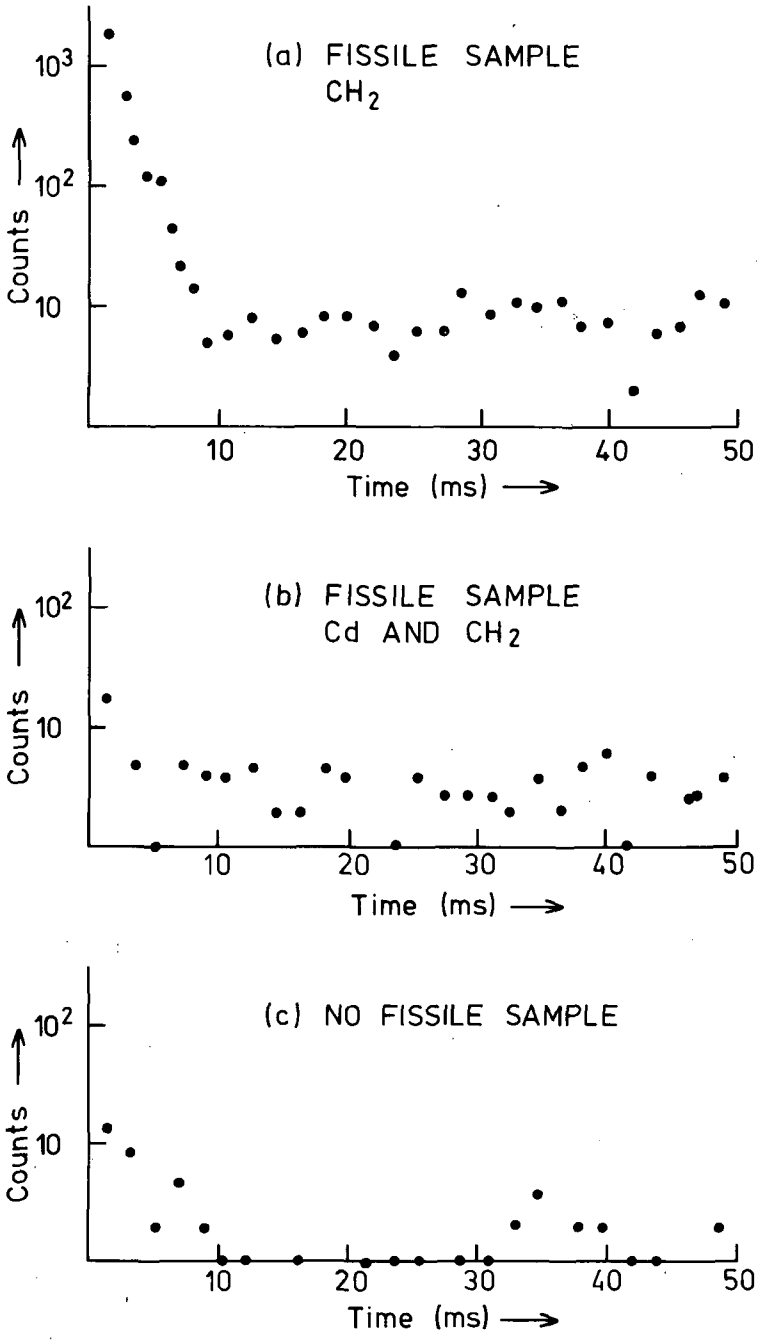

Fig. 1.10 Fast neutron detector time spectra for periods up to 50 ms following 14 MeV neutron pulses: (a) 4.4 kg UO_2 (1.46% ^{235}U) surrounded by 7.6 cm CH_2 showing thermal neutron induced fission response during the 1-10 ms thermal neutron die-away period followed by delayed neutron response at longer times; (b) same sample surrounded by 1 mm Cd inside the CH_2 showing absence of thermal neutron induced fission response and present of a reduced but still detectable delayed neutron response; (c) system background in absence of fissile sample

However, we note that 14 MeV neutron induced fission still results in a detectable delayed neutron signal above the background levels with no fissile material shown in Fig. 1.10c.

1.13.1.5 Pulsed neutron source development (B.H. Armitage and J.W. Leake)

The principal obstacle to the introduction of a number of active neutron interrogation systems in the UK nuclear industry is the reliability of pulsed neutron sources. As much of the envisaged future use is in plant environments, consideration has been given to a common specification for a pulsed neutron generator which is simple to operate. The need is for a reliable long lived pulsed neutron source operating at 10 Hz with a neutron output of around 10^7 neutrons per pulse.

Experience at Harwell has been gained with a Marconi Avionics NK 51 pulsed neutron generator. This consists of a sealed tube within which deuterons are accelerated on to a tritiated erbium target, a separate high voltage transformer and a control unit. Problems encountered with the system include electrical breakdown in the EHT connections and leakage of insulating gas.

Following discussions with Marconi Avionics a development programme was proposed aimed at producing more reliable and longer lived tubes. Thus, by increasing the diameter of the canister an improvement in the high voltage characteristics can be expected. It is also proposed to run lifetime tests on tubes incorporating new features such as an anti-sputter guard, a suppressor electrode, the use of low sputter coefficient materials and the use of an alternative target material. For a more constant neutron output a mixed d and t beam which is accelerated on to a target containing the same mixture of isotopes is proposed in place of the conventional d on t reaction.

1.13.2 Fast Shuffler (E. Wood and A.R. Talbot)

One of the problems in waste assay is quantifying the mass of fissile material in waste drums when the fissile material is inhomogeneous. For example, the die-away technique described in sect. 1.13.1 utilises a thermal interrogation flux and so self-shielding gives rise to underestimates of the fissile content. Although the ^{252}Cf shuffler technique cannot approach the sensitivity of the die-away technique, it can be designed to produce a harder neutron spectrum for interrogation and hence reduce the effects of self-shielding.

The technique is based on the detection of delayed neutrons from fission. The sample under investigation is irradiated by neutrons from a ^{252}Cf source for about 10 s; the amount of moderator surrounding the source can be varied to suit the application. The source is then transferred rapidly to a storage position and the delayed neutrons from fission are detected by BF_3 counters surrounded by moderator.

During the year, effort has concentrated on improving the mechanical performance of the fast shuffler described in UKNDC(83)P109, p.61. A large air reservoir (300 litres at a pressure of 2 atmospheres) has been installed to improve the consistency of the transit times from the irradiation position to the storage position (typical transit time is 200 ± 3 ms, with a counting period of 10 s). The performance of the shuffler has been satisfactory and plans are under way to test the reliability by running for long periods. Some problems have been encountered with corrosion of the support tubes which house the BF_3 detectors in the water moderator. It is planned to change from a water to a transformer oil moderator in the near future.

The sensitivity of the device (a few grams of fissile material) has been improved by additional shielding between the storage position for the ^{252}Cf source and the sample. However, there is still evidence of occasional interference problems and we propose to try to overcome these by installing an electro-optic system to link the experiment to the data collection system and controlling computer (VAX 11/750) which are located ~50 metres away. Future work will involve measuring the real waste samples discussed in sect. 1.13.1.3 above.

1.13.3 Evaluation of possible methods of monitoring the ^{235}U enrichment of centrifuge plants operating at low pressure (T.W. Packer and R. Howsley*)

It was shown in UKNDC(83)P109, p.62 that it is possible to determine the enrichment of uranium deposited on product header pipes in centrifuge plants by using a γ-ray spectrometer. The enrichment can be approximately determined by measuring the ratio of the 186 keV γ-rays emitted by ^{235}U to the number of 63 keV γ-rays emitted by ^{234}Th, a daughter of ^{238}U. Due to the presence of directly deposited thorium on the pipes it was established that a better enrichment value could be obtained by measuring the ratio of the 84 keV γ-rays emitted by ^{231}Th, a daughter of ^{235}U and the 63 keV γ-rays emitted by ^{234}Th.

---

*British Nuclear Fuels plc, Risley

In the preliminary measurements the 84 keV γ-ray determination was partially obscured by the presence of Pb K_{β_1} X-rays excited in the lead shielding. This problem has been eliminated by lining the shielding with 1 cm thick steel sheet. The measuring system has also been improved by using additional shielding to reduce the number of γ-rays emitted from the pipework within the centrifuge console being detected.

Two γ-ray spectrometers have been in operation at Capenhurst for six months, one monitoring the rate at which uranium is deposited on the product header of a centrifuge cascade from its initial commissioning, the other one on a test rig used to determine if there is exchange between the UF_6 gas in the pipe and the deposit.

(1) Measurements related to the mechanism by which uranium and its daughter products are deposited on the pipe

The intrinsic Ge detector used for the preliminary measurements has been used to monitor continuously the number of γ-rays emitted from the UF_6 gas and deposit on a product header pipe of a centrifuge cascade from when it was first commissioned.

A graph of the number of detected 63, 84 and 186 keV γ-rays, converted to estimated masses of uranium deposited on the pipe, as a function of the time the centrifuge cascade has been operating is given in Fig. 1.11 (63 keV readings low as ^{234}Th is not in equilibrium with ^{238}U). It is seen that approximately 50 μg cm^{-2} of uranium was deposited on to the pipe within the first few days. After 20 days operation the presence of approximately 20 μg cm^{-2} uranium equivalent of directly deposited thorium can be seen (i.e. 84 keV reading 20 μg cm^{-2} above 186 keV reading). The uranium was then deposited at an approximately linear rate of 10 μg cm^{-2} per month for the next three months. However, following a change in feed container the mass of uranium deposited increased by approximately 70 μg cm^{-2} in the three weeks before the feed container was changed again. In the three months since this time less than 10 μg cm^{-2} of uranium has been deposited. The variations in the 186 keV reading are at least partly due to changes in pressure and enrichment of the UF_6 gas.

These measurements are being continued to try to obtain more information on the variation in the rate of deposit of uranium on the pipes which has been shown to depend on the operating conditions of the plant.

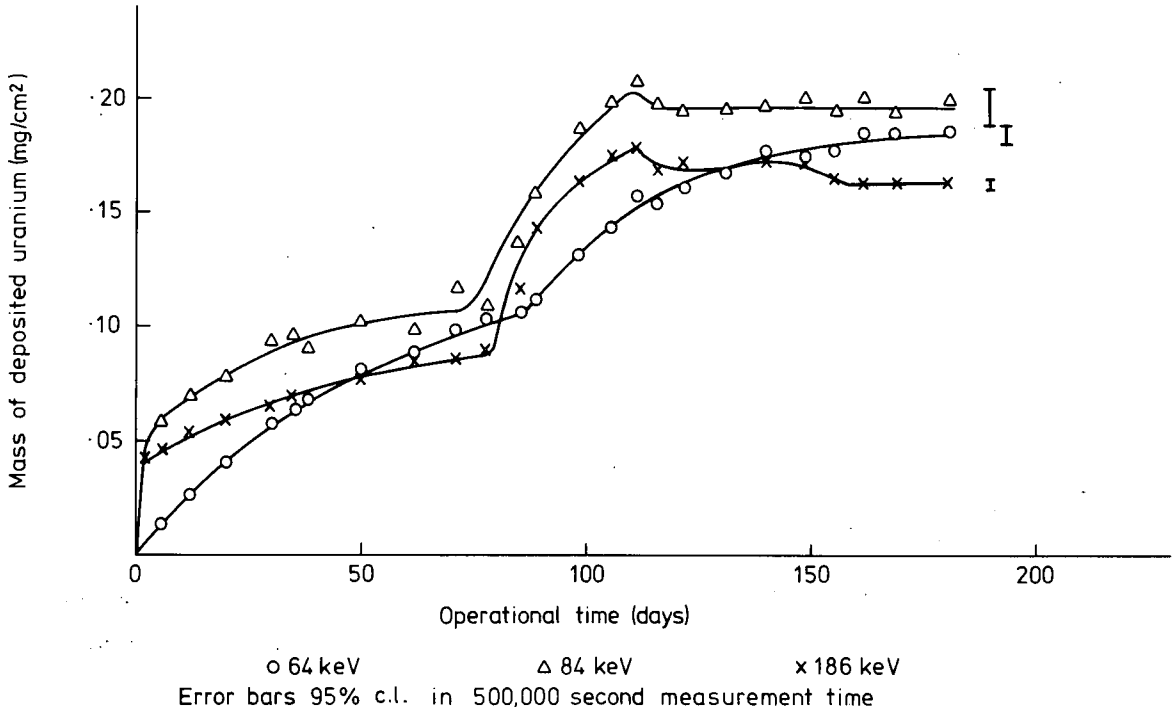

Fig. 1.11 Variation in the estimated mass of uranium deposited as a function of the operational time of the centrifuge cascade

(2) Measurements related to the possible exchange of UF_6 gas with the deposited uranium

It has been suggested that low enrichment UF_6 gas may exchange with highly enriched uranium deposit, hence preventing an inspector using the γ-ray spectrometer technique from detecting the misuse of the centrifuge plant. A γ-X detector, which is approximately three times more sensitive than the intrinsic Ge detector for measuring 63 keV γ-rays, was therefore used to measure continuously the number of γ-rays emitted from the UF_6 gas and the deposit on a new pipe in a test rig in which the UF_6 gas samples of different enrichments could be recirculated.

Depleted UF_6 gas was recirculated around the rig for a week and an estimated 45 $\mu g\ cm^{-2}$ of uranium was deposited on the pipe. Enriched uranium (7%) was introduced into the rig for 6 weeks and 14 $\mu g\ cm^{-2}$ of enriched uranium was deposited. As these values are very similar to those shown in Fig. 1.11 for the operational centrifuge, it was established that the systems were behaving in a similar fashion. A further 14 $\mu g\ cm^{-2}$ of uranium

was deposited in the 12 weeks after depleted UF_6 was reintroduced. Although this rate of deposit was lower than that obtained when recirculating the enriched gas, even if the change in deposition rate was entirely due to exchange between the depleted UF_6 gas and the enriched uranium deposit, it would only be equivalent to a maximum exchange of 0.5 $\mu g\ cm^{-2}$. It is probably less than this value as the rate of deposit tends to decrease with the time the centrifuge plant has been operating (see Fig. 1.11). Even if the exchange is as high as 0.5 $\mu g\ cm^{-2}$ this will not significantly affect the measured enrichment when using the γ-ray spectrometer and would not prevent an inspector from detecting whether the centrifuge plant had been misused and had produced higher enriched uranium than the declared value. It was also confirmed by measuring the number of 84 keV and 63 keV γ-rays emitted by ^{231}Th and ^{234}Th respectively during the periods when the UF_6 gas was removed from the rig, that approximately 25 $\mu g\ cm^{-2}$ uranium equivalent of thorium is directly deposited on to the pipe.

These latest results confirm the original conclusions that the γ-ray spectrometer is capable of determining the ^{235}U enrichment of uranium deposited on pipe walls, thus enabling an inspector to detect misuse of the centrifuge plant. The main unknown is the rate at which the uranium is deposited as this will define the minimum mass of enriched UF_6 that can be produced which cannot be detected by the inspector. The emphasis is now being placed on measuring the mass of uranium that has been deposited in centrifuge cascades that have been in operation for different times.

1.14 Neutron diagnostic systems for JET

1.14.1 I Measurement and calculation of JET time-resolved neutron yield monitors (M.T. Swinhoe and O.N. Jarvis)

Two types of fission detector assemblies (^{235}U and ^{238}U) were designed to monitor the neutron yield from JET* as a function of time (see UKNDC(83)P109, p.66). The absolute neutron detection efficiencies for monoenergetic and Am/Be and ^{252}Cf neutron spectra have been calculated using the Monte Carlo transport code MORSE (AERE PR/NP 30, p.145) for both types of assembly. The detection efficiency was also measured for 2.5 and 14 MeV neutrons (using the 0.5 MeV Van de Graaff accelerator) and for calibrated Am/Be and ^{252}Cf sources. The measured and calculated values, shown in Table 1.6 are in very good agreement, the mean measured/calculated ratio for the

---

*Joint European Torus, Culham

^{235}U assembly being 1.00, and for the ^{238}U assembly 1.03. (A paper has been accepted for publication in Nucl. Instr. and Meth.)

Table 1.6

Comparison of measured and calculated responses of ^{235}U and ^{238}U fission detector assemblies

	Measured		Calculated	Measured / Calculated
^{235}U assembly:				
2.5 MeV (30 cm)	$(1.85\pm.09)\times10^{-4}$	$(n^{-1}\ sr^{-1})$	$(2.00\pm.12)\times10^{-4}$	0.925±.072
2.5 MeV (2m)	$(0.47\pm.03)$	$(n^{-1}\ cm^{-2})$	$(0.42\pm.02)$	1.119±.087
14 MeV	$(0.33\pm.02)$	$(n^{-1}\ cm^{-2})$	$(0.34\pm.02)$	0.970±.085
Am/Be	$(1.06\pm.07)\times10^{-4}$	$((source\ n)^{-1})$	$(1.17\pm.02)\times10^{-4}$	0.906±.063
Cf	$(1.10\pm.08)\times10^{-4}$	$((source\ n)^{-1})$	$(1.04\pm.04)\times10^{-4}$	1.058±.085
				0.996±.036
^{238}U assembly:				
2.5 MeV	$(5.80\pm.35)\times10^{-4}$	$(n^{-1}\ cm^{-2})$	$(5.92\pm.18)\times10^{-4}$	0.979±.067
14 MeV	$(1.02\pm.05)\times10^{-3}$	$(n^{-1}\ cm^{-2})$	$(0.95\pm.05)\times10^{-3}$	1.074±.076
^{238}U bare**				
2.5 MeV	$(7.20\pm.43)\times10^{-4}$	$(n^{-1}\ cm^{-2})$	$(6.90\pm.41)\times10^{-4}$	1.043±.090
14 MeV	$(1.54\pm.08)\times10^{-3}$	$(n^{-1}\ cm^{-2})$	$(1.51\pm.09)\times10^{-3}$	1.020±.078
				1.029±.040

**Without lead shield (10 cm thick)
(Errors given are one standard deviation)

1.14.2 I 14 MeV neutron spectrometers for deuterium-tritium plasmas
P. Dixon, C.A. Uttley and D. West)

Design studies for three systems are in progress prior to preparation of detailed reports, including budgetary cost estimates, for submission to JET for their assessment and selection.

(1) Magnetic transport system

This system conveys protons, ejected in the forward direction by 14 MeV neutrons from a thin foil ('proton radiator') placed in vacuum near the JET torus, out of the torus hall and into a low background region in the diagnostics hall where their energy can be measured in Si diode detectors. Two bends in the beam line are used to ensure achromatism and prevent

exposure of the detectors to neutrons emitted either directly from the torus or after scattering from any part of the torus hall. The achromatism ensures that, for a given aperture of lenses and beam pipe, a maximum momentum spread of protons is transmitted. It is important to keep the aperture in the shield wall to a minimum as the cost of the subsequent shielding in the diagnostics hall as well as the cost of quadrupoles and bending magnets is sensitively dependent on the aperture. An intermediate beam focus is arranged near the point of emergence from the torus hall where a triplet field lens is placed. Such a system was used successfully at Nimrod[1]. The system proposed uses a beam pipe of diameter 20 cm and transmits an energy bite $\frac{\Delta E}{E} = \pm 0.063$. The overall length is 26 m of which about one half lies outside the torus hall. Shielding calculations using the Monte Carlo program MORSE indicate that 50 cm thickness of concrete round the beam pipe would provide adequate biological shielding in the torus hall at 20 keV operation except near the main shield and at the beam's end where 75 cm thickness is needed.

In d-t plasmas at 5 keV plasma temperature the expected fluence at the foil with a 20 cm diameter collimator to select the volume of plasma viewed is 6×10^8 neutrons per shot. A 5.4 cm dia. disc of polyethylene 2.5 mg cm^{-2} thick would then give 3300 counts per shot. The overall energy resolution is 70 keV. A single thermonuclear peak would require only 210 counts total for a 10% determination of plasma temperature.

Consideration has been given to the presence of hydrogen adsorbed in the walls of the vacuum tube which could give rise to background protons. Provided stainless steel is used the degree of outgassing required is readily accomplished.

(2) Si diode neutron spectrometer

This method makes direct use of the reaction $^{28}Si(n,\alpha)^{25}Mg$ (threshold 2.75 MeV) in the Si detector itself. The peak from the total energy released when alpha particles leave the residual nucleus ^{25}Mg in its ground state would be used. Excited states in ^{25}Mg exist at 0.585 MeV, 0.975 MeV, 1.612 MeV, 1.965 MeV and above and in addition there is an (n,p) reaction with a threshold of 4.0 MeV. Apart from the complexity of the spectrum there are other disadvantages of the technique such as the small fraction of

counts in the α_0 peak (0.3%). The maximum count rate in the detector is of the order 10^5 cps so the count rate in the α_0 peak is much more restricted. Radiation damage also constitutes a difficulty. In spite of these problems the system seems feasible if one is prepared to replace the detector after about 1000 shots (1 month). If the detector is located in a shielded enclosure outside the torus hall and a hole in the main shield of about 2.5 cm radius is used, together with a matching precollimator near the torus, then the background of energy-degraded neutrons striking the detector will be only about one-sixth of the neutrons direct from the plasma. In these conditions 3000 counts per burst in the α_0 peak with an energy resolution of about 100 keV are easily achieved at 5 keV plasma temperature.

Very similar shielding arrangements are needed for the system described in the next section and they could both be accommodated in the same shielded enclosure and with the same precollimator. The two detectors are complementary, since the Si detector is capable of operating at lower plasma temperatures (lower neutron fluxes). Preliminary trials have been carried out using the 0.5 MV Van de Graaff accelerator and are encouraging.

(3) Annular radiator proton recoil spectrometer

The design constraints on this spectrometer are that it should have an efficiency $\sim 10^{-4}$ and a resolution not greater than 2.5% fwhm. The basic unit of the spectrometer is an annular radiator of 6 mg cm^{-2} polyethylene of internal radius 7 cm and external radius 8 cm with a 1.5 cm radius HP germanium detector placed axially 40 cm behind the plane of the radiator. The efficiency of this detector for 14 MeV neutrons is 2.23×10^{-5} and the energy resolution is 2.4% (fwhm). The desired efficiency of 10^{-4} is achieved by arranging four units in tandem and follows an existing design which has been applied to fast neutron spectroscopy by Kang and Chung[2]. These workers observed an improvement by a factor of 5 in the signal-to-background ratio from 14 MeV neutron irradiations when using HP Ge detectors rather than Si detectors due to the reduced (n,p) and (n,α) cross-sections in germanium. The spectrometer will be sited in the diagnostic hall behind an annular collimator located in the biological shield wall. In this position the expected count rate will be ~250 recoil protons s^{-1} during a discharge at a plasma temperature of 5 keV, and the spectrometer is intended to operate at higher temperatures where count rates ~1000 s^{-1} can be achieved with an adequate energy resolution.

---

(1) C. Whitehead et al. Nucl. Phys. B48 (1972) 365.

(2) H.D. Kang and M.K. Chung, J. Kor. Phys. Soc. 8 (1975) 9.

2. CHEMICAL NUCLEAR DATA

2.1 Introduction

During 1983 the Chemical Nuclear Data Committee (Chairman J.G. Cuninghame, Secretary R. Bett) met twice and the Data Library Sub-Committee (Chairman A. Tobias (CEGB), Secretary H.E. Sims) three times. There have also been a number of meetings of the special working group which is overseeing the completion of the CASCADE data processing code.

The Data Library Sub-Committee considered and discussed the problem of what data should be put into the Joint European File, which is to comprise preferred nuclear data for the whole of Europe. A consistency checking method was developed and participants from all countries contributing to JEF were persuaded to accept it. As a result, there is now an agreed set of decay data selected from the British (i.e. CNDC) and French national files and these data will be included in the first edition of JEF.

The problem of fission yield data is more difficult to solve. The American (Meek and Rider) data set is in an unsatisfactory state as a result of the retirement of B.F. Rider and, in any case, is not necessarily available for European use. The UK file needs updating following the retirement of E.A.C. Crouch. A plan is now well on the way to acceptance for a three year contract to be given to Brmingham University to do this; costs will be shared between Harwell, Winfrith, CEGB and BNFL. This updated set should then be acceptable for the JEF.

The CASCADE code has now been completed and development frozen. Manuals are being written and should be ready by Easter 1984, at which time the code will be passed to the NEA Data Centre. Copies will be available on the main computers at Harwell, Winfrith and CEGB Berkeley.

Support for measurement of chemical nuclear data has been withering and stands at between 1 and 2 scientist-years in the whole of the UK. This support has been used for measurement of:

(i) certain parameters of actinide fission in fast neutron fluxes,

(ii) half-life and decay measurements of actinides, and

(iii) development of methods for the measurement of decay data of fission products having half-lives in the range 1 s - 1 h.

2.2 Alpha-particle spectrometry and low-level measurement seminar (K.M. Glover, M. Ivanovitch, A.E. Lally (AERE))

A Seminar on Alpha Particle Spectrometry and Low Level Measurement under the auspices of the International Committee for Radionuclide Metrology

was held at Harwell, 11-13 May, 1983. The Seminar was attended by 180 delegates representing countries world wide. The proceedings will be published in Nucl. Instr. Meth., May 1984.

2.3 Fission measurements

2.3.1 Fast reactor nuclear data measurement (J.G. Cuninghame, H.E. Sims (AERE))

Work on this project has been mainly concerned with a change from fission yield measurements to studies of the decay schemes of very short lived fission products for the elements Mo - Ag and the rare earths ($t_{\frac{1}{2}} \sim 1$ s - 1 h). A computerised irradiation and helium jet recoil transport system has been developed for the work. It involves the use of a PDP-11/34 computer controlling both a PET and a MOUSE microcomputer, together with elaborate data acquisition software for both single and multi-parameter experiments. With this equipment complete sets of measurements can be made semi-automatically, the fission products being produced by the irradiation of ^{238}U with high energy α-particles from the Harwell Variable Energy Cyclotron. The entire system has been tested with fission products from a ^{252}Cf source and with products from the nuclear reaction $^{109}Ag + ^{12}C \rightarrow ^{121}I\ *$.

Fig. 2.1 shows the system as it is now set up. The development work is being completed by attempting to add a limited chemical separation to the products of the He jet, thus simplifying the rather complicated γ-ray spectra of mixed fresh fission products. One promising region of investigation substitutes CO as carrier gas for the jet instead of He and this appears to bring out carbonyl-forming fission products preferentially. In addition, in an experimental system the collected products are rapidly removed ($\sim$1 s) from the tape by dissolution in a jet of hot HNO_3 and then subjected to rapid separation by high performance liquid chromatography or reversed phase chromatography.

Fig. 2.2 gives an example of the sort of activities which were identified during the He jet test runs in which ^{109}Ag was bombarded with ^{12}C ions. The unknown peaks listed are almost certainly from the virtually unknown isotope ^{115}I.

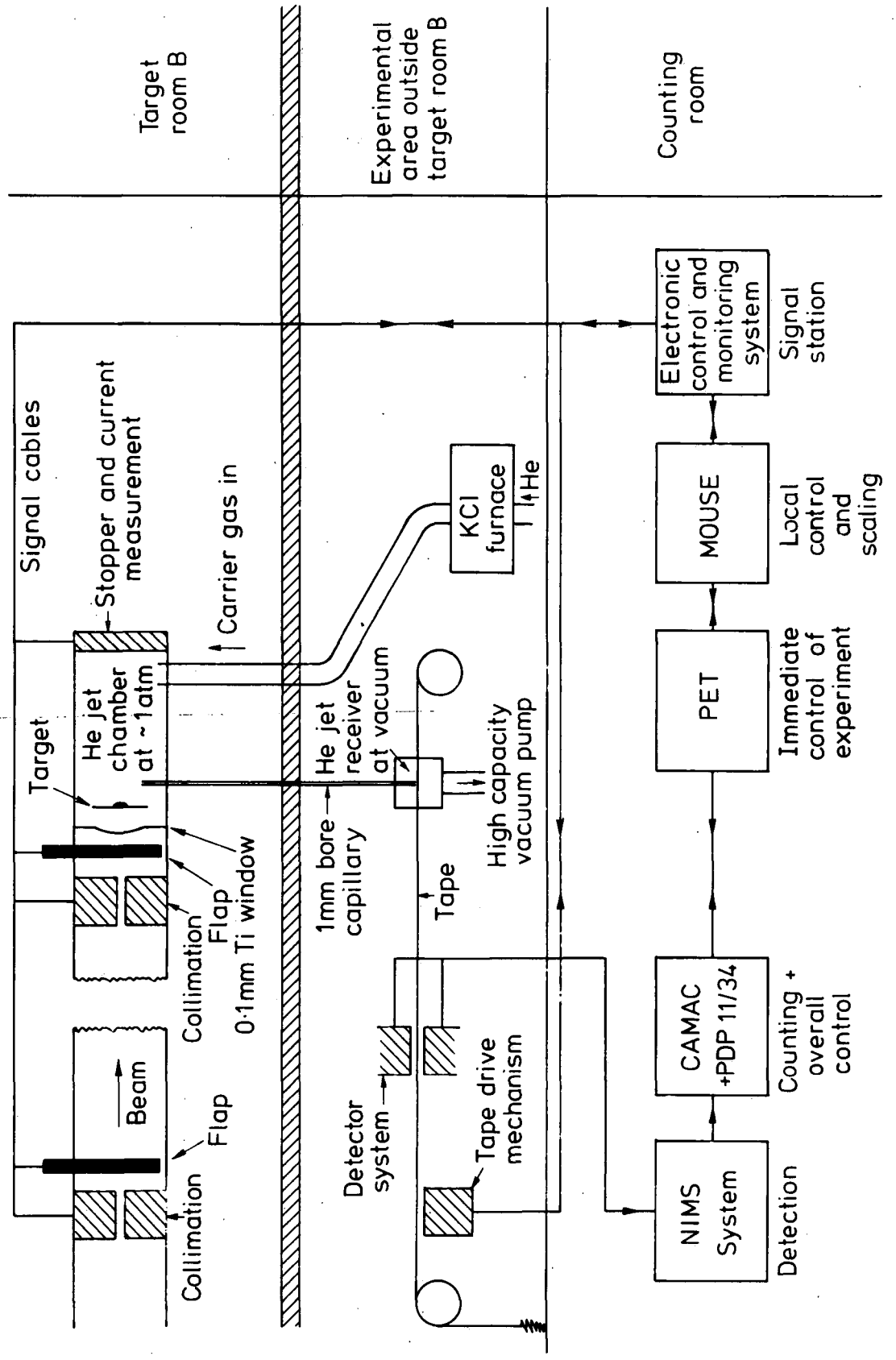

Fig. 2.1 Helium jet transport system on the Variable Energy Cyclotron. Control and data requisition are by computers

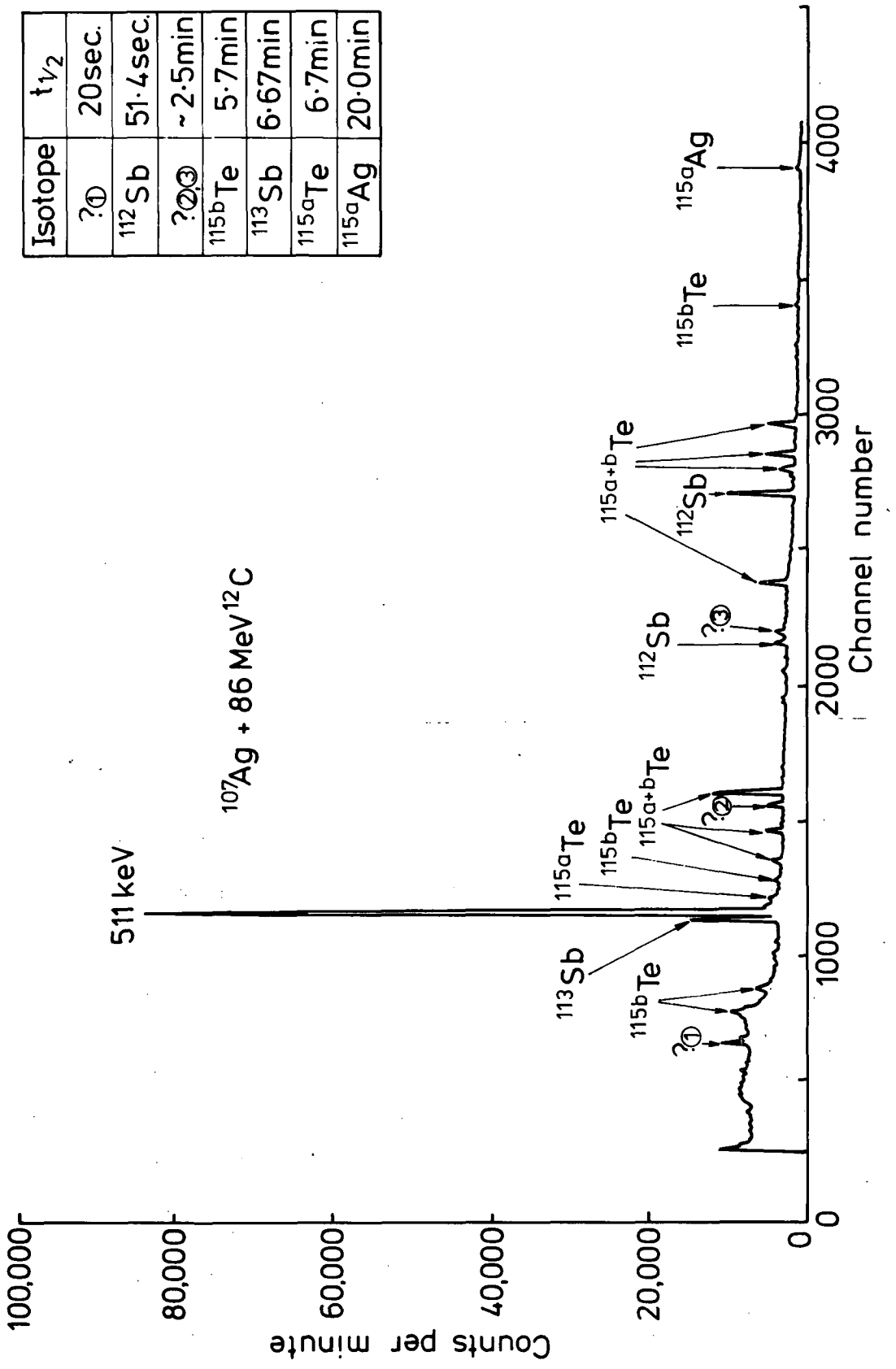

Fig. 2.2. An example of a gamma ray spectrum taken during helium jet trial runs

2.3.2 Program development using the PET/MOUSE system (J.G. Cuninghame, J.A.B. Goodall, H.E. Sims (AERE))

Programs for control and monitoring of irradiations using the helium jet system are now running routinely.

2.3.3 PDP-11 development (J.G. Cuninghame, H.E. Sims (AERE); Members of F. International)

A DEC LSI 11/23 computer has been installed with a double density floppy disk drive and 20 MB Winchester disk configured as four RLØ1 disks. This computer supports at present 5 VDUs, a DECwriter and fast printer with a TSX operating system (a multi-use RT-11). This has facilitated program development and the running of general programs, thus freeing the PDP-11/34 for sophisticated counting and experimental work.

Four new LeCroy ADCs have been purchased as replacements for ageing and unreliable NE ADCs. These ADCs have three additional 'tag' bits and the use of these has allowed the near completion of the multiparameter data acquisition program. However it was discovered that these ADCs suffer from a design fault which can cause UNIBUS errors; this has been overcome temporarily - Lecroy hope to solve the problem properly in the near future.

2.3.4 Rapid chemical separations of fission products (H.E. Sims (AERE); G. Blower, G.W.A. Newton, V.J. Robinson, G. Quirk (Manchester University))

In the first year of this project two helium jet transport systems were built, one at the Daresbury Laboratory and one at the University Research Reactor, Risley. The latter is a dual purpose unit and the former has three functions.

At Daresbury there is a cryostatic helium jet which transports short-lived isotopes over about 1 m using pure helium at 77°K and below. There is also a conventional KCl aerosol helium jet and a rabbit system. These have required considerable engineering development and there are no results yet with this system. The microprocessor control has been developed and the system will be ready for use in Jan. 1984.

At the University Research Reactor, Risley the system has been built to transport fission products from the thermal neutron fission of ^{235}U using either CO/He or KCl aerosol/He gas mixtures. For the latter, quantitative transport of the fission products is obtained without any chemical separation, but for the former (CO/He), some separation seems to be achieved. There is a significant number of gamma rays in the transported material as shown in Table 2.1; so far only some of these have been

identified but work is progressing. In addition there are eight gamma lines with $t_{\frac{1}{2}} < 2$ m requiring further investigation.

The VEC helium jet system will be used in future work on this project, in addition to the systems mentioned above.

Table 2.1

Gamma rays from isotopes from ^{235}U thermal fission transported by CO/He mixtures

Measurement		Identified as			
E_γ (keV)	$t_{\frac{1}{2}}$	Isotope	$t_{\frac{1}{2}}$	energy keV	(abundance) %
191.7	12 m				
211.9	27.2 m				
219.7	1.34 m				
256.4	4.8 m				
278.5	18 m				
345.0	3.5 m				
358.8	12.3 m				
408.6	11 m				
455.5	43 m				
463.4	33 m	^{138}Cs	32.2 m	462.8	(30.7)
512.2	23 m				
546.0	-				
591.4	5.1 m				
697.6	3 m				
794.2	-				
840.6	6.5 m	^{130}Sb	6.3 m	839.4	(100)
943.4	-	^{131}Sb?			
974.8	-	^{131}Sb?			
989.9	-	^{132}Sb?			
1010.8	30 m	^{138}Cs	32.2 m	1009.8	(29.8)
1032.9	14 m	^{89}Sb	15.4 m	1031.9	(53.6)
1248.0	14 m	^{89}Rb	15.4 m	1247.0	(46.7)
1436.3	27 m	^{138}Cs	32.2 m	1435.9	(70)

2.3.5 Comparison of heavy-ion and fission yields (H.E. Sims (AERE); G. Blower, G.W.A. Newton, V.J. Robinson, G. Quirk, (Machester University))

This project is in its final stages. Its purpose has been to look at elements which are formed in symmetrical fission of uranium isotopes e.g. Y to I, but to form them in heavy-ion reactions using Nb and Mo targets. The efficiency of transport by helium jet techniques have been measured and the results used for the fission studies. A large number of systems have been studied, using ^{3}He, ^{12}C, ^{14}N and ^{16}O beams on Nb and Mo targets, and absolute yields of various products have been measured. The latest systems to be studied were ^{3}He and ^{16}O on ^{92}Mo (97.4% enriched). The ^{3}He experiment was conducted to investigate ^{90m}Tc ($t_{\frac{1}{2}}$ = 49.2 s). The relative abundances of the two main gamma peaks are:

E_γ	a_γ(literature)	a_γ(this work)
948.1	100	100
1054.3	100	58

Careful measurements, allowing for ^{88m}Nb decay, have revealed a discrepancy in the literature gamma abundance of the 1054.3 keV peak.

In the case of $^{92}Mo(^{16}O,xy)Z$ reactions a wide range of products have been identified and these are of considerable interest in a study of the mechanism of damped transfer reactions. As an example the absolute yields of yttrium isotopes at four energies are shown in Table 2.2. These are interesting because they involve the transfer of three protons from the target to the projectile, a reaction mode not accounted for in many models.

A Ph.D thesis which contains all the data on the Nb and Mo reaction systems is being prepared.

2.3.6 Tritium yields (I.C. McKean, H.E. Sims, H.H. Willis (AERE))

Work continues to be held up for lack of staff. A further delay has been imposed by the loss of fumehoods that were to have been used for ^{3}He separations. These separations will now be carried out in a glove box and a case is now being prepared for submission to the Glove Box Working Party for permission for the work to proceed.

Table 2.2

Absolute yields of yttrium isotopes in the reaction

$^{92}Mo(^{16}O,^{16}O\ 3pxn)^{89-x}Y$

Product	^{16}O Energy (MeV)	Absolute cross-section (mb)
^{84g}Y	185.1	2.6
"	177.0	2.7
"	169.4	2.0
"	159.7	0
^{85g}Y	185.1	9.6
"	177.0	8.8
"	169.4	8.4
^{86g}Y	185.1	15.9
"	177.0	13.2
"	169.4	12.0
^{87m}Y	185.1	26.3
"	177.0	20.9
"	169.4	23.7

^{85g}Y, ^{86g}Y and ^{87m}Y are cumulative yields for that mass chain

2.3.7 ^{236}Pu alpha-particle energy (R.A.P. Wiltshire (AERE); A. Rytz (BIPM Paris))

The alpha particle energy of ^{236}Pu has been measured as a collaborative project. The ^{236}Pu was prepared by VEC irradiation using the reaction

$$^{238}U(p,3n)\ ^{236}Np \xrightarrow[\beta]{22h}\ ^{236}Pu \quad (50\ MeV)$$

The irradiated target was processed chemically and the plutonium fraction separated. Sources were prepared at Harwell for measurements in the BIPM uniform field magnetic spectrometer. The measurements gave the following values:

	Energies (keV)	Abundances (%)
α_0	5767.66 ± 0.08	69.26 ± 0.45
α_{47}	5721.00 ± 0.10	30.56 ± 0.45

A measurement of the ^{228}Th alpha particle energy is planned for 1984.

2.3.8 ^{235}U fission mass and counting intercomparison and standardisation (R.A.P. Wiltshire (AERE); B.L.H. Burbidge (AEE Winfrith))

The accuracy of the ^{235}U fission cross-section does not meet the requirement for reactor calculations. A major factor is the uncertainty associated with the mass of the deposit constituting the target in a cross-section measurement, the deposit normally being assayed by alpha counting. The group has participated in an international counting intercomparison and standardisation of ^{235}U fission deposits co-ordinated by Poenitz of Argonne National Laboratory. Uniform ^{235}U deposits, 20 mm diameter, were prepared by vacuum evaporation on to stainless steel substrates, and assayed both at Harwell and Winfrith by defined solid angle counting, and at Harwell in a medium geometry counter. The uranium isotopic composition was assayed mass spectrometrically. The fission cross-section measurements were performed at Argonne. The sample masses on the two foils measured by Harwell and Winfrith were in close agreement with the values obtained by Argonne.

Foil	Sample mass (Harwell/Winfrith) quoted μg uranium	Sample mass (Argonne) quoted μg uranium
HAR A	346.1 ± 2.2	346.5 ± 1.6
HAR B	348.0 ± 2.2	346.8 ± 1.6

The combined uncertainties take account of those arising from deposit diameter, uniformity, isotopic impurities, dead-time correction, back-scatter and self-absorption corrections.

2.4 Cross-section measurements

2.4.1 Integral experiments to measure the partial capture cross-sections for the production of ^{242m}Am and ^{242}Cm from ^{241}Am and ^{244}Cm from ^{243}Am using ZEBRA (R.A.P. Wiltshire, K.M. Glover and B. Whittaker, (AERE))
(WRENDA 1276, 1278, 1280, 1281, 1283, 1284)

The purified ^{241}Am fractions remaining from the ZEBRA core 21 samples have been retained and archived for future measurements of the $^{242m}Am/^{242g}Am$ production branching ratio by the ingrowth of ^{242}Cm from ^{242m}Am.

2.4.2 PFR high power reaction rate samples (R.A.P. Wiltshire, K.M. Glover, W. Snooks, D. Anstee (AERE))
(WRENDA 1277, 1282, 1305, 1306, 1308, 1310)

150 μg samples of ^{241}Am and ^{243}Am have been irradiated in the mid and outer core regions of PFR for measurement of the production rates of ^{242}Cm and ^{244}Cm. The samples were irradiated in silica ampoules. These have been

dissolved and the products analysed by alpha and gamma spectrometry on sources prepared directly from the irradiated material without prior separation of americium and curium. The data from these measurements are at present being evaluated.

2.5 Decay Data

2.5.1 ^{235}Np decay data (B. Whittaker (AERE); J.L. Campbell (Guelph University, Canada))

A 3 μCi ^{235}Np source in the form of a high purity solid deposit on a mylar substrate was prepared at Harwell for K and L X-ray measurements at Guelph University, where the source was analysed by a high resolution LEPS detector and computer fitting codes. The K and L X-ray emission rates were measured by reference to the detector efficiency curve derived from a set of gamma standards used in an international intercomparison exercise. On 22/3/83 the X-ray rates were found to be 1980 s^{-1} and 3.904 x 10^4 s^{-1} respectively. The source was returned to Harwell and is being used as a standard. In the course of the Guelph measurements a previously unreported shoulder was observed at 89 keV. To improve the quality of this data a 30 μCi ^{235}Np source has been prepared at Harwell and loaned to Guelph. The absolute L and K X-ray intensities measured at Guelph are in good agreement with Nichols' evaluated data:

	Guelph measurement	Nichols' evaluation
Total K-shell X-ray intensity %	1.96 ± 0.20	1.94 ± 0.20
Total L-shell X-ray intensity %	37.8 ± 4.0	34.0 ± 5.0

2.5.2 ^{235}Np alpha branching B. Whittaker (AERE))

Quantities of ^{235}Np can be assayed either by 2π proportional alpha counting and alpha spectroscopy using a surface barrier detector or by K_α X-ray counting. However the results of an assay using these two methods were discrepant, being 510 and 330 μCi respectively. This was attributed to an error in the alpha branching fraction.

The ^{235}Np alpha branching fraction has been remeasured using two sources of 9 and 4 μCi respectively prepared on tantalum discs from freshly purified ^{235}Np. The 3 μCi ^{235}Np source calibrated at Guelph was corrected

for decay using a ^{235}Np half-life value of 396.1 days and used as standard for direct comparison of the K_α X-ray emission rates. The sources were counted using a 2π gas flow proportional counter and a silicon surface barrier detector for the alpha measurements and a co-axial Ge(Li) detector for the X-ray activity. Using a value of 1.96% for the total K X-ray absolute intensity and established relative intensities for the K_α doublet and K_β multiplet, values of 0.00270% and 0.00268% for the alpha branching of the two sources were obtained. Using the new value, a better agreement was obtained between the ^{235}Np yield measured by alpha assay and that obtained by K_α X-ray assay, 265 and 330 μCi respectively.

2.5.3 ^{235}Np half-life (B. Whittaker (AERE))

This is being measured using a ^{235}Np solution internally spiked with ^{241}Am, and a tentative half-life of 385 ± 4 days has been reported. Further work during this period has been retarded by detector problems.

2.5.4 ^{237}Pu half life (B. Whittaker (AERE))

^{237}Pu decays by electron capture to ^{237}Np producing a 59.5 keV gamma ray and characteristic Np X-rays. The half-life of ^{237}Pu is being measured by observing the decay of the K_α and K_β X-rays and the 59.5 keV gamma ray at weekly intervals. It is anticipated that the measurement will be completed during 1984.

2.5.5 ^{242}Cm half-life (R.A.P. Wiltshire (AERE))

In a fast reactor with plutonium as the fuel there is a build up of ^{242}Cm; it is therefore important to know the alpha and spontaneous fission decay constants. The spontaneous fission half-life is particularly important since fission neutrons can lead to problems associated with reactor control, fuel handling and reprocessing of spent reactor fuel.

The IAEA International Nuclear Data Committee have recommended a value for the ^{242}Cm alpha half-life of 162.8 ± 0.4 days. A recent measurement by Usuda and Umezanta in Japan gave a value of 161.35 ± 0.30 days, considerably lower than any previously reported value. The IAEA indicated that additional measurements were required. The ^{242}Cm half-life has been measured by direct decay using a defined solid angle counter - a value of 163.03 ± 0.16 days was obtained, in good agreement with the IAEA recommended value. Measurements were made on four sources over a period of 490 days. The ^{238}Pu in-growth was measured directly by alpha spectrometry and the ^{243}Cm content was measured after 400 days by mass spectrometry. The overall

uncertainty of the measurement was ±0.1%. Measurement of the spontaneous fission half-life of ^{242}Cm is planned.

2.6 Chemical Nuclear Data Library Sub-Committee

During the year the Data Library Sub-Committee (DLSC) lost the services of Mr. B.S.J. Davies (CEGB). This resulted in reorganisation of the DLSC, which became: A. Tobias (Chairman, CEGB/BNL), H.E. Sims (Secretary, AERE), K.M. Glover (AERE), A.L. Nichols (AEEW), M.F. James (AEEW), V. Barnes (BNFL), and D.G. Vallis (AWRE).

2.6.1 Data Library development

The current status of the UKCNDC data libraries is summarised in Table 2.3.

Efforts have begun to construct a new fission product decay data library, UKFPDD-3. Decay data which had been extracted from the Evaluated Nuclear Structure Data File (ENSDF) for UKFPDD-2 have been re-examined and processed by COGEND[1] to produce ENDF/B-V format decay data. These have been supplemented by recently published data for ~40 short-lived nuclides which have also been processed to ENDF/B-V format. The remaining fission product data, which in UKFPDD-2 had been taken from either US-ENDF/B-IV or an earlier UK evaluation, have still to be updated. These data will be taken from either ENSDF or the CEA data libraries and will be supplemented by appropriate theoretical data, possibly from the JNDC data library.

The activation product decay data library UKPADD-1 has been processed to ENDF/B-V format. Work has progressed on the evaluation of nuclides for a new library UKPADD-2. A total of 60 evaluations have so far been completed, of which 56 have been processed into ENDF/B-V format.

The fission yield data base and evaluation codes used by Crouch at AERE Harwell are in the process of being implemented at AEE Winfrith. It is intended that these will be used to provide a partially updated evaluation of both constrained and unconstrained fission yields. The DLSC is also considering ways in which these yield data could be completely updated.

The current status and future development of the UKCNDC data libraries have been described by members of the DLSC in a number of conference papers and publications during the year[2-5].

Table 2.3

UK Chemical Nuclear Data Libraries status, Oct. 1983

Data	Present Status	File Development
1. Fission Product Decay Data	Exists as UKFPDD-2 (ENDF/B-IV format); replaces UKFPDD-1 Total no. of nuclides = 855 Radioactive nuclides = 736 Ground state = 175 1st excited state = 133 2nd excited state = 5 Nuclides with spectra = 390 Total no. of γ lines = 11978 Total no. of β^- lines = 3592 Total no. of β^+ lines = 91	Data acquisition for future revision. Some data have been converted to ENDF/B-V format.
2. Activation Product Decay Data	Available in ENDF/B-IV and V format for 91 nuclides as UKPADD-1	60 nuclides have been evaluated for UKPADD-2, 56 are in ENDF/B-V format.
3. Heavy Element and Actinide Decay Data	Completion of UKHEDD-1, including spontaneous fission data in June 1982. Data in ENDF/B-V format for: Total no. of nuclides = 125 Ground state = 111 1st metastable state = 13 2nd metastable state = 1 Total no. of alpha lines = 767 Total no. of β^- lines = 527 Total no. of β^+ lines = 39 Total no. of γ lines = 3475 Total no. of discrete electrons = 6755 Total no. of X-rays = 381.	Report AEEW-R1407 has now been issued.
4. Fission Yields	Available in ENDF/B-IV format, based on Crouch's second round of adjustment (Crouch 3). 60 new compilations have been added. Yields to isomeric states have been calculated on basis of ENDF/B-IV ratios and are included.	Crouch's data files and programs will be used (in ENDF/B-IV and V formats) to produce updated libraries of both unconstrained and constrained yields. These will also generate most of the necessary documentation.
5. Delayed Neutrons	Tomlinson data are still recommended.	Delayed neutron emission probabilities and half-lives of precursors have been evaluated. The DLSC requires access to these data. Neutron spectra await evaluation.
6. (α,n) cross-sections	A library now exists for all α emitters in oxide fuel; for use with UKHEDD-1.	Published as DIDWG paper DIDWG(82)P268

Spectral data from the decay data files may be accessed via the retrieval system described by Tobias (CEGB report RD/B/5170N81 (1981)).

(1) CEGB report RD/B/N4147.

(2) A.L. Nichols and A. Tobias, 'Evaluated Decay Data for Reactor Applications: The UKCNDC Data Libraries', ICRM Seminar on Alpha Particle Spectrometry and Low Level Measurement: Intercomparisons and Evaluations, Harwell, May 1983, to be published Nucl. Instr. Meth. (1984).

(3) A.L. Nichols, 'Revision of the Evaluated UKCNDC Activation Product Decay Data Library', ICRM Seminar on Applied Radionuclide Metrology, Geel, May 1983, Int. J. Appl. Radiat. Isot. 34 (1983) 1249.

(4) A. Tobias, 'The UKCNDC Data Libraries', UK Nuclear Data Forum, Imperial College Reactor Centre, Silwood Park, Ascot, Dec. 1983.

(5) A. Tobias, B.S.J. Davies, A.L. Nichols, M.F. James, 'The UKCNDC Radioactive Decay Data Libraries', BNES Journal, 22 (1983) 445.

2.6.2 Brookhaven Conference

The DLSC was represented by A. Tobias (CEGB) and M.F. James (AEEW) at the Specialists Meeting on the Yields and Decay Data of Fission Products held at Brookhaven National Laboratory USA, Oct. 1983. An invited paper on Problems in Decay Heat Evaluation was presented by M.F. James.

At the meeting the 'Pandemonium effect' for short-lived fission products was noted. This results in an overestimate of average beta energies and corresponding underestimate of average gamma energies derived from decay schemes. The direct measurement of these parameters for separated fission products was recommended. In addition the use of beta strength functions to derive these quantities was encouraged in preference to values derived from decay schemes for short-lived high Q value nuclides.

The meeting warmly encouraged the continued free exchange of decay data libraries between different countries, and reinforced previous recommendations for a standard format, namely ENDF/B-V which is used by the DLSC.

2.6.3 Joint Evaluated File

The DLSC is represented by Tobias, Nichols and James on the International Working Group responsible for setting up the fission yield and decay data components of the Joint Evaluated File (JEF). Nichols and Tobias have examined the decay data present in both the French and UK data libraries and have proposed selection criteria to be applied in the construction of JEF1. These were discussed at a meeting of the Working Group earlier in the year at which it was agreed that data selection would be based upon decay scheme consistency.

James has examined the available fission yield evaluations considered for JEF. The CEA data file uses the chain yields of Meek and Rider in conjunction with a simple Gaussian independent yield. In contrast the Crouch evaluation is completely independent of the US evaluation work and has utilised a number of physical constraints in the production of an adjusted set of data. James has proposed that the Crouch evaluation is adopted for the JEF because in an addition to those items noted above it forms a valuable basis for future work.

2.6.4 CASCADE

Development of this suite of programs has been completed by G. Evangelides (Daresbury Laboratory), and a number of draft manuals written. They have been critically reviewed and discussed by the Data Library Sub-committee, and following revision and editing will be reconsidered early in 1984. It is intended to release the program and this documentation to users and to the NEA Data Centre in the summer.

3. REACTOR PHYSICS DIVISION, AEE WINFRITH

(Division head: Dr. J.R. Askew)

3.1 Cross-section processing codes (R.W. Smith, M.F. James)

The US cross-section processing package NJOY has been provided with an option for the generation of cross-section point-by-point tabulations from resolved resonance parameters using the UKAEA code SIGAR7. Using this facility unbroadened cross-section point-by-point tabulations over the resolved energy range have been produced for all the materials in the ENDF/B-V Dosimetry Library. Results from NJOY and NJOY/SIGAR7 routes have been processed into the format of the 620 SAND-2 group structure and sent to the IAEA at Vienna as the UK contribution to Stage 1 of the IAEA Cross-Section Processing Code Verification Project. Work on the broadening option is nearing completion, these results constituting Stage 2 of the IAEA exercise.

3.2 Resonance parameter evaluation of the isotopes of iron (R.W. Smith)

The resonance parameter evaluation for ^{54}Fe has been completed.

3.3 Heavy element decay data (A.L. Nichols, M.F. James)

The following report has been issued:

Radioactive Heavy Element-Decay Data for Reactor Calculations, A.L. Nichols and M.F. James, AEEW-R 1407 (1983).

3.4 Activation product decay data (A.L. Nichols)

Work on the development of a new activation product decay data library (UKPADD-2) has continued. Data for 56 nuclides (H to Cd) have been processed into the ENDF/B-V format.

4. DIVISION OF RADIATION SCIENCE AND ACOUSTICS, NATIONAL PHYSICAL LABORATORY

(Superintendent: Dr. K.C. Shotton)

4.1 ^{252}Cf neutron source emission rate intercomparisons (E.J. Axton and A.G. Bardell) (organised by BIPM*)

4.1.1 NBS Source SR144 coordinator E.J. Axton (NPL))

(Emission rate approximately 4.5×10^7 s^{-1} at the start of the intercomparison.)

Measurements were made between September 1978 and March 1983 by twelve participants, and these, listed in chronological order, are:

Laboratory*	Country	Reference date	Method
NBS	USA	May 1978	relative to source NBS1
BIPM	-	October 1978	$MnSO_4$ bath
PTB	FRG	January 1979	gold foil integration
CNEN	Italy	April 1979	$MNSO_4$ bath
CEN, Bruyeres-le-Chatel	France	July 1979	BF_3 counter/moderator; relative to $\bar{\nu}$ (^{252}Cf)
ASMW	GDR	July 1980	$MnSO_4$ bath
VNIIM	USSR	October 1980	$MnSO_4$ bath; gold foil integration; associated particle counting
VGKRI	USSR	January 1981	$MnSO_4$ bath
ETL	Japan	January 1981	$MnSO_4$ bath
NPL	UK	May 1981	$MnSO_4$ bath
BARC	India	-	$MnSO_4$ bath
LMRI	France	-	$MnSO_4$ bath
NBS	USA	February 1983	relative to source NBS1

It was not possible to send the intercomparison source to India. To enable Indian participation a bilateral comparison was accomplished between NPL and BARC by means of an NPL ^{252}Cf source.

In addition to the above programme a bilateral comparison was

*For abbreviations see UKNDC(82)P105 p. 71

accomplished between NPL and INEL as part of the ^{252}Cf programme.

After the measurement programme was completed, a request was received from the Institute of Atomic Energy, Beijing (IAEB) for a bilateral comparison between IAEB and NPL using an NPL ^{252}Cf source. Instead, arrangements have been made to send the SR144 source to China.

Eight of the twelve participants have submitted full reports on their work, two have submitted brief statements, and two have so far provided no information. In view of the intended 'blind' nature of the comparison it is not considered advisable at this stage to divulge fully the results received so far. Full reports have been promised for early June by three laboratories. A full report will be prepared as soon as the full data set is available. It is not proposed to delay the analysis further to include the Chinese participants.

Including INEL, ten laboratories used the manganese bath method, two used the gold foil integration method, and one used associated particle counting. One laboratory made measurements relative to $\bar{\nu}$ for ^{252}Cf. The NBS measurements were relative to the NBS standard Ra-Be (γ,n) source NBS1 which was calibrated in an unconventional manganese bath containing a mixture of light and heavy water. With the exception of one laboratory the manganese bath values form a cluster with a standard deviation between 0.4 and 0.5% depending on the choice of half-life. Other results differ from these by up to 7.8%. This summary is based on the results as received, no attempt having been made to adjust results to standard cross-section data or standard corrections.

In view of the importance of the purity of the manganese sulphate solution in the $MnSO_4$ bath method used by the majority participants in the comparison, two laboratories agreed to assay samples of solution from various participants. VGKRI undertook to analyse the samples by neutron activation analysis to determine the presence of rare earths. Six laboratories took advantage of this offer. The report states the levels of Sm, Eu and Gd in samples from GDR, France, India, USSR, Japan and UK. CBNM undertook to determine the Mn content by several methods, and to determine impurity levels for a number of other elements including B. Approximately seven laboratories took advantage of this offer. No results are available yet but it is believed that the measurements have been completed.

The duration of the calibration was 4.8 years, a period long compared with the half-life of ^{252}Cf, the choice of which has become a problem. The

source contains a mixture of Cf isotopes, of which the neutron emitters are ^{250}Cf, ^{252}Cf and ^{254}Cf. In order to correct the data as received to a single reference date, it is necessary to know the relative abundances present at the time of the assay together with certain associated nuclear data. The only controversial datum is the half-life of ^{252}Cf, for which values between 2.638 and 2.651 years are in use at different laboratories.

4.1.2 NBS Source SR255Z (coordinator W.G. Alberts (PTB))

(Emission rate $\sim 10^9$ neutrons s^{-1} at the start of the comparison.)

Only three laboratories are participating in the comparison. NBS completed measurements in 1977 and PTB the following year. The source is currently at NPL, where difficulties were encountered in the safe handling of the source. Measurements are expected to be completed in 1984.

4.2 Fast neutron fluence intercomparisons (organised by BIPM)

4.2.1 Transfer method using the $^{115}In(n,n')^{115m}In$ reaction at 2.5, 5.0 and 14.8 MeV (coordinator H. Liskien (CBNM))

Seven laboratories participated at 2.5 MeV, four at 5.0 MeV and nine at 14.8 MeV. All measurements were completed in 1981 and a detailed analysis of the results was presented by the coordinator. The analysis involved careful consideration of the correlations between the measurements of the different laboratories and between the measurements at different energies by the same laboratory. A clear distinction was made between the uncertainties in the neutron fluence measurements at each laboratory and those inherent in the intercomparison method.

The results for the two lower energies were reasonably satisfactory and will be published in 1984. However at 14.8 MeV difficulties occurred with the rather large corrections for room-scattered and target-scattered neutrons, which have a disproportionate effect due to the high value of the reaction cross-section at low neutron energies relative to that at 14.8 MeV. The comparison, therefore, serves to highlight the difficulties involved in the practical measurements of neutron capture cross-sections, some of which can be required as secondary standards for the measurement of neutron fluence, and in the calibration of certain instruments used for the measurement of neutron dose equivalent in the field of radiation protection. Some laboratories withdrew their results and others submitted revised values which were not always 'blind'. It was therefore decided that a thorough study of the corrections involved should be carried out using Monte Carlo calculations and other methods.

4.2.2 Transfer methods using $^{115}In(n,\gamma)^{116m}In$ reaction at 0.144 and 0.565 MeV (coordinator T.B. Ryves (NPL))

Six laboratories are participating in sequence in this comparison. Measurements at four laboratories have already been completed. The comparison is proceeding satisfactorily and measurements are expected to be completed by the end of 1984.

4.2.3 Transfer method using twin ^{235}U and ^{238}U fission chambers (coordinator D.B. Gayther (AERE))

The two chambers, one containing ^{235}U and the other containing ^{238}U fissile deposits, have been assembled. Tests with neutron sources show that the design specification has been achieved. Trial runs on pulsed Van de Graaff accelerators at AERE and NPL revealed no problems.

The chambers must be regarded as transfer devices for the intercomparison of neutron fluence measurements: the ^{235}U chamber at 0.144, 0.565, 2.5, 5.0 and 14.8 MeV, and the ^{238}U chamber at 2.5, 5.0 and 14.8 MeV. It will be possible to relate the measurements to the fission cross-sections of ^{235}U and ^{238}U, provided that corrections can be applied for loss of fragments in the fissile deposits and for the effect of neutron scattering in the deposit backings. Accordingly, great care was taken to characterize the fissile deposits. The total fissile mass present in each chamber was determined by direct weighing and checked by medium-geometry alpha counting. Additional foils were made and destructively assayed to confirm these measurements. The fissile content of each chamber has thus been determined with an uncertainty of 0.2%, but the figure will not be released until all the fluence measurements have been made. The uniformity of the thickness of each fissile deposit has been checked by measurements taken on autoradiographs and also by alpha counting from selected regions. For most measurements, the slight variation (a few per cent) in deposit thickness across the foils is of no consequence for the intercomparison, but for certain techniques, such as the associated particle technique, the variation in thickness must be known. The autoradiographs and selected alpha-counting data are still being analysed to determine this variation.

One laboratory has completed measurements, and eight others have agreed to participate.

4.3 The $^{65}Cu(n,2n)$ cross-section at 14 MeV (G. Winkler*, T.B. Ryves)
(WRENDA 510)

A paper describing the above work has been published[1] with the following abstract:

The cross-sections for the reaction $^{65}Cu(n,2n)^{64}Cu$ were measured at 13.692, 14.473 and 14.822 MeV using the activation technique with an accuracy of 1.4 - 1.5% relative to well known cross-sections for the reference reaction $^{27}Al(n,\alpha)^{24}Na$. The reaction $^{3}H(d,n)^{4}He$ was used to produce the neutrons. Activity measurements were performed with a 12.7 x 12.7 cm NaI(Tl) well-type detector using a recently measured value for the β^{+}-branching ratios of ^{64}Cu.

The new cross-section values were incorporated in a combined re-evaluation of the $^{65}Cu(n,2n)^{64}Cu$ cross-section and some other important cross-sections at 14.70 MeV yielding a consistent set with uncertainty (1σ) of 0.6 - 2.0%. The uncertainty for the evaluated $^{65}Cu(n,2n)^{64}Cu$ cross-section could be reduced to 1.2%.

---

(1) G. Winkler and T.B. Ryves, Ann. Nucl. Energy 10 (1983) 601.

4.4 Indium cross-sections between 14 and 18 MeV (T.B. Ryves, Ma Hongchang**)
(WRENDA 660)

The final results have now been published[1] with the following abstract:

The cross-sections for the reactions $^{113}In(n,2n)$ and (n,n') and $^{115}In(n,n')$, (n,p) and (n,α) at 14 MeV, and $^{115}In(n,2n)$ from 14 to 18 MeV were measured by the activation technique. Special emphasis was placed on the accuracy of the results, and so full experimental details are included. The correlations between the measurements are considered, these being especially important for $^{112m,g}In$.

Isomeric cross-section ratios were measured at 14.3 MeV: σ_m/σ_g = (4.32 ± 0.20) for $^{113}In(n,2n)^{112m,g}In$ and σ_m/σ_g = (4.59 ± 0.03) for $^{115}In(n,2n)^{114m,g}In$. The results were compared with other published values, which show a very wide spread so that these cross-sections cannot be considered well known at the present time.

During the course of the work half-lives were measured for

---

*IRK Vienna

**Institute of Atomic Energy, Beijing

^{112g}In (14.97 ± 0.10 min), ^{112m}In (20.56 ± 0.06 min) and ^{114g}In (71.6 ± 0.1 s). The decay scheme of ^{114m}In was investigated, and γ-ray intensities and a total internal conversion coefficient of 5.101 ± 0.061 for the 190 keV γ-ray were obtained. In the case of ^{112m}In arguments are presented to support the theoretical internal conversion coefficient for the 156 keV γ-ray of 6.80.

---

(1) T.B. Ryves et al. J. Phys. G (Nucl. Phys.) 9 (1983) 1549.

4.5 Nuclear decay scheme measurements (P. Christmas, D. Smith, M.J. Woods, R.A. Mercer, T.B. Ryves

Half-life measurements have been continued for ^{152,154}Eu: provisional results are 4934 ± 4 d and 3138 ± 6 d respectively.

The results of the ^{64}Cu decay scheme measurements have now been published[1] with the following abstract:

The branching ratios in the decay scheme of ^{64}Cu, which decays by the emission of positrons and electrons and by electron capture, have been determined by six distinct and partially correlated measurements. From these data, best estimates, including covariances, are obtained by a generalised least-squares criterion. The electron-to-positron ratio was determined by β spectrometry and separately by a 4πβγ coincidence-counting method using a gas proportional counter. The total β branching ratio was determined by a 4πβγ method using a liquid scintillation technique. The positron branching ratio was estimated firstly by comparison using a Ge(Li) detector of the emission rates of annihilation γ-rays from sources of ^{64}Cu and ^{22}Na of known activity, and secondly by counting with a calibrated NaI well crystal the total γ-rays from a copper foil of known activity which had been irradiated in a standard thermal neutron field. In addition, the yield of the low-intensity 1.34 MeV γ-ray was determined with a calibrated Ge detector. Furthermore, an absolute counting technique using the liquid scintillator system was devised to determine the disintegration rate of ^{64}Cu, and from the β spectrometry, the electron and positron end-point energies were accurately measured.

---

(1) P. Christmas et al Nucl. Instr. Meth. 215 (1983) 397.

5. BIRMINGHAM RADIATION CENTRE, UNIVERSITY OF BIRMINGHAM

(Director: Professor J. Walker)

5.1 Delayed neutron spectrum measurements (J.G. Owen, D.R. Weaver and J. Walker)

(WRENDA 979)

Measurements of near-equilibrium delayed neutron spectra from fast fission of ^{235}U have been continued with our two ^{3}He spectrometers. Two sets of measurements have been made with fission induced by neutrons from a thick beryllium target bombarded by deuterons of 1.5 or 3 MeV from the Dynamitron accelerator; at these energies the Be(d,n) reaction gives neutrons of maximum energy 5.8 MeV or 7.4 MeV respectively. The spectrum obtained from the older, Technion detector at a deuteron energy of 1.5 MeV is shown in Fig. 5.1.

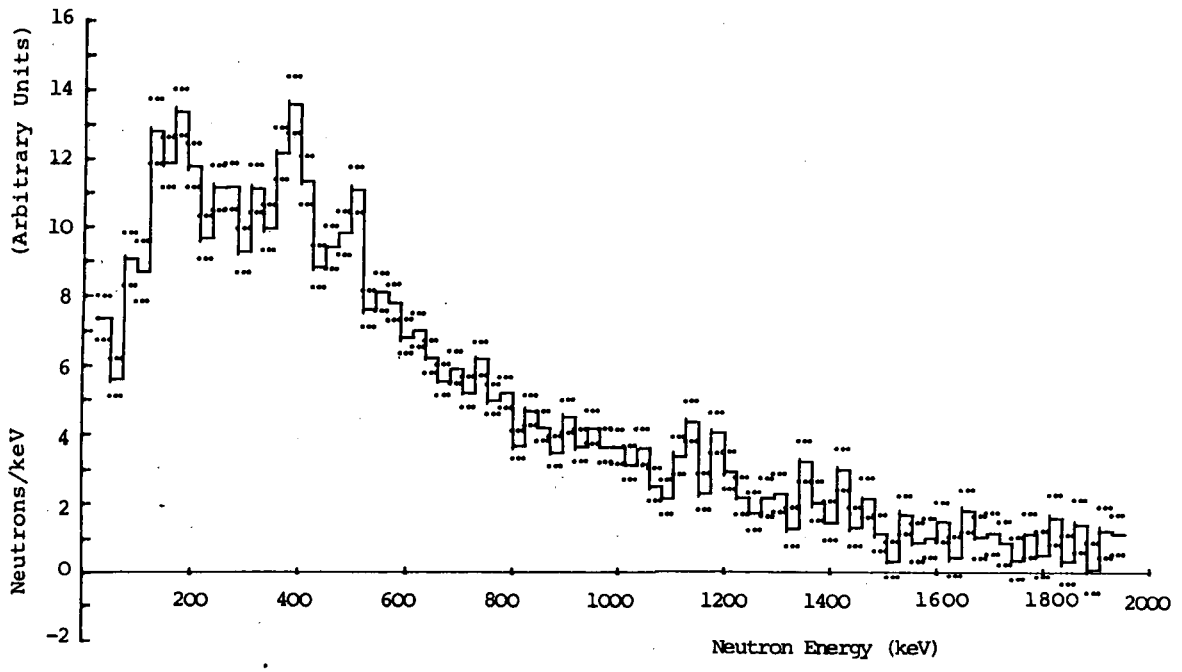

Fig. 5.1 The delayed neutron spectrum from ^{235}U irradiated with neutrons from the Be(d,n) reaction. (The delayed neutrons were measured using the older detector). (Errors are marked by dots and represent ±1 s.d.).

Following the IAEA Meeting on Delayed Neutron Properties[1], we were asked to undertake an international comparison of delayed neutron spectra in an attempt to resolve a long-standing discrepancy between results from

proton recoil and ^{3}He spectrometers. To facilitate this we developed a method of determining the full covariance error matrix for the unfolded spectra[2], and the group from Washington University, Seattle, were kind enough to supply us with their raw proton recoil data and unfolding code[3], so that we could carry out the necessary statistical analysis. During the course of modifying their code to run on our own computer, we discovered a discrepancy between the algorithm used to calculate the delayed-neutron intensity from the source and what we would have expected. The code actually calculates the neutron density at the detector, but unfortunately this is not simply proportional to the neutron yield of the source. A modification has been made to the code, and the revised spectra agree much better with the results from our ^{3}He spectrometer, as shown in Fig. 5.2. A joint paper giving details of the modification is in preparation, and it is felt that this work goes much of the way towards resolving the discrepancy between ^{3}He and proton recoil spectrometers.

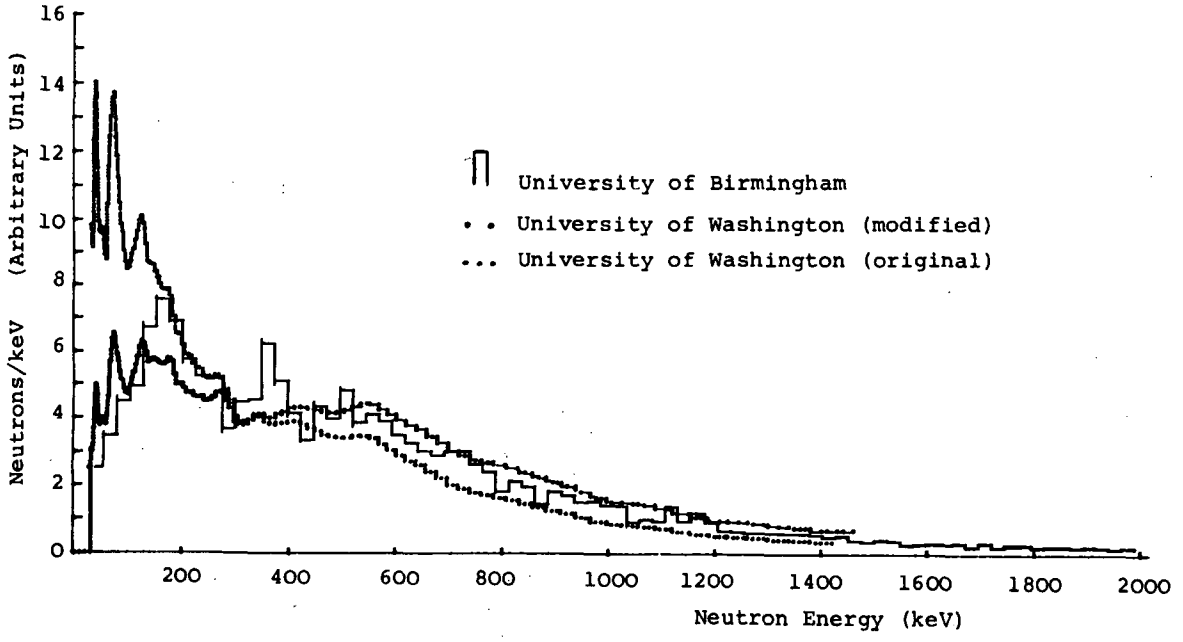

Fig. 5.2 Comparison of delayed neutron spectra from ^{235}U. (The Birmingham measurement was made using the ^{3}He spectrometer.)

(1) Proc. Consultants Meeting on Delayed Neutron Properties, Vienna (March 1979) Int. Nucl. Data Comm. Rep. INDC(NDS)-107/G+ Special (1979).

(2) J.G. Owen, D.R. Weaver and J. Walker, Nucl. Instr. Meth. 188 (1981) 579-593.

(3) G.W. Eccleston and G.L. Woodruff, Nucl. Sci. Eng. 62 (1977) 636.

6. DEPARTMENT OF PHYSICS, UNIVERSITY OF BIRMINGHAM

6.1 Measurements relating to tritium production in fusion reactor breeder blankets (D.A. Naylor and M.C. Scott)

(WRENDA 35, 39, 63, 65, 67, 68)

Measurements of tritium production from $^{6}Li(n,\alpha)$ and $^{7}Li(n,n'\alpha)$ reactions in different fusion reactor breeder blanket mock-ups have now been completed, although the comparison with calculations is not yet complete. The measurements involved ~1 tonne of LiF arranged in six 1 x 1 x 0.15 m slabs; this makes it easy to simulate different breeder blanket arrangements such as the inclusion of a graphite reflector or a stainless steel first wall. Each slab had a re-entrant hole running to the centre in the plane parallel to the square face and a hole at right angles through the centre, enabling tritium production to be measured throughout the assembly. During measurements all voids were filled with cylinders of LiF. Tritium production during neutron irradiation was measured by placing LiOH pellets within the LiF assembly and subsequently measuring the tritium produced within the pellets. The LiOH pellets were encapsulated in a LiOH case, the LiOH then being sealed in an aluminium container. The container was sealed using an interference fitted lid* to prevent tritium produced in the bulk LiF from diffusing into the LiOH pellet and being absorbed. Some of the results are shown in Fig. 6.1 for a graphite reflected LiF assembly with no first wall material, the source of the neutrons being at the centre of the front (1 x 1 m) face. The increase in tritium production in ^{6}Li associated with the graphite reflector at the back face can be readily seen as the up-turn over the last ~10 - 20 cm.

*The body of the container was shrunk by cooling in liquid nitrogen to allow the lid to be fitted.

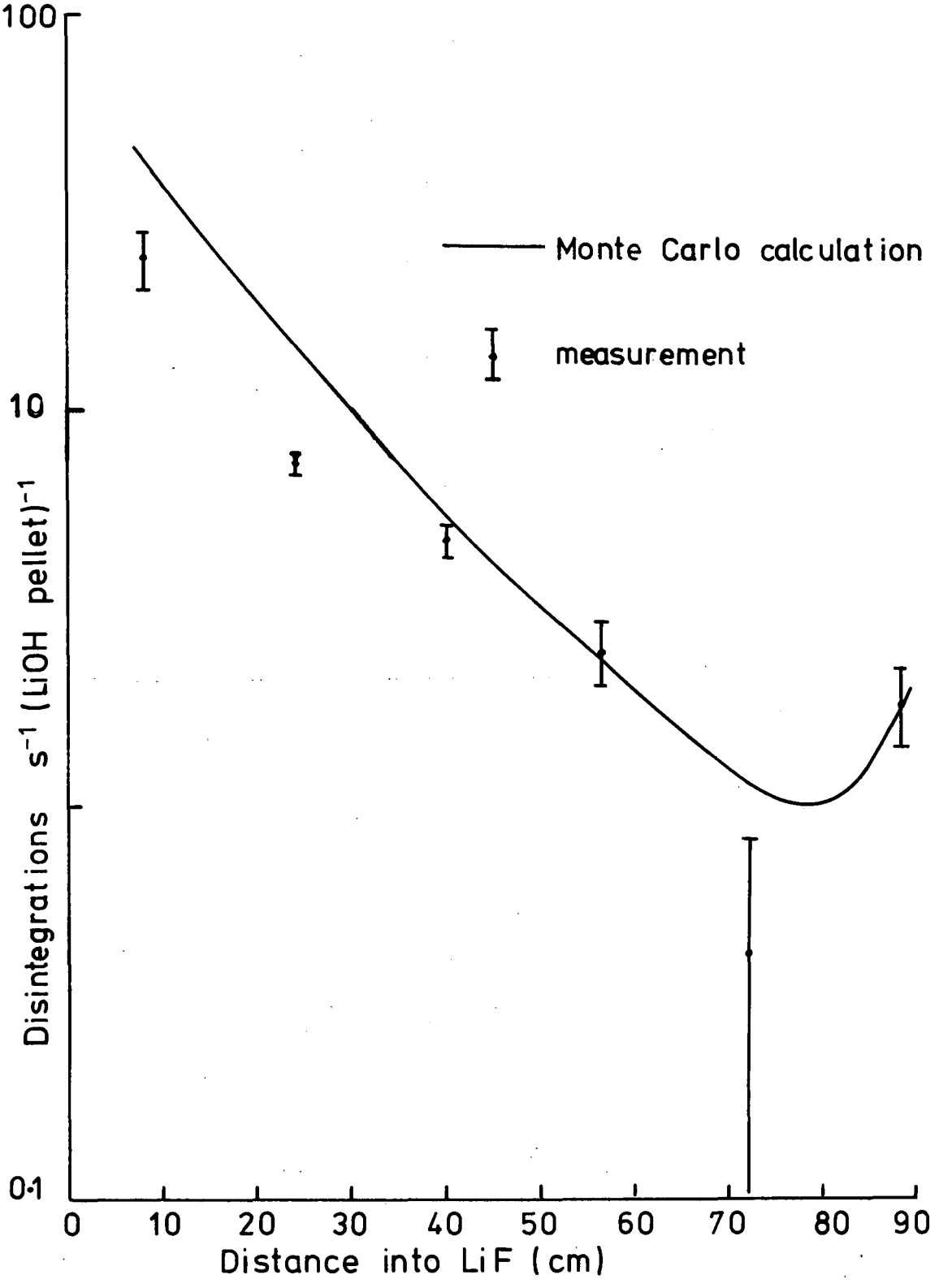

Fig. 6.1 Comparison of calculated and measured tritium disintegration rates per pellet as a function of distance into the LiF assembly for 1.18×10^{16} neutrons incident on a graphite reflected LiF assembly. This disintegration rate is of course a measure of the tritium production within the LiF assembly.

7. DEPARTMENT OF PHYSICS, UNIVERSITY OF ASTON IN BIRMINGHAM

7.1 The effect of multiple scattering on fast neutron scattering in iron and concrete (A.J. Cox and S.T.P. Anvarian) (WRENDA 341)

The angular distribution from 0 to 90° of 14 MeV neutrons elastically scattered from various thicknesses of iron and concrete have been measured using an associated particle time-of-flight technique to determine the neutron energy. There appears to be no previous published data for concrete.

The 14 MeV neutrons were generated by the $^{3}H(d,n)^{4}He$ reaction using a rotating water cooled $^{3}H/Ti$ target. Deuteron beams from both a 150 kV SAMES type J accelerator and the Birmingham Radiation Centre 3 MV Dynamitron accelerator were used.

The alpha-particles associated with neutron production and emitted at 90 ± 6° to the deuteron beam direction were used to give the zero-time signal and to monitor the neutron flux. These alpha-particles were detected using a thin 0.5 mm NE102A plastic scintillator mounted on a 56AVP photomultiplier tube. The count rate from the alpha detector was corrected for background radiation and counts due to fast neutron detection. The alpha detector was shielded from elastically scattered deuterons by a 0.0044 mm thick Al foil.

The neutron detector was a cylindrical block* of NE102A plastic scintillator, 5 cm thick and 10 cm in diameter, mounted on a 56AVP photomultiplier tube via a conical perspex light guide. The neutron detector was shielded by concentric cylinders of paraffin wax, boric oxide and lead. It was also shielded from the neutron source by a paraffin wax shadow bar. The time resolution of the spectrometer was found to be 2.5 ± 0.2 ns FWHM.

The concrete samples consisted of normal Harwell type 5 concrete with a density of 2.5 g cm^{-3}. Each was 23 cm long by 15 cm broad, while the thickness varied from 7.6 cm to 25.4 cm corresponding to 0.69 to 2.3 mean free paths respectively. The iron samples were slabs 20 cm long by 17 cm broad with thicknesses ranging from 2 cm to 8 cm corresponding to 0.44 to 1.7 mean free paths respectively.

---

*manufactured by Nuclear Enterprises Ltd.

The samples were placed 20 cm from the neutron source at an angle of 83° to the incident deuteron beam in order to intercept along the normal all the neutrons from the source associated with the alpha-particles detected at 90° to the beam. The neutron flight path between the sample and the detector was 140 cm.

Table 7.1 shows the differential elastic scattering cross-sections for the concrete samples. The errors shown were obtained by combining the individual errors in quadrature. In the published literature no data were found with which to compare the present results. The variation of the differential elastic scattering cross-section with sample thickness for iron is shown in Table 7.2.

Table 7.1

Differential cross-section for elastic scattering of 14 MeV neutrons from concrete*

Scattering angle	Sample thickness (cm)	Cross-section (mb sr^{-1})
35°	5.00	155 ± 13
	7.62	130 ± 10
	12.70	145 ± 12
	17.78	160 ± 14
	25.40	170 ± 16
55°	5.00	66 ± 6
	7.62	51 ± 4
	12.70	58 ± 5
	17.78	68 ± 6
	25.40	112 ± 11
75°	5.00	47 ± 4
	7.62	46 ± 4
	12.70	48 ± 4
	17.78	59 ± 5
	25.40	104 ± 10
85°	5.00	29 ± 3
	7.62	35 ± 3
	12.70	49 ± 4
	17.78	57 ± 5
	25.40	101 ± 10

*Assumes atomic weight of concrete = 33.35

Table 7.2

Differential cross-section for elastic scattering of 14 MeV neutrons from iron

Scattering angle	Sample thickness (cm)	Cross-section (mb sr^{-1})
25°	2	368.5 ± 30.1
	4	374.6 ± 30.9
	6	376.2 ± 33.6
	8	420.6 ± 36.9
45°	2	75.3 ± 6.4
	4	80.6 ± 6.8
	6	95.7 ± 8.3
	8	102.7 ± 9.2
65°	2	27.8 ± 2.6
	4	34.6 ± 3.1
	6	38.2 ± 3.5
	8	39.6 ± 3.7
85°	2	23.3 ± 2.3
	4	24.7 ± 2.3
	6	28.8 ± 2.7
	8	40.2 ± 3.7
90°	2	21.1 ± 2.1

Both sets of cross-sections were found to follow the equation:

$$\sigma = \sigma_o \, e^{\alpha x}$$

where σ is the measured differential cross-section, σ_o is the differential cross-section in the limit of zero thickness, α is a parameter obtained from the experimental results and x is the sample thickness in units of mean free paths. Values of the parameter α were found to be 0.38 ± 0.10 and 0.26 ± 0.10 (mean free path)$^{-1}$ for concrete and iron respectively.

8. DEPARTMENT OF PHYSICS, UNIVERSITY OF EDINBURGH

8.1 The polarization and differential cross-section for elastic scattering of 3 MeV neutrons (J.R.M. Annand*, R.B. Galloway and H. Savalooni) (WRENDA 1004, 1005)

The programme of measurements of the angular dependence of polarization due to elastic scattering and of the elastic differential cross-section for 3 MeV neutrons is continuing (see UKNDC(83)P109, p.102). Descriptions have been published of the 24 detector fast neutron polarimeter used for this work[1], of the influence of light attenuation in the NE213 scintillation counters on the recoil proton spectra recorded[2], and of the finite sample size correction procedure adopted for our data along with tests on iron samples of masses 760 and 250 g[3]. Measurements as well as appropriate optical model, Hauser-Feshbach and coupled channels calculations have been made on U, Bi, Pb, Tl, Hg, W and Sn. Measurements are being made on Sb and will continue on I, Te and In.

---

(1) J.R.M. Annand and R.B. Galloway, Nucl. Instr. Meth. 206 (1983) 431.

(2) J.R.M. Annand and R.B. Galloway, Nucl. Instr. Meth. 211 (1983) 421.

(3) J.R.M. Annand and R.B. Galloway, Nucl. Instr. Meth. 211 (1983) 453.

8.2 Polarization of neutrons from the $^{7}Li(d,n)^{8}Be$ reaction (R.B. Galloway and A.M. Ghazarian) (WRENDA 70)

The angular dependence of the polarization of neutrons from the $^{7}Li(d,n)^{8}Be$ reaction to the ground state of ^{8}Be as well as relative differential cross-sections for the ground state neutrons had been determined for 510 and 450 keV deuterons (see UKNDC(83)P109, p. 103-4). Measurements have been made of the reaction yield from 100 - 500 keV. The mean deuteron energies in the target corresponding to 510 and 450 keV incident energies were found to be 460 and 400 keV respectively. The absolute differential cross-section scale was determined by comparison with the yield from the $^{3}H(d,n)^{4}He$ reaction using a target of ^{3}H absorbed in Ti. From this calibration the relative differential cross-section data for

---

*Now at the Physics Department, University of Ohio

450 keV incident deuteron energy (see UKNDC(83)P109, p.104) can be interpreted in absolute terms with the zero degree differential cross-section corresponding to 1.4 mb sr^{-1}. The uncertainty in the absolute scaling is ±25%.

8.3 2.5 MeV neutron elastic and inelastic differential scattering cross-sections (M.N. Erduran and R.B. Galloway)
(WRENDA 812)

Equipment has been assembled with which it is intended to complement the work in this laboratory on neutron polarization and elastic scattering by making inelastic differential cross-section measurements. Unpolarized neutrons, i.e. at 90° centre of mass, from the $^{2}H(d,n)^{3}He$ reaction are used and the neutron yield is monitored by the protons from the $^{2}H(d,p)^{3}H$ reaction. Three neutron detectors view the scattering sample through tapered collimators in a wheel filled with paraffin wax which can be rotated to obtain different scattering angles. The neutron detectors are of NE213 with pulse shape discrimination against gamma rays. Proton recoil spectra are recorded and unfolded. Calculated differential cross-sections will be smeared in energy to match the energy resolution of the experimental system for comparison with and testing of model calculations. The equipment has been tested by making measurements on Fe. Proton recoil spectra have been collected for scattering through 20° to 150° by Bi, Hg, I, Sn and In. Cross-section normalisation is by scattering from a polythene sample. The unfolding of the proton recoil spectra to give neutron energy spectra is in progress.

9. NUCLEAR PHYSICS LABORATORY, OXFORD UNIVERSITY

9.1 Neutron inelastic scattering

9.1.1 The inelastic scattering of neutrons by ^{238}U (P.E. Hodgson and A.M. Kobos)*

A simple method of calculating the cross-section for the inelastic scattering of neutrons by deformed nuclei has been developed. The compound nucleus and direct interaction contributions are calculated, and approximate provision is made for the capture and fission processes. The method is applied to analyse the scattering of 0.2 -5 MeV neutrons by ^{238}U to both discrete and continuum states[1].

9.1.2 The inelastic scattering of neutrons by ^{232}Th (P.E. Hodgson and A.M. Street)*

The method of analysis described in sect. 9.1.1 is being applied to (n,n') on ^{232}Th with an improved program** that includes the fission and capture channels. The transmission coefficients are now calculated by the Hoffmann-Tepel-Weidenmüller formalism.

9.2 The neutron optical potential (P.E. Hodgson)

A review paper[2] has been written with the following abstract:
The nucleon optical model is described, with particular reference to the analysis of neutron scattering and reaction cross-sections. The central, spin-orbit and isospin terms in the potential are defined, and the results of phenomenological determinations of their parameters reviewed. The methods used to determine the asymmetry and isospin terms are described in detail. The optical potential at negative energies may be determined from the properties of the single-particle states and thus enables its behaviour at both positive and negative energies to be studied. Some of the methods used to calculate the optical potential from the nucleon-nucleon interaction are described, and the results compared with the phenomenological potential. The coupled-channels formalism enables both elastic and inelastic scattering from collective nuclei to be analysed simultaneously. Some analyses made in this way are reviewed, together with similar analyses of charge-exchange isoabric analogue state reactions.

---

*Work in collaboration with B.H. Patrick and M.G. Sowerby (AERE).

**Developed by Theoretical Physics Division, AERE.

(1) P.E. Hodgson and A.M. Kobos Ox. Univ. Nucl. Phys. Lab. preprint 5/84; also submitted to Nucl. Sci. Eng.

(2) P.E. Hodgson Ox. Univ. Nucl. Phys. Lab. preprint 14/84; to be published in Rep. Prog. Phys.

10. DEPARTMENT OF PHYSICS, UNIVERSITY OF LIVERPOOL

10.1 Nuclear data evaluation (N.J. Ward)

During the course of 1983, the data evaluation effort at Liverpool has continued. The review of data for A = 66 nuclides was accepted for publication in Nuclear Data Sheets. Data on A = 67 nuclides was submitted for publication and work on the A = 65 mass-chain has progressed.